A STUDY OF LAMINAR FORCED FILM CONDENSATION OF VAPOR FLOWING IN CROSS-FLOW DIRECTION THROUGH THE ANNULAR SPACE BETWEEN TWO CONCENTRIC CYLINDERS

A THESIS SUBMITTED TO
THE GRADUATE SCHOOL OF NATURAL AND APPLIED SCIENCES
OF
MIDDLE EAST TECHNICAL UNIVERSITY

BY

AHMET KORAY ATILGAN

IN PARTIAL FULLFILLMENT OF THE REQUIREMENTS
FOR
THE DEGREE OF MASTER OF SCIENCE
IN
MECHANICAL ENGINEERING

SEPTEMBER 2006

Approval of the Graduate School of Natural and Applied Sciences

Prof. Dr. Canan ÖZGEN
Director

I certify that this thesis satisfies all the requirements as a thesis for the degree of Master of Science

Prof. Dr. S. Kemal İDER
Head of Department

This is to certify that we have read this thesis and that in our opinion it is fully adequate, in scope and quality, as a thesis for the degree of Master of Science

Assoc. Prof. Dr. Cemil YAMALI
Supervisor

Examining Committee

Prof. Dr. Faruk ARINÇ (METU, ME) _____

Assoc. Prof. Dr. Cemil YAMALI (METU, ME) _____

Prof. Dr. Mecit SİVRİOĞLU (Gazi Unv., ME) _____

Prof. Dr. Kahraman ALBAYRAK (METU, ME) _____

Dr. Tahsin ÇETİNKAYA (METU, ME) _____

I hereby declare that all information in this document has been obtained and presented in accordance with academic rules and ethical conduct. I also declare that, as required by these rules and conduct, I have fully cited and referenced all material and results that are not original to this work.

Name, Last name : Ahmet Koray ATILGAN

Signature :

ABSTRACT

A STUDY OF LAMINAR FORCED FILM CONDENSATION
OF VAPOR FLOWING IN CROSS-FLOW DIRECTION
THROUGH THE ANNULAR SPACE BETWEEN
TWO CONCENTRIC CYLINDERS

Atılgan, Ahmet Koray

M. S., Department of Mechanical Engineering

Supervisor : Assoc. Prof. Dr. Cemil YAMALI

September 2006, 85 pages

In this study laminar forced film condensation of vapor flowing in cross-flow direction through the annular space between two concentric cylinders was investigated numerically. To achieve this, governing equations of the vapor and the condensate flow in cross-flow direction between two concentric cylinders were developed. After obtaining the equations in integral forms by using the finite difference technique the vapor boundary layer thicknesses on the inner and outer cylinders and the condensate layer thickness was obtained as a function of the angular position on the cylinders. It was assumed that the condensation took place on the outer surface of the inner cylinder only and the outer cylinder was assumed to be insulated. The computer program developed is capable to calculate the condensate film thickness, vapor boundary layer thickness, the heat flux and the heat transfer coefficient and the interface velocity between the condensate and the vapor layer as a function of the angular position on the cylinders. Effects of changing the free stream velocity flowing in the channel, the radius of the inner cylinder, the temperature difference between the saturated vapor and the wall and the annular space between the concentric cylinders were investigated numerically by using the computer

program and the results were presented graphically. Results showed that by increasing the free stream velocity of the vapor in the core, the film thickness decreased and by increasing the radius of the inner cylinder, the temperature difference between the saturated vapor and the wall and the annular space, the film thickness increased.

Keywords: Film Condensation, Concentric Cylinders, Film Thickness, Laminar Flow

ÖZ

KONSANTRİK İKİ SİLİNDİRİN ARASINDAKİ BOŞLUĞA ÇARPRAZ AKIŞ YÖNÜNDE AKAN BUHARIN LAMİNER ZORLANMIŞ FİLM YOĞUŞMASININ İNCELENMESİ

Atılgan, Ahmet Koray
Yüksek Lisans, Makine Mühendisliği Bölümü
Tez Yöneticisi: Doç. Dr. Cemil YAMALI

Eylül 2006, 85 sayfa

Bu çalışmada, konsantrik iki silindirin arasındaki boşluğa çarpraz akış yönünde akan buharın laminer zorlanmış film yoğuşması nümerik olarak incelenmiştir. Bu amaç doğrultusunda iki silindirin arasında çarpraz akış yönünde akan buharın ve yoğuşan tabakanın denklemleri geliştirilmiştir. Sonlu farklar tekniği kullanılarak integral formunda denklemler elde ediltikten sonra iç ve dış silindirlerin buhar sınır tabakası ve yoğuşan tabakanın kalınlıkları silindirin açısal fonksiyonu olarak elde edilmiştir. Yoğuşmanın sadece iç silindirde olduğu ve dış silindirin yalıtılmış olduğu kabul edilmiştir. Yoğuşan tabakanın kalınlığını, iç ve dış silindirlerin buhar sınır tabakası kalınlıklarını, ısı akısını, ısı transfer katsayısını ve yoğuşan ve buhar tabakası arasındaki arayüzün hızını silindirin açısal fonksiyonu olarak hesaplayan bir bilgisayar programı geliştirilmiştir. Kanal içinde akan buharın hızının, iç silindirin yarıçapının, doymuş buhar ve duvarın sıcaklığının ve konsantrik silindirler arasındaki boşluğun değişiminin etkisi program kullanılarak nümerik olarak incelenmiş ve sonuçlar grafiklerle gösterilmiştir. Sonuçlara göre, kanal içinde akan buharın hızının artırılmasıyla yoğuşan film tabakasının kalınlığının azaldığı, iç silindirin yarıçapının, doymuş buhar ve duvar arasındaki sıcaklığın ve silindirler

arasındaki boşluğun artırılmasıyla yoğuşan film tabakasının kalınlığının arttığı anlaşılmıştır.

Anahtar Kelimeler: Film Yoğuşması, Konsantrik Silindirler, Film Kalınlığı, Laminer Akış

To My Parents,

ACKNOWLEDGMENTS

I would like to thank my supervisor, Assoc. Prof. Dr. Cemil YAMALI for his continous guidance, support and valuable contribution throughout this study.

I express my deepest gratitude to my mother Deniz ATILGAN, my father İbrahim ATILGAN and my dear friend Betül ACAR for their encouragements throughout my education and my thesis period.

TABLE OF CONTENTS

LIST OF FIGURES

FIGURES

LIST OF SYMBOLS

d	Annular space between the cylinders	[m]
D	Diameter	[m]
f	Function	
f_x	Body Force	[N]
F	Differentiable function	
g	Gravity	[m/s^2]
h	Heat transfer coefficient due to condensation	[$W/(m^2.K)$]
h_{fg}	Latent heat of evaporation	[J/kg]
J	Jacobean matrix	
k_{liq}	Thermal conductivity of the condensate	[W/(m.K)]
L	Characteristic Length	[m]
m	Mass flow rate	[kg/s]
m_{con}	Mass flow rate of the condensate	[kg/s]
m_0	Mass flow rate per unit area entering the boundary layer through the (porous) surface	[kg/s]
m_δ	Mass flow rate per unit area entering the boundary layer from the free stream	[kg/s]
$m_{\infty 1}$	Mass flow rate from the core region to the vapor boundary layer of the inner cylinder	[kg/s]
$m_{\infty 2}$	Mass flow rate from the core region to the vapor boundary layer of the outer cylinder	[kg/s]
n	Number of points	
q	Heat flux	[W/m^2]
p	Pressure	[Pa]
r_0	Radius of the inner cylinder	[m]
R	Real numbers	
Re	Reynolds number	
T	Temperature	[°C, K]
T_{sat}	Temperature of saturated vapor	[K]

T_w	Temperature of the wall of inner cylinder	[K]
u	Velocity	[m/s]
u_l	Velocity of the condensate	[m/s]
u_{v1}	Velocity of the vapor layer of the inner cylinder	[m/s]
u_{v2}	Velocity of the vapor layer of the outer cylinder	[m/s]
U	Free stream velocity at inlet	[m/s]
U_∞	Free stream velocity	[m/s]
x	Coordinate parallel to surface of the inner cylinder	
y	Coordinate normal to surface of the inner cylinder	

Greek Letters

γ'''	Production of c per unit volume	
δ	Film thickness of the condensate	[m]
Δ_1	Boundary layer thickness of the vapor of the inner cylinder	[m]
Δ_2	Boundary layer thickness of the vapor of the outer cylinder	[m]
Δ_d	The difference of thicknesses between the vapors boundary layers	[m]
ΔT	Temperature difference between the saturated vapor and the wall of the inner cylinder	[K]
Δx	Distance between the two points over the inner cylinder in the solution procedure by using Newton's method	[m]
θ	Angular position measured from the top of the cylinder	[degree]
μ_l	Dynamic viscosity of the condensate	[Pa.s]
μ_v	Dynamic viscosity of the vapor	[Pa.s]
ρ_l	Density of the condensate	[kg/m^3]
ρ_v	Density of the vapor	[kg/m^3]
τ	Shear stress	[Pa]
τ_{xx}	Axial diffusion flux of c	
τ_{yx}	Transverse diffusion flux of c	
φ_{x0}	Axial diffusion flux of c at the wall	
$\varphi_{x\delta}$	Axial diffusion flux of c at the free stram	
φ_{y0}	Transverse diffusion flux of c at the wall	
$\varphi_{y\delta}$	Transverse diffusion flux of c at the free stram	

CHAPTER 1

INTRODUCTION

In this chapter, theoretical information is given about condensation by explaining its physical meaning and kinds. In addition to this, information about the condensation outside a cylinder and in the presence of noncondensable gas in vapor and also general information about flow regimes are given.

1.1. Condensation

Condensation is simply defined as changing phase from vapor state to liquid state. It occurs by bringing the vapor temperature under its saturation temperature. During a phase change a certain amount of subcooling takes place in the condensate and the latent heat released during the condensation is removed through the condensate by conduction. As the vapor diffuses into the condensation region, the pressure decreases from the bulk of the vapor to the vapor condensate interface.

Condensation is classified as bulk condensation and surface condensation. In the bulk condensation vapor condenses as droplets suspended in a gas phase. When condensation occurs randomly within the bulk of the vapor, this is called homogenous condensation. On the other hand, if it occurs on foreign particles existing in the vapor, it is called as heterogeneous condensation.

Surface condensation occurs by bringing vapor in contact with a surface that has the temperature below the saturation temperature of the vapor. This type of condensation

is widely used in industrial applications. Surface condensation is classified as filmwise condensation and dropwise condensation.

1.1.1. Filmwise Condensation

When the liquid wets the surface and this surface is blanketed by a condensate film, it is called filmwise condensation. This film creates a thermal resistance to heat transfer and a temperature gradient through the condensate occurs. In 1916 Nusselt performed an analytical investigation of filmwise condensation. He assumed the flow is laminar but neglected the vapor drag force and fluid acceleration. Furthermore, he assumed a linear temperature distribution and parabolic velocity profile for liquid phase. By making these assumptions he achieved the realistic results although he simplified the actual physical problem considerably by his assumptions. According to his study, the heat transfer coefficient in filmwise condensation over a flat plate is given as:

$$h = \left[\frac{g \rho_l (\rho_l - \rho_v) h_{fg} k_l^3}{4 \mu_l (T_{sat} - T_w) x} \right]^{1/4} \tag{1.1}$$

1.1.2. Dropwise Condensation

In dropwise condensation, surface is coated with a substance which inhibits from wetting the surface. In applications dropwise condensation is desired because heat transfer rates in this condensation can be ten times higher than filmwise condensation or much more. By the advantage of this type of condensation, a considerable decrease in condenser surface area is possible. To maintain dropwise condensation various surface coatings such as gold, silicones and Teflon are used. Due to oxidation and surface fouling, the effectiveness of these coatings decreases as vapor

condenses on the condenser surface and therefore, after a period of time dropwise condensation reversed to filmwise condensation. Also at high rate of condensation accumulation of droplets on the condenser surface causes to decrease the effectiveness of dropwise condensation.

For all these reasons condensers are designed with the assumption that filmwise condensation will take place in the condenser.

1.2. Condensation Outside a Single Horizontal Cylinder

Film condensation outside horizontal cylinders occurs in many engineering applications. For example, in shell-and-tube condensers which are widely used in power plants and processing industries employs condensation on horizontal cylinders.

In forced film condensation, in which vapor flows over a condenser surface, the shear stress exerted by the vapor on the surface film affects the rate of condensation. Vapor flowing over a condenser surface reduces the thickness (and thus thermal resistance) of the liquid film, which results in an enhancement of the heat transfer rate. Using the profile of vapor velocity at the interface, the shear stress can be obtained and subsequently be used to find the condensate film thickness and heat transfer to the condensate surface. For film condensation outside a single horizontal cylinder, heat transfer coefficient is given as:

$$h = 0.729\left[\frac{g\rho_l\left(\rho_l-\rho_v\right)h_{fg}k_l^{\,3}}{\mu_l\left(T_{sat}-T_w\right)D}\right]^{1/4} \tag{1.2}$$

1.3. Condensation in the Presence of Noncondensable Gases in Vapor

Experimental studies showed that even small amounts of noncondensable gas in the vapor decrease heat transfer coefficient significantly. The reason for this decrease is explained in connection with the formation of a barrier which is caused by the accumulation of the noncondensable gas between the vapor and the condensate layer. When the vapor diffuses toward the vapor-condensate interface with the noncondensable gas, vapor condenses and the noncondensable gas remains and accumulates in the vicinity of the surface thus, forming a barrier them. Therefore, the existence of noncondensable gases slows down the condensation process and for that reason it is not desired. In the literature it has been shown that the vapor passing by at high velocities assist the condensation heat transfer by removing the stagnant noncondensable gas from the vicinity of the condensate [1].

1.4. Shear Stress

In the flow, fluid particles contacting surface attain zero velocity. These particles retard the motion of other particles adjoining layer. This retardation effect is formulated in terms of the shear stress "τ" between fluid layers which is given in Equation 1.3 below:

$$\tau = \mu \frac{du}{dy} \tag{1.3}$$

In this relation "μ" is called the dynamic viscosity which is a fluid property.

1.5. Boundary Layer

At a stationary surface over which a viscous fluid flows, the fluid particles adhere to the surface and the frictional forces between the fluid layers retard the motion of the fluid within a thin layer near the surface. In this thin layer, this is called the boundary layer, the velocity of the fluid decreases from its freestream value to a value of zero at the surface (no-slip condition).

Ludwig Prandtl introduces the boundary layer concept for the first time in 1904. According to Prandtl's boundary layer concept, under certain conditions viscous forces are of importance only in the immediate vicinity of a solid surface are large. In regions away from the solid surface where large gradients exists in fluid velocity, the fluid motion may be considered frictionless, i.e., potential flow.

There is, in fact, no precise dividing line between the potential flow region, where friction is negligible, and the boundary layer region. However, it is customary to define the boundary layer as that region where the velocity component parallel to the surface is less than 99 % of the freestream velocity. Since the velocity component parallel to the surface is varying, the continuity requires that there should also be a velocity component perpendicular to the surface [2].

1.6. Flow Regimes

There are two kinds of flow regime which are called laminar and turbulent. Characteristics of the flow strongly depends on the flow regime. Reynolds number given below "Re" is used to determine the flow regime whether it is laminar or turbulent:

$$\mathrm{Re} = \frac{\rho U_\infty L}{\mu} \tag{1.4}$$

1.6.1. Laminar Flow

In the laminar flow, fluid motion is orderly and it is possible to identify streamlines along which the fluid particles move. The flow is steady and two dimensional. The velocity component perpendicular to the surface contributes significantly to the transfer of momentum and energy through the flow layers [3].

1.6.2. Turbulent Flow

Fluid motion in the turbulent flow is highly irregular and is characterized by disorderly displacements of individual volumes of fluid within the flow. These displacements enhance the transfer of momentum and energy. Velocity, temperature, pressure and other properties change continuously in time, and the flow is unsteady and three dimensional. The structure of turbulence is a complex phenomenon which is still not fully understood, and semi-empirical methods are invariably used for the solution of engineering problems.

If the flow over a flat plate is considered, initially the boundary layer development is laminar, but at some critical distance from the leading edge small disturbances in the flow begin to and a transition process takes place until the flow in the boundary layer becomes fully turbulent [3].

1.6.3. Flow Separation

For the flow separation, there must be a driving force to slow down the wall flow and can make it go backward. This driving force is called a adverse pressure gradient. The flow over a flat plate is a boundary layer flow without pressure gradient and hence, there is no flow separation. But, for boundary layer flows such as the flow

over a cylinder or sphere, an adverse pressure gradient develops after some location in the flow, and the increasing downstream pressure causes the flow adjacent to the wall to separate [4, 5].

CHAPTER 2

REVIEW OF PREVIOUS STUDIES

The present work concerns the theoretical analysis of laminar forced film condensation on annular outer surface of inner cylinder of two concentric cylinders. In this section reviews of previous studies about laminar film condensation are described.

Laminar film condensation was first analyzed by Nusselt [6]. In his study, the effects of both energy convection and fluid accelerations within the condensate layer and the shear stress at the liquid-vapor interface are neglected. The flow is assumed throughout the film is laminar and only gravity forces are acted on the condensate layer. In the analysis a simple balance between gravity and shear forces is created. Heat transfer from vapor to liquid is only carried out by condensation. In the analysis all fluid properties assumed constant for the liquid film and a linear temperature profile distribution is accepted for the condensate layer.

Sparrow and Gregg [7] pointed out the effect of inertia forces and energy convection for gravity which induced condensate flow along vertical plate. First of all they get simple differential equations from partial ones of the boundary layer by using similarity transformation. Then they solved the equations which they obtained. It was noticed in the analysis that depending on overall energy balance, the liquid film thickness increases regularly related with the subcooling parameter $C_p\Delta T/h_{fg}$. The author obtained the heat transfer results for the parameter $C_p\Delta T/h_{fg}$ values between 0 and 2 for Prandtl numbers to between 0.003 and 100. It is suggested that the effect of inertia forces on heat transfer can be neglected for $Pr \geq 1$; however, when $Pr << 1$ for a constant value of the parameter $C_p\Delta T/h_{fg}$ (for liquid film thickness), this effect becomes significant and can not be neglected. Moreover it is showed that the

importance of the effect of inertial forces is directly proportional to the parameter $C_p\Delta T/h_{fg}$, they both increases. According to the study, for Pr << 1 the energy convection has a minor role; however, for Pr ≥ 1 it increases with the film thickness.

In later study Sparrow and Gregg [8] developed a similar boundary layer analysis for laminar film condensation on a horizontal cylinder which again concerns the effects of inertia and energy convection. Cartesian coordinates was used to model the problem for the cylinder. A similarity solution is presented which confirms the cylinder surface except the stagnation region where the boundary layer assumptions are invalid. Similar to the vertical plate case, it is found that for high Prandtl number fluids, the importance of effects of energy convection become greater and due to the increasing of film thickness, the heat transfer increases. On the contrary, for low Prandtl number fluids, where heat conductivity supersedes energy convection, the opposite conditions occur. Therefore, the effects of inertia forces become more important and due to the increasing film thickness, the heat transfer decreases at that time. Furthermore, it is found that the film thickness rise rather slowly over the upper portion of the cylinder and this continues until it reaches infinity at the lower stagnation point.

Koh, Sparrow and Hartnett [9] first studied the boundary layer approach with the shear force at the liquid-vapor interface and developed it for laminar film condensation of stationary vapor along a vertical plate. It seems to be significant that the interfacial shear brings about the liquid to induce vapor velocities and then to reduce the heat transfer. Therefore, the authors get the solutions of two-phase boundary layer equations which include the inertia forces and energy convection for the problem which is concerned. The consideration of the shear force at the liquid surface is obtained by applying a force balance at the interface. In the analysis, doers used similarity transformation and they noticed that the effect of interfacial shear on heat transfer is extremely small that can be neglected for Pr ≥ 1. However, if the liquid metals are considered, the interfacial shear seems to cause a vital reduction in heat transfer. It is also clear that is one increases the thickness of the condensate film, it makes the interfacial shear and inertia forces to be more effective in reducing heat transfer which is valid for all Prandtl numbers. The effect of the parameter

$(\rho\mu)_l/(\rho\mu)_v$, which comes from the balance of shear force at the liquid-vapor interface, on heat transfer is small enough to be neglected.

Chen [10] made analysis about the effect of interfacial shear at the liquid-vapor interface. This was developed by applying on modified integral method for laminar film condensation along a vertical plate. The author accepted the ratio $(\rho\mu)_l/(\rho\mu)_v$ is small enough to be neglected and the vapor drag at the edge of the liquid film is approximately equal to the momentum of the entering vapor. Then, the author found lower heat transfer rates comparing to Sparrow and Gregg [7] (at low Prandtl numbers) as a result of vapor drag. That resembles the study of Koh, Sparrow and Hartnett [9]. Furthermore, if the acceleration parameter $k\Delta T/\mu_l h_{fg}$ is not small, an excessive negative velocity gradient at the interface appears.

Later Chen [11] made another study which focuses on the effect of interfacial shear at the liquid-vapor interface for the case of laminar film condensation on a horizontal cylinder. The modified integral method (which is used with the assumptions for the vertical plate case) is chosen to apply to the cylinder. According to the results, the velocity and temperature profiles are gotten for the condition that is $(\rho\mu)_l/(\rho\mu)_v << 1$. Moreover similarity is found existing near the top stagnation point and the most part of the tube approximately. Hence, this analysis proves that the inertia forces which are stronger for the top half of the cylinder, comparing with the vertical plate case, have greater effect on heat transfer, however the values of $k\Delta T/\mu_l h_{fg} < 0.5$, this situation does not occur.

In a later study, the two-phase boundary layer equations of laminar film condensation along a vertical plate is solved by Koh [12] who obtained the results by using an integral method. Similar to other studies given in references [9, 10], Koh included inertia forces, energy convection and interfacial shear to the analysis. In the study it is shown that why the parameter $(\rho\mu)_l/(\rho\mu)_v$ does not play a significant role and hence only two parameter which are $C_p\Delta T/h_{fg}$ and Pr are involved in film condensation problem. It is found that the subcooling parameter $C_p\Delta T/h_{fg}$ which increases the heat transfer for $Pr > 1$, on the contrary it decreases the heat transfer for $Pr < 1$. The calculations showed that heat transfer results and velocity profiles are completely

harmonious with the results of the boundary layer equations which are developed by Koh, Sparrow and Hartnett [9] (max. deviation of 5 %).

Churchill [13] also found a similarity solution which is approximately the same as the model of Koh, Sparrow and Hartnett [9]. The author used the solutions to determine the effects of inertia, interfacial shear and the heat capacity of the condensate. According to results, the effects of inertia of the condensate and interfacial shear on heat transfer can be admitted as significant for $Pr < 5$. Moreover, as previously shown, the heat capacity of the condensate seems to increase the rate of heat transfer for $Pr > 1$ and to decrease for $Pr < 1$. The author also examined the effect of surface curvature on laminar film condensation which occurs outside and inside of the vertical tubes. Therefore, for Nusselt numbers less than 26, this effect makes the heat transfer greater for condensation outside the tube, then has the opposite effect inside the tube accordingly.

Taghavi [14] made a study about the effect of surface curvature for laminar film condensation on a horizontal cylinder. In his analysis he assumed that inertia forces and energy convection is negligible small and also the shear at the condensate surface is zero. Moreover, when he presents the effect of surface curvature, the solution of the momentum equation in cylindrical coordinates is used. After that, the author shows the results in terms of the solution which is valid for the case of curvature effect can be neglected which means the solution of the momentum equation is showed in Cartesian coordinates. Consequently, the author found that the assumption of the surface curvature effect, which is neglected, is reasonable for the range of ordinary Nusselt numbers (deviation < 1 %).

Marchello and Henderson [15] searched for the role of tube diameter and surface tension on film condensation of stationary vapor for horizontal tubes. The authors obtained a set of $h_{measured}/h_{Nusselt}$ ratio with help of the collected data of other many observers. After the set was provided, least suitable squares were used. Then, they invented a correlation for the h_m/h_{Nu} ratio involving the corrections related to the effects of surface tension and pipe diameter which are considerable at the bottom of

the tube. This correlation contains the Ohnesorge number which is expressed as $\mu/(\rho g D \sigma)^{1/2}$.

Laminar film condensation in forced flow was initially analyzed along a horizontal plate by Koh [16]. The author incorporated energy convection, on the other hand excluded inertia and gravity forces. By the time, the solutions of the ordinary differential equations, which are obtained by similarity transformation of the partial layer equations, are necessary for the analysis. The interfacial shear was included by writing a force balance at the vapor-liquid interface as done by Koh, Sparrow and Hartnett [9]. Then they declared the results as a function of parameters which are $C_p\Delta T/h_{fg}$ with $(\rho\mu)_l/(\rho\mu)_v$ and Prandtl number. According to the findings of the author, for low Prandtl number liquids, energy transfer by convection is as small as to be neglected; also the heat transfer is inversely proportional to the parameter $C_p\Delta T/h_{fg}$. That means, the heat transfer decreases consistently, when the parameter $C_p\Delta T/h_{fg}$ increases. On the other hand, for high Prandtl number liquids; the energy convection is exactly significant and while the condensate film thickness increases, heat transfer possesses its minimum values.

Laminar film condensation of flowing vapor along a horizontal plate and over a horizontal cylinder was analyzed by Shekriladze and Gomelauri [17]. They all neglect pressure gradient, energy convection, condensate subcooling, inertia and gravity forces. Likewise in the studies of Chen and Churchill [10, 11, 13], the vapor drag was accepted to occur from the momentum transferred which is due to the vapor suction. For the plate case, correlations for the effects of inertia forces and energy convection were found. These effects on heat transfer were neglected due to being small for ordinary liquids. Then, for the horizontal cylinder, a relation was initially found for the mean heat transfer coefficients. After that, they shaped this relation in order to modify related to the case that 65 % of heat is transferred up to the minimum separation angle of 82°. Finally the authors expressed that on a certain analytical solution is out of possibility for condensation in a gravitational field.

Denny and Mills [18] also studied on laminar film condensation of flowing vapor on a horizontal cylinder. However, they made their analysis by including the gravity

forces unlike Shekriladze and Gomelauri [17] did. The authors focused on an analytical solution of the problem for the case that inertia forces, energy convection pressure gradient around the cylinder are neglected. They compared the exactness of the solution with certain numerical solutions which are also take place in this study. The authors declared that according to the results of the analysis, when Φ (angle measured from the vertical axis) reaches a value higher than 140°, the negligible inertia assumption is disturbed. In spite of that situation, the results were deserved to be considered. Since, in fact, in ordinary cases, 85% of total condensation occurs when $\Phi<140°$, also the effects of surface tension near the bottom of the tube cannot be ignored. Moreover, the pressure gradient brings about an augmentation in overall heat transfer coefficient; and while Φ increases, its effect on local heat transfer decreases.

Fujii, Uehara and Kurata [19] carried out a research about the effect of vapor velocity on laminar film condensation of flowing vapor on a horizontal cylinder. In their study, it is observed that they all include gravity forces, inertia forces for the vapor boundary layer, energy convection and pressure gradient. They also found a solution for the problem of the interfacial shear with the help of the model of Koh, Sparrow ad Hartnett [9]. The authors admitted potential flow outside the vapor boundary layer; also they used the power series expansion. So, they found a similarity solution. Furthermore, they developed a simple expression for the average and local heat transfer coefficient. Due to the fact that they made experiments about the condensation of steam; they added comparisons between the theoretical results and experimental ones to their study. According to that, it was seen that for high oncoming velocities the effect of body forces on heat transfer can be neglected because of being small; and the ρμ ratio is significant. Consequently, it is also observed that the local heat transfer coefficients at the upper part of the tube become greater related to increasing oncoming velocity.

The effect of pressure gradient for forced convection film condensation on a horizontal cylinder was studied by Rose [20]. Doer omitted the inertia forces and adopted a simpler Shekriladze and Gomelauri model for the vapor drag which is necessary as the primary object was to investigate the effect of pressure gradient in

the analysis. The author also made an assumption of the potential flow outside the vapor boundary layer. Overall, the analysis showed that by the time the parameter $\rho gd/8\rho gU_{\infty}^{2}$ has values under unity, the pressure gradient becomes important. The author also proves that the pressure gradient reaches to higher heat transfer coefficients for the upper part of the cylinder and it brings about instability in the condensate film at some location over the rear half.

There exists a fact that the approximations such as zero gravity, negligible inertia and energy convection probably supplies many situations, however, one should avoid a generalization over the all of the governing parameters. Therefore, Gaddis [21] transformed the governing partial differential equations into ordinary ones in order to solve the full two-phase boundary layer equations for laminar film condensation of flowing vapor on a horizontal cylinder. He obtained different results for quiescent vapor and liquid metals, and for ordinary liquids. If quiescent vapor (Re=0) and liquid metals are considered, when inertia forces in the condensate film and shear forces at the interface are ignored, a significant increase in heat transfer occurs, but subcooling in the condensate is ineffective. On the other hand, if ordinary liquids are taken in consideration, when the inertia forces in the condensate film and shear forces at the interface are again ignored, however this seems to have unimportant effect on heat transfer; by contrast liquid subcooling leads to a reduction of 5% in heat transfer. For flowing vapor (Re=0), as long as flow separation is not observed, an increase of Reynolds number causes an increase in heat transfer. Consequently, the author showed that for the value of $Re=10^{5}$, a separation of flow from the wall occurs at $\Phi=126°$.

A study which is on numerical analysis of laminar film condensation of vapor flowing downwards a horizontal cylinder was performed by Karabulut and Ataer [22]. The authors include the inertia forces, pressure gradient and energy convection in the two-phase boundary layer equations. Unlike Gaddis [21], who transformed the basic equations into a set of ordinary differential equations, they applied a direct numerical method to the basic equations. After discretizing the basic equations of the boundary layer first, they found the solutions of the discretized equations numerically. Moreover, the authors noticed that flow separation occurs at

Φ=108° under certain conditions which require steam with a freestream velocity of 20 m/s and temperature difference of 10°C. When they compare the condensate thickness in different situations that are with and without the pressure gradient, they experienced the instability of the condensate flow over the lower part of the cylinder due to the pressure gradient. However, they found that the effect of the pressure gradient on heat transfer is inconsiderable. It was also proved that the effect of pressure gradient on heat transfer reduces the condensate film thickness; therefore, it increases the heat transfer from the interface to the wall. The researchers also investigated for errors due to neglecting inertia forces and energy convection. Then, it was noticed that these errors are insignificant except for the cases in which oncoming velocity and ΔT are high.

Memory, Adams and Marto [23] analyzed laminar film condensation on horizontal elliptical tubes under the condition of free and forced convection. The authors added the effect of surface tension to their study. They assumed the shear force at condensate film edge as zero for free convection. On the other hand, they include interfacial shear and pressure gradient around the tube for the cases of forced convection. According to results of the analysis of free convection, it can be clearly seen that comparing to a circular tube of equivalent surface area, an improvement of 11% in mean heat transfer coefficient is noticed due to an elliptical tube with major axis vertically placed. At a given oncoming velocity for forced convection, 2% decrease occurs in the mean heat transfer coefficient because of a reduction in interfacial shear. However, for the same pressure drop across each tube, heat transfer was 16% higher than the one for the elliptical tube. By researchers it is also concluded by the researchers that the surface tension effect on mean heat transfer coefficient can be neglected since it is small enough.

Rao and Sarma [24] investigated the condensation of vapor on a laminar falling film of the liquid coolant. In their study, it is mentioned that the dynamics of the falling film had an important effect on the condensation heat transfer rates. Furthermore, with shorter coolant film thickness would be more effective in terms of condensation heat transfer rates than its calculated by Nusselt for direct contact condensers.

Variable wall temperature and the effects of pressure gradient for film condensation on a horizontal tube with flowing vapor downward on it were analyzed by Hsu and Yang [25]. It is stated that the mean heat transfer coefficient is slightly increased with the wall temperature variation amplitude "A". When the pressure gradient is not taken account, the mean heat transfer coefficient is decreased with A. On the contrary, it is increased with A by taking account the pressure gradient. Moreover, the mean heat transfer coefficient is not affected by the pressure gradient for the low and high vapor velocities. With increasing pressure gradient effect the mean heat transfer coefficient is decreased considerably.

Mosaad [26] made a study about free and forced convection laminar film condensation on an inclined circular tube. In the analysis some approximations were obtained for the evaluation of the interfacial shear stress. A numerical investigation was made to obtain local and mean Nusselt numbers by the effects of vapor velocity and gravity forces. Furthermore, an explicit simple expression was formulated by the author to calculate the mean Nusselt number for an inclined tube with infinite length.

Browne and Bansal [27] published a review paper about condensation heat transfer on horizontal tube bundles particularly for shell-and-tube type condensers. After reviewed by authors over 70 paper, which were published about condensation, they obtained some conclusions. Firstly, according to the authors, surface geometry is very important on condensation. And then, condensate inundation substantially affects tubes with three dimensional fins first, smooth tubes second and finally integral-fin tubes. Moreover, enhancement due to vapor shear on smooth tubes is greater than that on integral-finned tubes. Finally, the coolant velocity has a large effect for enhanced tube surfaces by means of overall heat transfer coefficient. On the contrary it has minimal effect for smooth tubes.

Test sections were prepared to investigate the condensation of flowing vapor onto horizontal tube banks by Kutateladze and Gogonin [28]. In their experiments R12 and R21 were used. The results obtained by the authors were compared with the previous works. According to their results, when the vapor velocity is low, the condensate flow rate only affects the condensation heat transfer on tube banks.

Kutateladze, Gogonin and Sosunov [29] investigated the condensation heat transfer by the effect of the condensate flow rate. In their study, the horizontal smooth tube banks with different diameters were analyzed. It is mentioned that at $Re > 50$, the heat transfer is contributed by the condensation on supercooled drops and discrete liquid streamlets. And also it is stated that the starting length of the thermal boundary layer is affected by both Reynolds number and the diameter of the cylinder.

In another study by Kutateladze and Gogonin [30] about the condensation of flowing vapor on a horizontal cylinder was made. It is stated that the friction on the liquid-vapor state depends on the magnitude of the cross flow of the substance. It also determines the film thickness and the condensation heat transfer of flowing vapor.

Different from geometries in condensation studied at previous works mentioned above, in this study the effect of using two concentric cylinders on the condensation heat transfer is investigated.

CHAPTER 3

ANALYSIS

Firstly geometry of the problem is described briefly in this part. And then, with the help of the assumptions and conservation laws which are the conservation of mass and momentum, the governing equations are obtained. After obtaining the nonlinear equations for the variables, which are the condensate film thickness, vapor boundary layers of inner and outer cylinders, the velocity at the interface and also free stream velocity in the core, these variables are solved with the computer code which uses finite difference method in order to solve these equations.

3.1. Description of the Problem

As seen in Figure 3.1 the saturated vapor with the velocity U_∞ at 100°C flows through the annular space between the two concentric cylinders. In Figure 3.2 the physical model is shown in Cartesian coordinates schematically just for simplicity. As the vapor flows through the annular space, the condensate film thickness and vapor boundary layers starts increasing. The vapor boundary layer of the inner cylinder is expected to be thinner compared to the one over the inner surface of outer cylinder because there is the mass transfer by the condensation from the vapor to the condensate layer. Furthermore in forced film condensation thinner condensate film thickness is expected compared to the one with stagnant vapor. Since in forced film condensation while vapor flows along the surface, the flow of the vapor as a result of shear stress increases the average velocity of the liquid and thus decreases the film thickness. Therefore the thermal resistance of the condensate film decreases which

results on this helps to increase in the condensation heat transfer which is desired in applications.

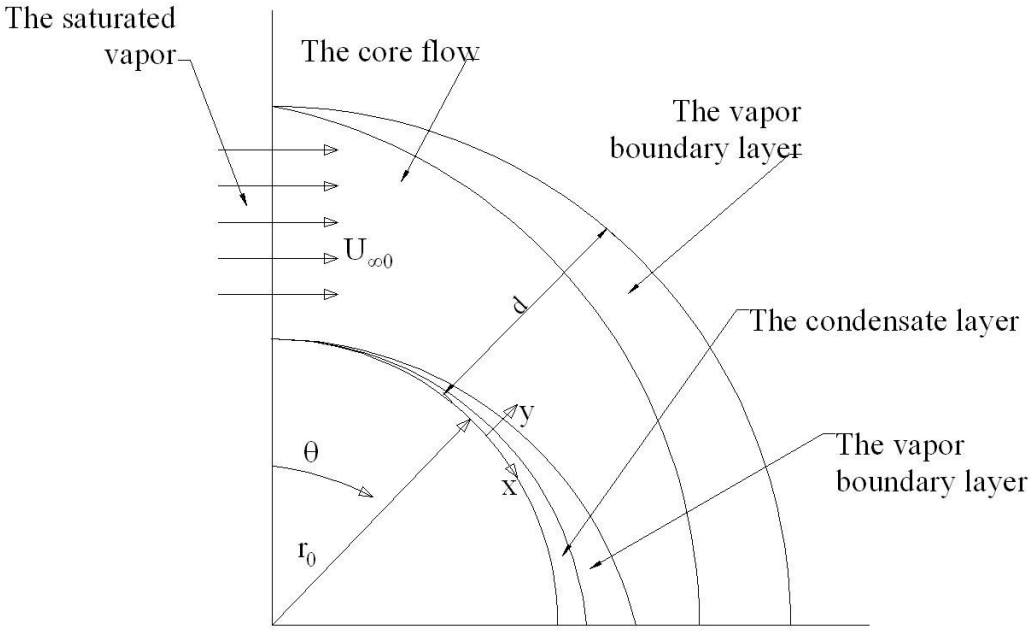

Figure 3.1 Physical Model of the Problem

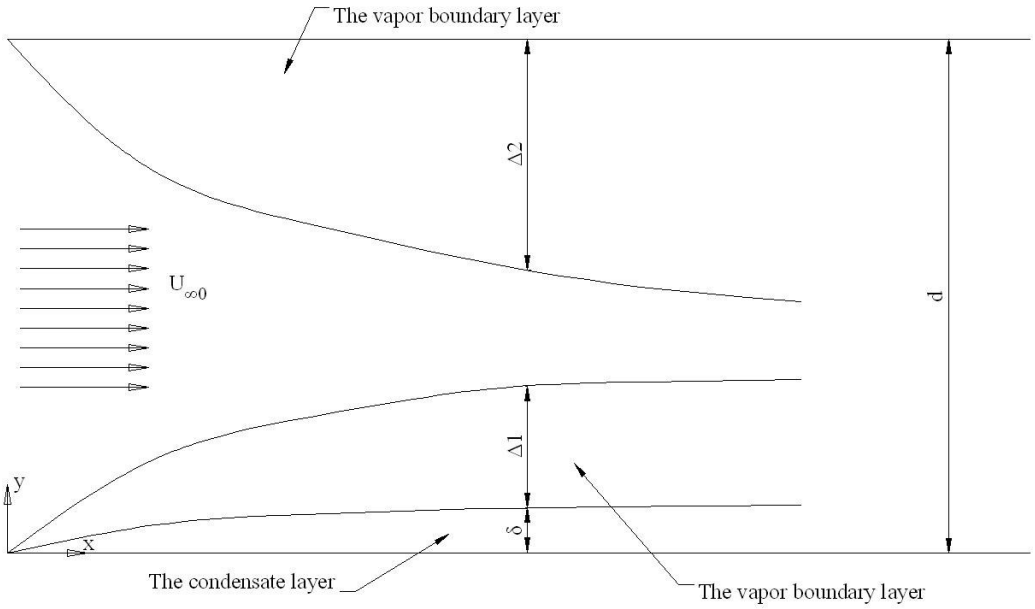

Figure 3.2 Simplified Model in Cartesian Coordinates

3.2. Governing Equations

By applying the principles of conservation of mass and momentum on the condensate and vapor boundary layer, governing equations are obtained in order to investigate the condensation for the geometry in this study. Before starting to analyze some assumptions should be made:

- The gravitational force is neglected.
- Condensation takes place on the outer surface of inner cylinder only.
- All the vapor layers are at uniform temperature.
- Temperature variations at the interface between liquid and vapor phases are insignificant.

- Mass transfer from vapor to liquid is only carried out by condensation.
- Velocity profiles for the condensate and vapor layers are both assumed to be linear to simplify the solution procedure.
- All the flow regimes are laminar.
- All the properties of vapor and liquid are assumed constant in the flow.
- Thicknesses of the condensate film and vapor boundary layers are very small compared with the radiuses of the inner and outer cylinders. Consequently the curvature effects are neglected and a single x axis is used as coordinate axis in the radial direction.
- Steady state is assumed.
- Potential flow is assumed for the core region between the vapor boundary layers of inner and outer cylinders, respectively.

Analysis is started by writing general integral formulation which states a general balance principle involving property c per unit mass. Applying this principle to the differential-integral control volume shown in Figure 3.3, Equation 3.1 can be obtained for two-dimensional boundary layers [31].

$$\frac{\partial}{\partial t}\int_0^\delta \rho c dy + \frac{\partial}{\partial x}\int_0^\delta \rho c u dy - m_\delta c_\delta - m_0 c_0 - \varphi_{x\delta}\frac{\partial \delta}{\partial x} + \frac{\partial}{\partial x}\int_0^\delta \varphi_x - \varphi_{y0} + \varphi_{y\delta} - \int_0^\delta \gamma''' dy = 0 \qquad (3.1)$$

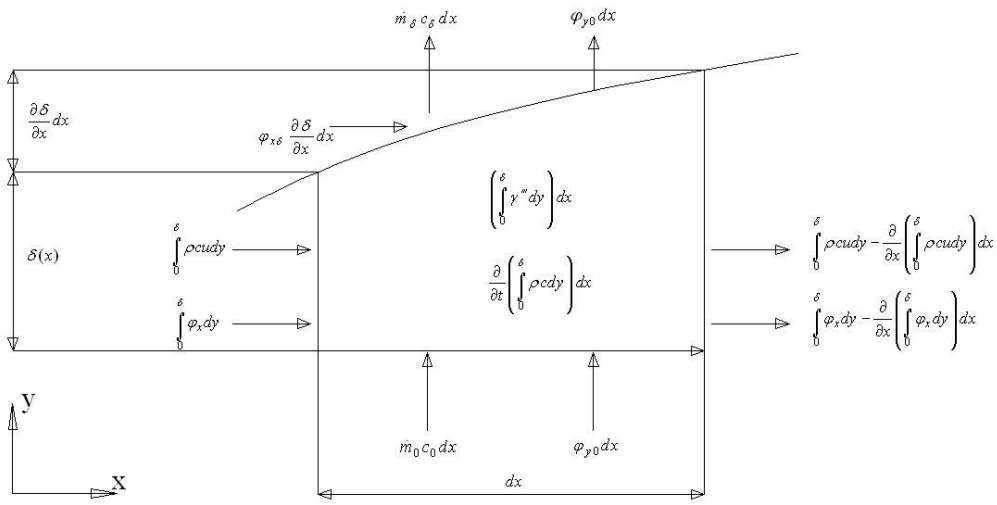

Figure 3.3 General Balance Principle for the Differential-Integral Control Volume of Boundary Layer

In Equation 3.1, m_δ and m_0 are the mass flow rate per unit area entering the boundary layer from the free stream and through the surface (porous or condensation surface), respectively. By using the Leibnitz rule, fifth and sixth terms in Equation 3.1 can be combined to a single term, which represents the axial (streamwise) fluxes of c, as shown in Equation 3.2

$$\varphi_{x\delta} \frac{\partial \delta}{\partial x} - \frac{\partial}{\partial x} \int_0^\delta \varphi_x = -\int_0^\delta \frac{\partial \varphi_x}{\partial x} dy \tag{3.2}$$

According to the boundary layer approximation, the diffusive contributions to these fluxes may usually be ignored. Transverse diffusion fluxes of c are φ_{y0} at the wall and $\varphi_{y\delta}$ at the free stream, where $\varphi_{y\delta}$ is usually zero by the physics of the problem. γ''' is the production of c per unit volume. By deriving the conservation of mass for c=1, φ=0, γ'''=0, Equation 3.3 is obtained:

$$\frac{\partial}{\partial t}\int_0^{\delta}\rho dy+\frac{d}{dx}\int_0^{\delta}\rho udy-m_{\delta}-m_0=0 \tag{3.3}$$

For the steady form, Equation 3.4 is obtained:

$$\frac{d}{dx}\int_0^{\delta}\rho udy-m_{\delta}-m_0=0 \tag{3.4}$$

Multiplying Equation 3.3 by c_{δ} and subtracting the result from Equation 3.1, Equation 3.5 is obtained below:

$$\begin{aligned}\frac{\partial}{\partial t}\int_0^{\delta}\rho cdy-c_{\delta}\frac{\partial}{\partial t}\int_0^{\delta}\rho dy+\frac{\partial}{\partial x}\int_0^{\delta}\rho cudy-c_{\delta}\frac{\partial}{\partial x}\int_0^{\delta}\rho udy-m_0(c_0-c_{\delta})+\\ +\int_0^{\delta}\frac{\partial\varphi_x}{\partial x}dy-\varphi_{y0}+\varphi_{y\delta}-\int_0^{\delta}\gamma'''dy=0\end{aligned} \tag{3.5}$$

To obtain the balance of momentum in x, c=u, c_{δ}=U, c_0=0, φ_x=-τ_{xx}+p, φy=-τ_{yx}, γ'''=ρf_x are used in Equation 3.5 and ignoring axial diffusion τ_{xx} and the variation in pressure and body force across the boundary layer and assuming steady flow, Equation 3.6 is obtained below:

$$\frac{d}{dx}\int_0^{\delta}\rho u^2dy-U\frac{d}{dx}\int_0^{\delta}\rho udy+m_0U-\delta\left(pf_x-\frac{dp}{dx}\right)+\tau_{yx}\Big|_{y=0}-\tau_yx\Big|_{y=\delta}=0 \tag{3.6}$$

To start to derive the equations velocity profiles should be expressed for the condensate liquid and vapor phases. As it is mentioned in assumptions to avoid complexities in problem linear velocity profiles are chosen for the condensate, vapor boundary layers, respectively in Equations 3.7, 3.8 and 3.9:

$$u_l=ay+b \tag{3.7}$$

$$u_{v1}=ky+l \tag{3.8}$$

$$u_{v2} = my + n \tag{3.9}$$

Boundary conditions are:

At $x = 0, \quad 0 \le y \ge d$: $\delta = \Delta_1 = \Delta_2 = 0 \, , U_\infty = U$

At $y = 0, \quad x \ge 0$: $u_l = 0$

At $y = \delta, \quad x \ge 0$: $u_l = u_{v1} = U_{\text{int}} \, , \tau = \mu_l \dfrac{\partial u_l}{\partial y} = \mu_v \dfrac{\partial u_{v1}}{\partial y}$

At $y = \delta + \Delta_1 \, , x \ge 0$: $u_{v1} = U$

At $y = d - \Delta_2 \, , x \ge 0$: $u_{v2} = U$

At $y = d \, , x \ge 0$: $u_{v2} = 0$

Using these boundary conditions and the assumptions above in Equations 3.7, 3.8 and 3.9, velocity profiles are obtained for the condensate and vapor layers in Equations 3.10, 3.11 and 3.12, respectively:

Velocity profile for the condensate layer:

$$u_l = \frac{U_{\text{int}}}{\delta} y \tag{3.10}$$

Velocity profile for the vapor boundary layer of the inner surface of the cylinder:

$$u_{v1} = \frac{U - U_{\text{int}}}{\Delta_1} y + U_{\text{int}} - \frac{U - U_{\text{int}}}{\Delta_1} \delta \tag{3.11}$$

Velocity profile for the vapor boundary layer of the outer surface of the cylinder:

$$u_{v2} = \frac{U}{\Delta_2} y \tag{3.12}$$

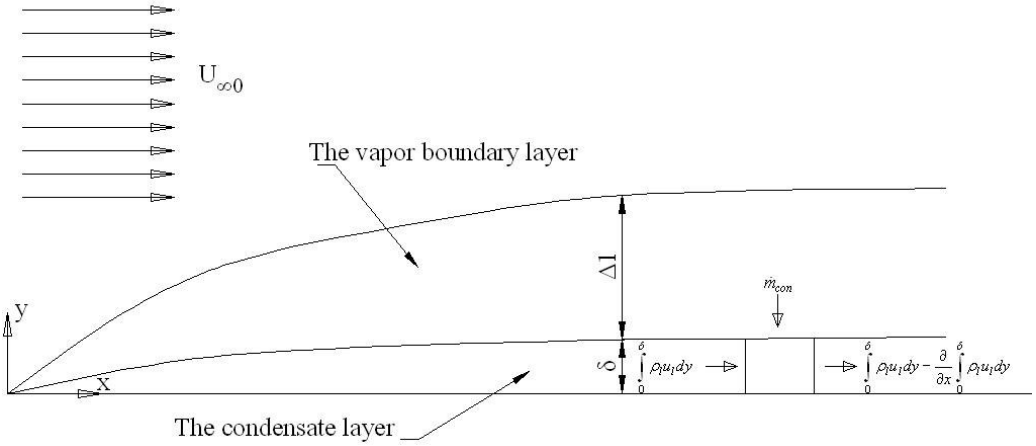

Figure 3.4 The Differential-Integral Control Volume for the Condensate Layer

The analysis is started by using the integral method mentioned before in Equations 3.1 to 3.6 derived for the differential-integral control volume for the condensate layer in Figure 3.4. By applying the conservation of mass principle on Figure 3.4, Equation 3.13 is obtained:

$$\left(\int_0^{\delta} \rho_l u_l dy\right) dx - \left(\int_0^{\delta} \rho_l u_l dy\right) dx - \left(\frac{\partial}{\partial x}\int_0^{\delta} \rho_l u_l dy\right) dx + \dot{m}_{con} dx = 0 \tag{3.13}$$

Mass entering into the differential integral control volume ($\dot{m}_{con}$) by condensation is obtained by assuming that the heat released during the condensation of vapor is conducted through the condensate layer. The heat released during the condensation and conducted through the condensate layer can be calculated by assuming a linear temperature variation in the condensate layer as shown below:

$$q'' = -kdx\frac{\partial T}{\partial y}\bigg| = kdx\frac{T_{sat} - T_w}{\delta} = kdx\frac{\Delta T}{\delta} \tag{3.14}$$

The rate of mass entering into the differential integral control volume can be expressed in terms of the heat released and conducted to the condensate layer becomes:

$$q'' = \dot{m}_{con} h_{fg} \tag{3.15}$$

$$\dot{m}_{con} = \frac{k_l \Delta T}{h_{fg}\delta} \tag{3.16}$$

Inserting $\dot{m}_{con}$ given by Equation 3.16 and the velocity profile for the condensate layer given in Equation 3.10 into Equation 3.13 the following equation for the conservation of mass in the condensate layer in the form of differential equation is obtained:

$$\frac{d}{dx}\left(\frac{U_{\text{int}}\delta}{2}\right) - \frac{k_l \Delta T}{\rho_l h_{fg}\delta} = 0 \tag{3.17}$$

Applying the conservation of momentum principle on the differential integral control volume in Figure 3.4 the following equations obtained:

$$\begin{aligned}\left(\int_0^\delta \rho_l u_l^{\,2} dy\right)dx - \left(\int_0^\delta \rho_l u_l^{\,2} dy\right)dx - \left(\frac{\partial}{\partial x}\int_0^\delta \rho_l u_l^{\,2} dy\right)dx + U_{\text{int}}\dot{m}_{con}dx + \\ +\delta\frac{dP}{dx}dx - \tau_s\big|_0\, dx + \tau_s\big|_\delta = 0\end{aligned} \tag{3.18}$$

In boundary layer theory the pressure variation in the transverse direction is neglected. Therefore, the variation of pressure in the condensate layer along the x direction is equal to the variation of the pressure along the x direction in the core

region. From the potential flow theory, this pressure variation can be obtained as follows:

$$\frac{dP}{dx} = -\rho_v U \frac{dU_\infty}{dx} \tag{3.19}$$

Shear stresses between the inner cylinder and the condensate layer and at the interface between the condensate and vapor boundary layer are obtained in Equations 3.20 and 3.21.

$$\tau_s\big|_0 = \mu_l \frac{du_l}{dy} = \mu_l \frac{U_{\text{int}}}{\delta} \tag{3.20}$$

$$\tau_s\big|_\delta = \mu_v \frac{du_{v1}}{dy} = \mu_v \frac{U - U_{\text{int}}}{\Delta_1} \tag{3.21}$$

Substituting the velocity profile, shear stresses and pressure variation along the x direction in Equation 3.18 the following the differential equation is obtained:

$$\begin{aligned} &\frac{d}{dx}\left(\frac{U_{\text{int}}{}^2 \delta}{3}\right) - U_{\text{int}} \frac{k_l \Delta T}{\rho_l h_{fg} \delta} - \frac{\rho_v}{\rho_l} \delta U \frac{dU}{dx} + \\ &+ \frac{\mu_l}{\rho_l} \frac{U_{\text{int}}}{\delta} - \frac{\mu_v}{\rho_l} \frac{U - U_{\text{int}}}{\Delta_1} = 0 \end{aligned} \tag{3.22}$$

By using the conservation of mass principle for the vapor boundary layer of the outer cylinder the following equation is obtained:

$$\left(\int_{d-\Delta_2}^{d} \rho_v u_{v2} dy\right) dx - \left(\int_{d-\Delta_2}^{d} \rho_v u_{v2} dy\right) dx - \left(\frac{\partial}{\partial x} \int_{d-\Delta_2}^{d} \rho_v u_v dy\right) dx + \dot{m}_{\infty 2} dx = 0 \tag{3.23}$$

Substituting the velocity profile given by Equation 3.9 in the Equation 3.23, the mass flow rate from the potential flow into the vapor boundary layer of the outer cylinder is obtained as follows:

$$\dot{m}_{\infty 2} = \rho_v \frac{d}{dx}\left(\frac{U\Delta_2}{2}\right) \tag{3.24}$$

Applying the conservation of mass principle for the potential flow that exists between two vapor boundary layers, the equation below is obtained.

$$\left(\int_{\delta+\Delta_1}^{d-\Delta_2} \rho_v U dy\right)dx - \left(\int_{\delta+\Delta_1}^{d-\Delta_2} \rho_v U dy\right)dx - \left(\frac{\partial}{\partial x}\int_{\delta+\Delta_1}^{d-\Delta_2} \rho_v U dy\right)dx - \\ -\dot{m}_{\infty 1}dx - \dot{m}_{\infty 2}dx = 0 \tag{3.25}$$

Substituting the mass flux given by Equation 3.24 into Equation 3.25, mass flow rate from the core region into the vapor boundary layer of the inner cylinder is obtained below.

$$\dot{m}_{\infty 1} = -\rho_v \left\{\frac{d}{dx}\left[U\left(d-\delta-\Delta_1-\Delta_2\right)\right] + \frac{d}{dx}\left(\frac{U\Delta_2}{2}\right)\right\} \tag{3.26}$$

By applying conservation of mass principle to the differential integral control volume for the vapor boundary layer of the inner cylinder the following integral equation is obtained.

$$\left(\int_{\delta}^{\delta+\Delta_1} \rho_v u_{v1} dy\right)dx - \left(\int_{\delta}^{\delta+\Delta_1} \rho_v u_{v1} dy\right)dx - \left(\frac{\partial}{\partial x}\int_{\delta}^{\delta+\Delta_1} \rho_v u_1 dy\right)dx - \dot{m}_{con}dx + \dot{m}_{\infty 1}dx = 0 \tag{3.27}$$

Substituting the velocity profile for the vapor, mass flow rate due to condensation ($\dot{m}_{con}$) and mass flow rate from the core into vapor boundary layer of the inner cylinder given by Equations 3.11, 16 and 26, respectively in Equation 3.27, the following equation for the conservation of mass in the vapor boundary layer of the inner cylinder is obtained.

$$\frac{d}{dx}\left[\frac{\Delta_1\left(U_{\text{int}}+U\right)}{2}\right]+\frac{k_l\Delta T}{\rho_v h_{fg}\delta}+\frac{d}{dx}\left[U\left(d-\delta-\Delta_1-\Delta_2\right)\right]+\frac{d}{dx}\left(\frac{U\Delta_2}{2}\right)=0 \qquad (3.28)$$

To solve the five unknowns which are the condensate film thickness, vapor boundary layer thicknesses of the inner and outer cylinders, the velocity at the interface of the condensate film and velocity boundary layer and the core velocity two more equations are needed. These two equations are obtained by applying the conservation of momentum principle for the core flow and the vapor boundary layer of the outer cylinder.

For the core flow by applying the conservation of momentum principle to the differential control volume the following equations are obtained.

$$\begin{aligned}\left(\int_{\delta+\Delta_1}^{d-\Delta_2}\rho_v U^2 dy\right)dx-\left(\int_{\delta+\Delta_1}^{d-\Delta_2}\rho_v U^2 dy\right)dx-\left(\frac{\partial}{\partial x}\int_{\delta+\Delta_1}^{d-\Delta_2}\rho_v U^2 dy\right)dx-U\dot{m}_{\infty 1}dx-\\ -U\dot{m}_{\infty 2}dx-(d-\Delta_1-\Delta_2-\delta)\frac{dP}{dx}dx=0\end{aligned} \qquad (3.29)$$

By substituting the core flow velocity gradient and mass fluxes to both vapor boundary layers given by Equations 3.19, 24 and 26 in Equation 3.29 the following differential equation for the conservation of momentum in the core flow is obtained.

$$\begin{aligned}\frac{d}{dx}\left[U^2\left(d-\Delta_1-\Delta_2-\delta\right)\right]-U\frac{d}{dx}\left[U\left(d-\Delta_1-\Delta_2-\delta\right)\right]-\\ -\left(d-\Delta_1-\Delta_2-\delta\right)U\frac{dU}{dx}=0\end{aligned} \qquad (3.30)$$

If the conservation of momentum principle is applied on the differential integral control volume for the vapor boundary layer of the outer cylinder, the following equations are obtained.

$$\left(\int_{d-\Delta_2}^{d}\rho_v {u_{v2}}^2 dy\right)dx-\left(\int_{d-\Delta_2}^{d}\rho_v {u_{v2}}^2 dy\right)dx-\left(\frac{\partial}{\partial x}\int_{d-\Delta_2}^{d}\rho_v {u_{v2}}^2 dy\right)dx+U\dot{m}_{\infty 1}dx- \\ -\Delta_2\frac{dP}{dx}dx-\tau_s\big|_d\,dx=0 \tag{3.31}$$

Substituting the velocity profile, mass flux from the core region, pressure gradient and the surface tension from Equations 3.12, 19, and 26 in Equation 3.31 the following equation for the conservation of the momentum of the vapor boundary layer of the outer cylinder is obtained.

$$\frac{d}{dx}\left(\frac{U^2\Delta_2}{3}\right)-U\frac{d}{dx}\left(\frac{U\Delta_2}{2}\right)-\Delta_2 U\frac{dU}{dx}+\frac{\mu_v}{\rho_v}\frac{U}{\Delta_2} \tag{3.32}$$

After determining the condensate film thickness from the solution of the sets of equations obtained above the heat flux due to condensation of the vapor to the inner cylinder can be calculated by the following equation.

$$q''=k_l\frac{T_{sat}-T_w}{\delta} \tag{3.33}$$

After calculating heat flux the heat transfer coefficient for the condensation of the vapor flowing annularly between the cylinders can be obtained by the equation that defines the condensation heat transfer coefficient as given below.

$$q''=h(T_{sat}-T_w) \tag{3.34}$$

Substituting heat flux give by Equation 3.33 in Equation 3.34 the local heat transfer coefficient due to condensation can be obtained as.

$$h=\frac{k_l}{\delta} \tag{3.35}$$

CHAPTER 4

SOLUTION METHOD

As explained in the previous section the governing equations of the condensation of the vapor flowing annularly and in cross flow direction between two cylinders can be reduced to five differential equations that has five unknowns in them. These are the film thickness of the condensate layer, boundary thicknesses of the vapor layers, the velocity at the interface and the velocity in the core. The system of differential equations transformed into ordinary set of equations by using forward difference technique. The set of ordinary equations in terms of five unknowns expressed above are nonlinear. To solve these nonlinear set of equations an iterative numerical method called Newton-Raphson method is used.

In this method the equations are expressed in such a way that all the terms are on one side of the equality sign so that all the terms are taken to be equal to zero and one starts the solution by assuming a value for the unknown which makes the equation reasonably close to the true zero, then replaces the function by its tangent (which can be computed using the tools of calculus) and computes the zero of this tangent (which is easily done with elementary algebra). This zero of the tangent will typically be a better approximation to the function's zero, and the method can be iterated.

Suppose f: [a, b] → R is a differentiable function defined on the interval [a, b] with values in the real numbers **R**. We start with an arbitrary value x_0 (the closer to the zero the better) and then define for each natural number n in Equation 4.1:

$$x_{n+1} = x_n - \frac{f(x_n)}{f'(x_n)} \tag{4.1}$$

Here, f' denotes the derivative of function f.

Newton's method will usually converge provided the initial guess is close enough to the unknown zero. Furthermore, for a zero of multiplicity 1, the convergence is at last quadratic in a neighborhood of the zero, which intuitively means that the number of correct digits roughly at least doubles in every step.

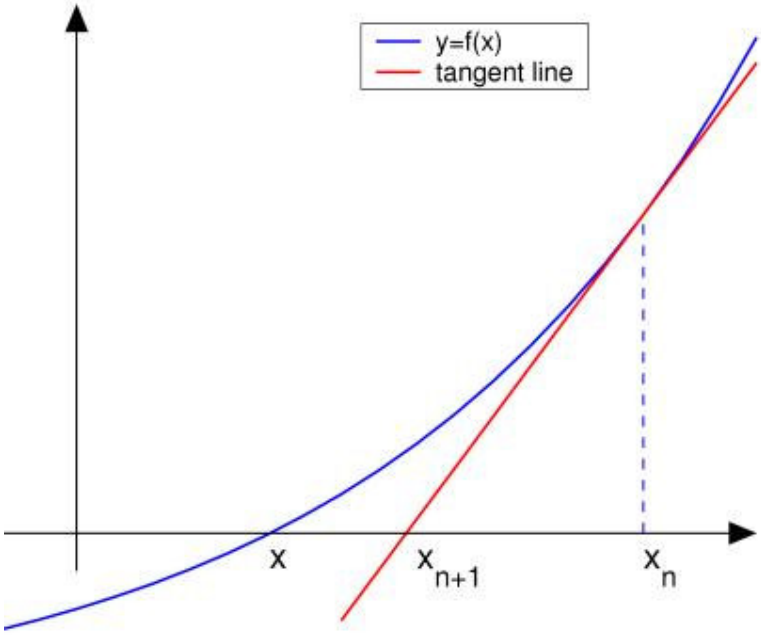

Figure 4.1 An Illustration of Newton's Method

Newton's method is used to solve systems of k (non-linear) equations, which amounts to finding the zeros of continuously differentiable functions F: $R^k \rightarrow R^k$. In the formulation one then has to multiply with the inverse of the k-by-k Jacobean matrix $J_F(x_n)$ instead of dividing by $f'(x_n)$ is shown in Equation 4.2.

$$J_F(x_n)(x_{n+1} - x_n) = -F(x_n) \tag{4.2}$$

Rather than actually computing the inverse of this matrix, one can save time by solving the system of linear equations for the unknown x_{n+1} - x_n. Again, this method only works if the initial value x_0 is close enough to the true zero. Typically, a region which is well-behaved is located first with some other method and Newton's method is then used to "polish" a root which is already known approximately.

In order to apply the Newton Rhaphon method to the five ordinary nonlinear equations which were obtained before are expressed in the following forms.

Conservation of mass in the condensate layer:

$$\frac{\frac{U_{\text{int}\,i+1}\delta_{i+1}}{2}-\frac{U_{\text{int}\,i}\delta_i}{2}}{\Delta x}-\frac{k_l\Delta T}{\rho_l h_{fg}\delta_{i+1}}=0 \tag{4.3}$$

Conservation of momentum in the condensate layer:

$$\begin{aligned}&\frac{\frac{U_{\text{int}\,i+1}{}^2\delta_{i+1}}{3}-\frac{U\,\text{int}_i{}^2\,\delta_i}{3}}{\Delta x}-U_{\text{int}\,i+1}\frac{k_l\Delta T}{\rho_l h_{fg}\delta_{i+1}}-\frac{\rho_v}{\rho_l}\delta_{i+1}U_{\infty i+1}\frac{U_{\infty i+1}-U_{\infty i}}{\Delta x}+\\&+\frac{\mu_l}{\rho_l}\frac{U_{\text{int}\,i+1}}{\delta_{i+1}}-\frac{\mu_v}{\rho_l}\frac{U_{\infty i+1}-U_{\text{int}\,i+1}}{\Delta_{1_{i+1}}}=0\end{aligned} \tag{4.4}$$

Conservation of momentum in the vapor boundary layer of the inner cylinder:

$$\begin{aligned}&\frac{\frac{\Delta_{1_{i+1}}(U_{\text{int}\,i+1}+U_{\infty i+1})}{2}-\frac{\Delta_{1_i}(U_{\text{int}\,i}+U_{\infty i})}{2}}{\Delta x}+\frac{U_{\infty i+1}(d-\delta_{i+1}-\Delta_{1_{i+1}}-\Delta_{2_{i+1}})-U_{\infty i}(d-\delta_i-\Delta_{1_i}-\Delta_{2_i})}{\Delta x}+\\&+\frac{k_l\Delta T}{\rho_v h_{fg}\delta_{i+1}}+\frac{\frac{U_{\infty i+1}\Delta_{2_{i+1}}}{2}-\frac{U_{\infty i}\Delta_{2_i}}{2}}{\Delta x}=0\end{aligned} \tag{4.5}$$

Conservation of momentum in the core region:

$$\frac{U_{i+1}{}^2\left(d-\Delta_{1_{i+1}}-\Delta_{2_{i+1}}-\delta_{i+1}\right)-U_i{}^2\left(d-\Delta_{1_i}-\Delta_{2_i}-\delta_i\right)}{\Delta x}-$$
$$-U_{i+1}\left[\frac{U_{i+1}\left(d-\Delta_{1_{i+1}}-\Delta_{2_{i+1}}-\delta_{i+1}\right)-U_i\left(d-\Delta_{1_i}-\Delta_{2_i}-\delta_i\right)}{\Delta x}\right]- \tag{4.6}$$
$$-\left(d-\Delta_{1_{i+1}}-\Delta_{2_{i+1}}-\delta_{i+1}\right)U_{i+1}\frac{U_{i+1}-U_i}{\Delta x}=0$$

Conservation of momentum in the vapor boundary layer of the outer cylinder:

$$\frac{\frac{U_{\infty i+1}{}^2\Delta_{2_{i+1}}}{3}-\frac{U_{\infty i}{}^2\Delta_{2_i}}{3}}{\Delta x}-U_{\infty i+1}\frac{\frac{U_{\infty i+1}\Delta_{2_{i+1}}}{2}-\frac{U_{\infty i}\Delta_{2i}}{2}}{\Delta x}-\Delta_{2_{i+1}}U_{\infty i+1}\frac{U_{\infty i+1}-U_{\infty i}}{\Delta x}+\frac{\mu_v}{\rho_v}\frac{U_{\infty i+1}}{\Delta_{2_{i+1}}} \tag{4.7}$$

A computer code in MATLAB is prepared to solve the nonlinear set of equations. Fsolve command in MATLAB solves systems of nonlinear equations of several variables using Newton-Raphson method with large optimization parameters. Trust-Region Dogleg Method is one of these optimization methods. The program written in MATLAB solves the equations for unknowns by the help of this optimization method. The program code is given at Appendix A and B. In the program unknowns are determined from stagnation point at the top to bottom of the cylinder. The solution is obtained by solving the five equations along the surface of the inner cylinder which is divided into 180 equal differences. The program solves five nonlinear equations at each angular position on the surface of the inner cylinder. The results obtained from the previous angular location are used to solve the set of nonlinear equations obtained for the next angular position and he solution continues in this manner till the bottom of the cylinder which is represented by the 180^{th} point.

CHAPTER 5

RESULTS AND DISCUSSIONS

In previous chapters the physical problem and the governing equations derived from the basic principles were explained. In this chapter with the help the computer code written in MATLAB the governing equations expressed in finite difference form which are obtained in Chapter 3 are solved and the film thickness, vapor boundary layer thickness, the velocity at the interface of liquid-vapor state, heat flux and local heat transfer coefficient were obtained. Results of the calculations are expressed in the form of graphs.

Moreover, the effect of the free stream velocity in the core, the radius of the inner cylinder, the temperature difference between the saturated vapor and the wall and the annular space between the concentric cylinders on the condensation process is studied.

The water is taken as the working fluid and the thermal properties of the vapor and the condensate is given as input. To obtain the results the free stream velocity was changed from 5 m/s to 40 m/s at an interval of 5 m/s. The radius of the inner cylinder and annular space between the inner and outer cylinder were fixed at 0.05 m and 0.005 m, respectively. Temperature of the saturated water vapor and the wall temperature were chosen as 373.15 K and 365 K, respectively. Fluid properties of the liquid and vapor phases, which are the density, enthalpy of phase change, thermal conductivity and dynamic viscosity, were chosen at these temperatures and are given below.

ρ_l = 963 [kg/m^3]

ρ_v = 0.596 [kg/m^3]

k_l = 0.677 [W/(m.K)]

μ_l = 0.306 x 10^{-3} [Pa.s]

μ_v = 0.12 x 10^{-4} [Pa.s]

h_{fg} = 2257 x 10^{3} [J/kg]

By using the output that are obtained by solving the governing equations with the help of the computer code developed in this study for each angular position on the cylinder, the heat flux and the local heat transfer coefficient are calculated with the help of the Equations 3.33 and 3.35.

The results of the calculations of film thickness for the free stream velocities (5, 10, 15, 20, 25, 30, 35 and 40 m/s) of the vapor in the core are shown in Figure 5.1. As seen in the Figure 5.1, the results show that the film thickness of the condensate layer increases with increasing angular position since along the angular direction more and more vapor condenses on the inner cylinder. It is also observed that the film thickness of the condensate layer decreases by increasing the free stream velocity of the vapor in the core since the boundary layer thickness is inversely proportional to Reynolds number. Reynolds number of the free stream increases as the velocity of the free stream of the vapor increases which results in decrease in the film thickness.

In addition to this, the shear stress at the interface between the condensate layer and the vapor boundary layer of the inner cylinder is increased by increasing the free stream velocity of the vapor in the core. This results in the dragging the condensate layer by the boundary layer of the vapor of the inner cylinder. Therefore, the film thickness of the condensate layer decreases by increasing the free stream velocity. The film thickness of the condensate at free stream velocity of 5 m/s is nearly three times larger than the film thickness at 40 m/s free stream velocity.

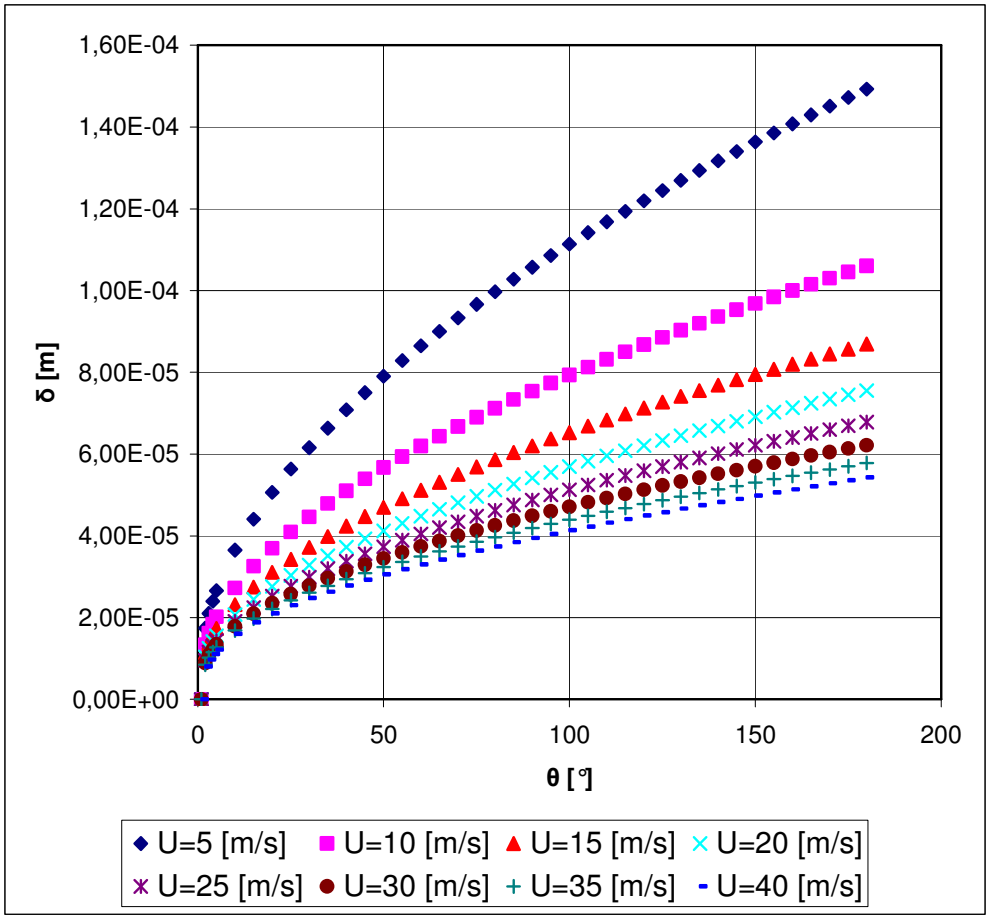

Figure 5.1 Variation of the Condensate Film Thickness with the Angular Position

In Figures 5.2 and 5.3, it is seen that by increasing angular position the boundary layer thicknesses of the vapor increase because of the mass transfer from the potential flow in the core to the boundary layers. The effect of the increasing velocity of the free stream of vapor in the core can be seen on the boundary layer thicknesses of the vapor in Figures 5.2 and 5.3. By increasing the free stream velocity of vapor in the core, the boundary layer thicknesses of the vapor also decrease just like the film thickness of the condensate layer decreases with an increase of the free stream velocity. It is observed in Figures 5.2 and 5.3 that the boundary layer thickness of the vapor on the outer cylinder is greater than the one on the inner cylinder. This is an expected result since there is a mass transfer from the vapor boundary layer of the

inner cylinder to the condensate layer because of the condensation. Therefore, the boundary layer thickness of the vapor on the outer cylinder is greater than the one on the inner cylinder at a given location. The difference of thicknesses between the boundary layers of the outer and inner cylinders (Δ_d) is calculated and the result is presented in Figure 5.4.

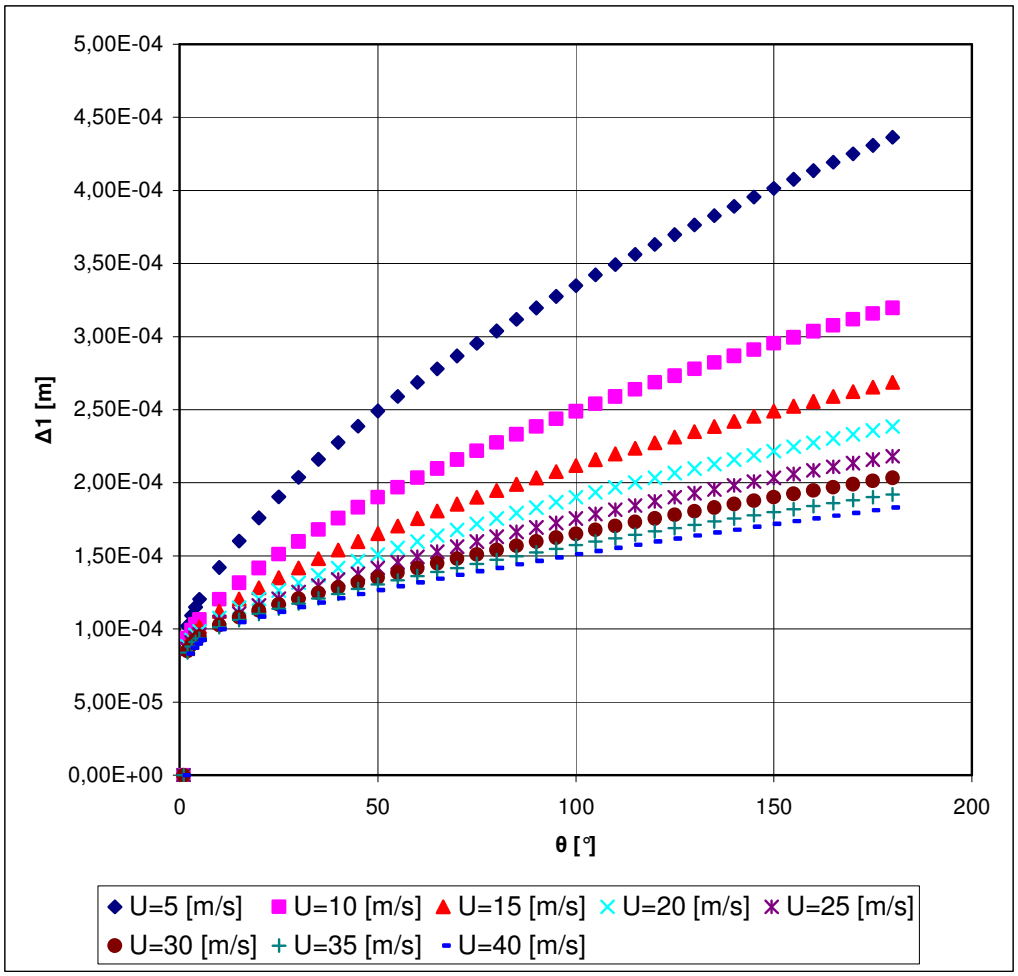

Figure 5.2 Variation of the Vapor Boundary Layer Thickness of Inner Cylinder with the Angular Position

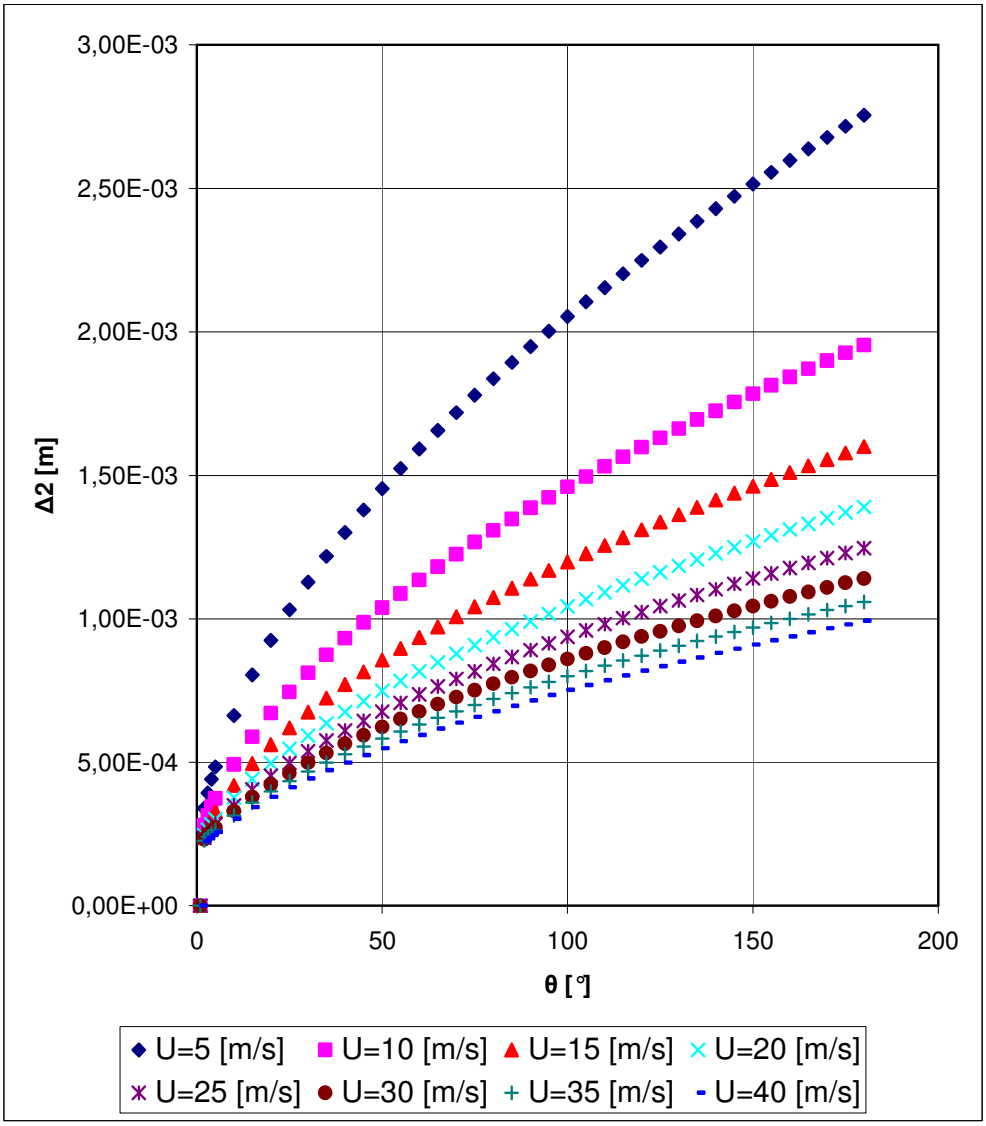

Figure 5.3 Variation of the Vapor Boundary Layer Thickness of the Outer Cylinder with the Angular Position

From the Figure 5.4, it can be seen that the difference between the boundary layer thicknesses of the outer and inner cylinders is decreased at larger free stream velocities of the vapor since at large free stream velocities the effect of the change of the free stream velocity on the boundary layer thickness is comparatively small.

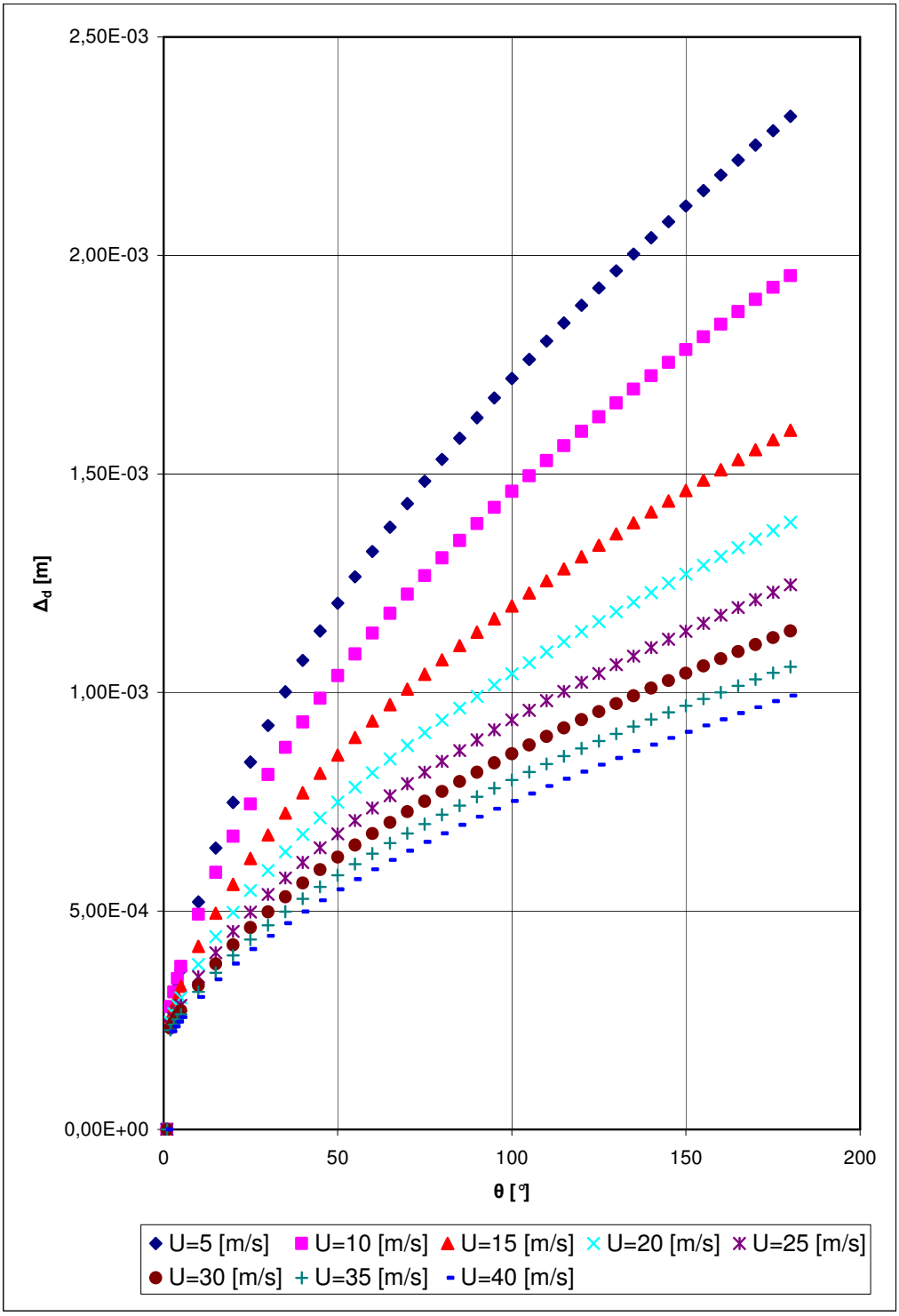

Figure 5.4 Variation of the Difference of the Vapor Boundary Layer Thicknesses of Two Cylinders with the Angular Position

As explained in Chapter 3, the heat flux and the local heat transfer coefficient are calculated by using of the film thickness of the condensate by using the Equations 3.33 and 3.35. In Figure 5.5, the variation of heat flux with the angular position was shown. The heat flux decreases with increasing angular position in accordance with the film thickness of the condensate since the heat flux is inversely proportional to the film thickness as can be seen in Equation 3.33. Heat flux increases by increasing the free stream velocity of the vapor in the core also for the same reason. Since increasing the free stream velocity, decreases the film thickness.

In Figure 5.6, the variation of local heat transfer coefficient with the angular position is shown. As it is in the heat flux variation, because of the inverse proportionality between the local heat transfer coefficient and the film thickness, the local heat transfer coefficient decreases with the angular position because of the increasing film thickness. The local heat transfer coefficient, on the other hand, increases with the free stream velocity of the vapor in the core because of increasing the film thickness.

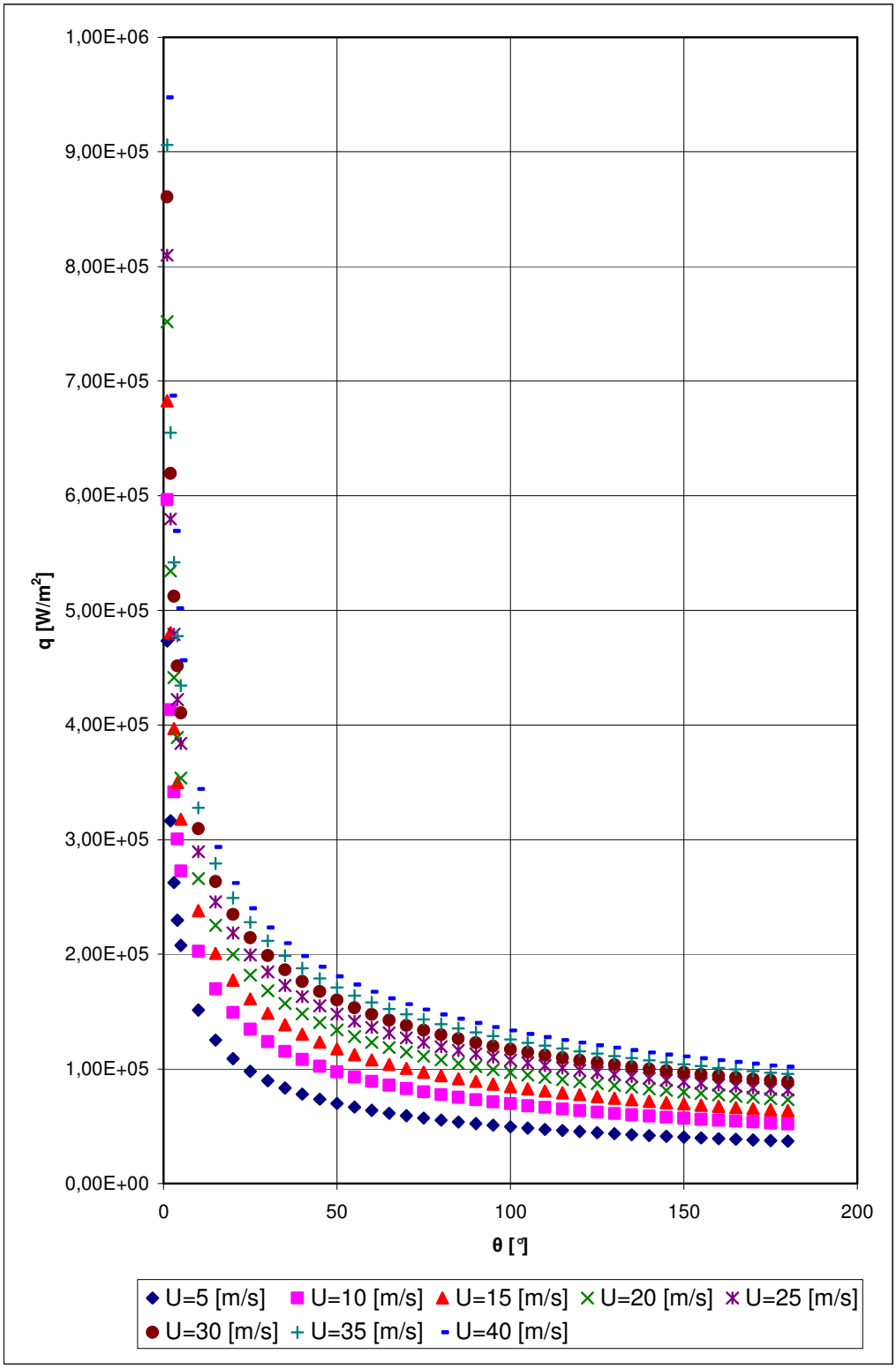

Figure 5.5 Variation of the Heat Flux with the Angular Position

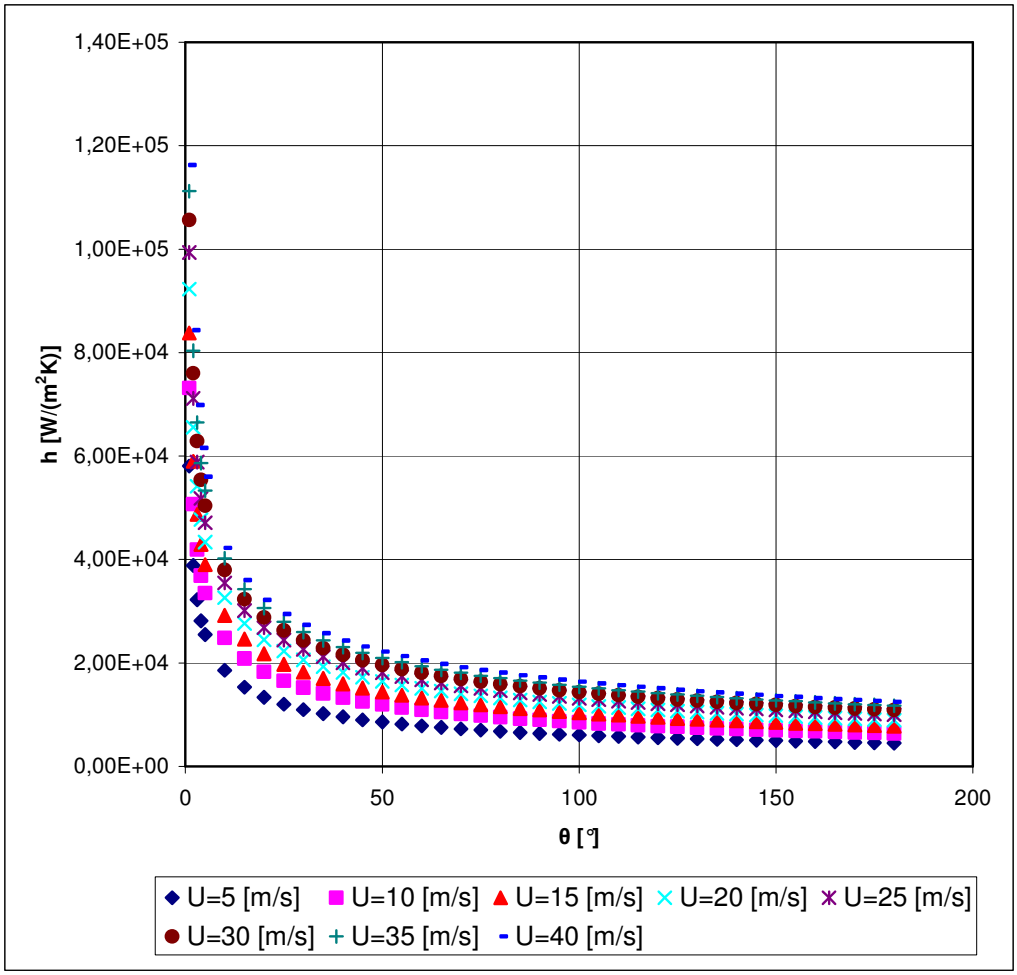

Figure 5.6 Variation of the Local Heat Transfer Coefficient with the Angular Position

In Figure 5.7, variation of the velocity at the interface with the angular position was shown. It can be seen in this figure that the velocity at the interface between the condensate and vapor layer of the inner cylinder increases by increasing the free stream velocity of the vapor in the core. The velocity at the interface is almost directly proportional with the free stream velocity in the core. Moreover, the interface velocity increases with angular position.

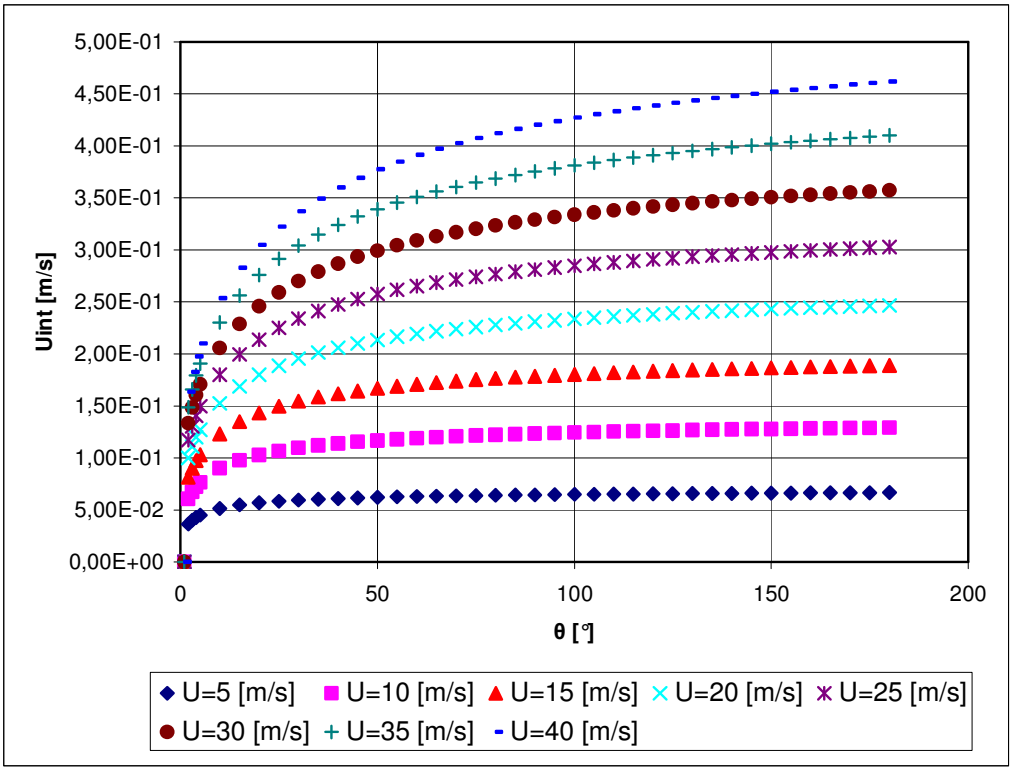

Figure 5.7 Variation of the Velocity at the Interface with the Angular Position

5.1. The Effect of Changing Radius of the Inner Cylinder on Condensation Heat Transfer

Variations of the film thickness, the boundary layer thicknesses of the vapor, the difference between two boundary layers, the heat flux, the local heat transfer coefficient and the velocity at the interface with angular position were shown in previous figures. This graphs were obtained for the radius of inner cylinder as 0.05 m as mentioned in Chapter 4. In the following figures the effect of changing radius of the inner cylinder were studied by changing the inner cylinder radius from 0.035 to 0.07 m at intervals of 0.005 m.

In Figures 5.8 and 5.9, the variations of the condensate film thickness with angular position at 5 m/s and 40 m/s by changing the radius of the inner cylinder are shown. As it is understood from the figures for the same angular position with an increase of the radius of the inner cylinder the condensate film thickness increases. This result can be explained by the reasoning that as the radius of the inner cylinder is the distance that the condensate travels, increases and the longer the distance that the condensate travels thicker the condensate film thickness becomes.

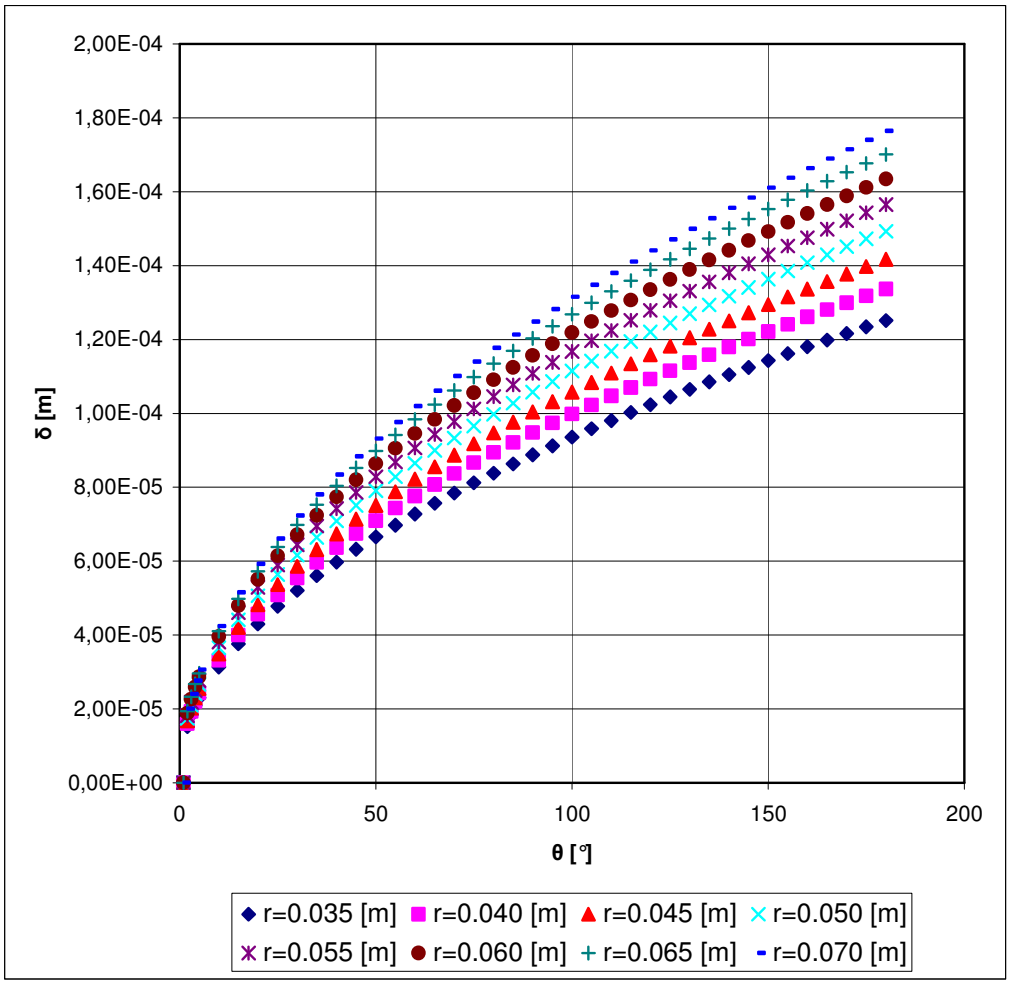

Figure 5.8 Variation of the Condensate Film Thickness with the Angular Position at Different Radiuses of the Inner Cylinder for U= 5 m/s

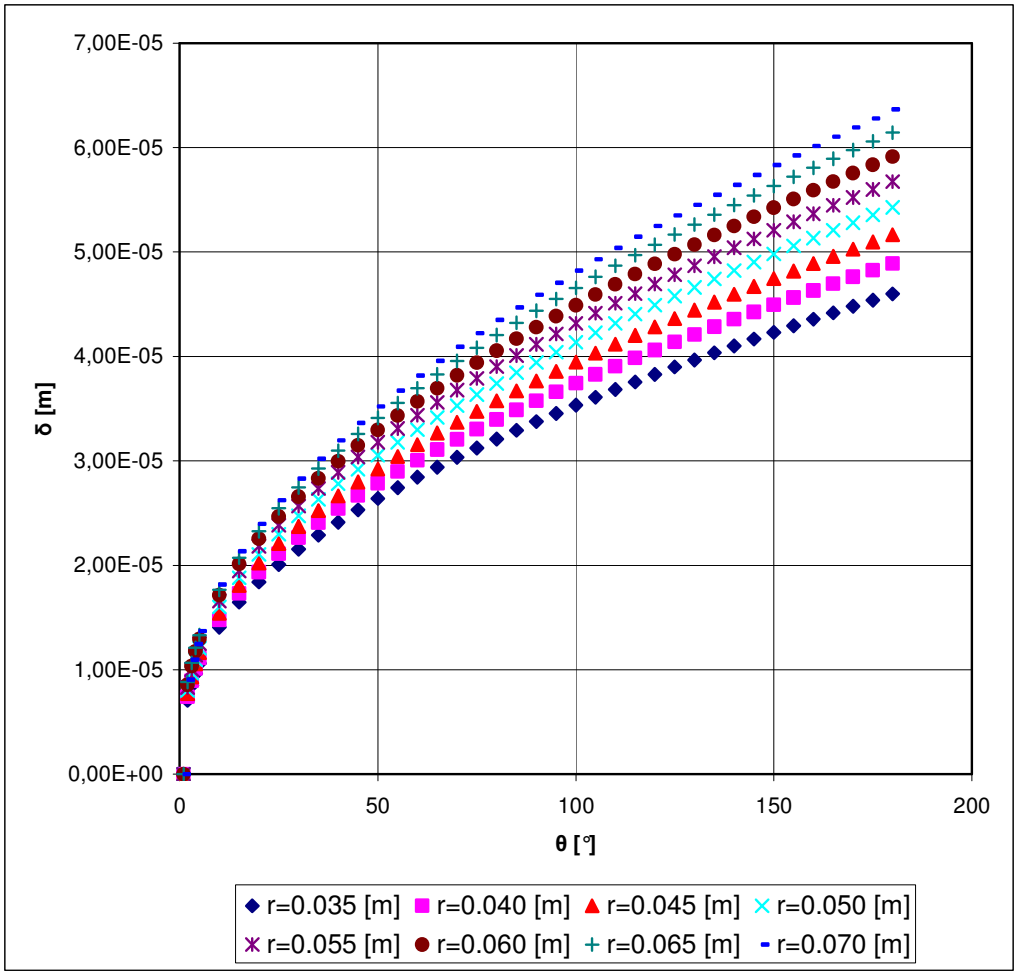

Figure 5.9 Variation of the Condensate Film Thickness with the Angular Position at Different Radiuses of the Inner Cylinder for U= 40 m/s

The effect of changing the radius of the inner cylinder on the boundary layer thicknesses of the vapor can be seen in Figures 5.10 and 5.11 for free stream velocity of 5 m/s and in Figures 5.12 and 5.13 for free stream velocity of 40 m/s. It is observed in these figures that by increasing the radius of the inner cylinder, boundary layer thicknesses of the vapor increases also. In addition to this, for the free stream velocity of 5 m/s of the vapor in the core at increment of the boundary layer thicknesses are greater compared to the free stream velocity of 40 m/s.

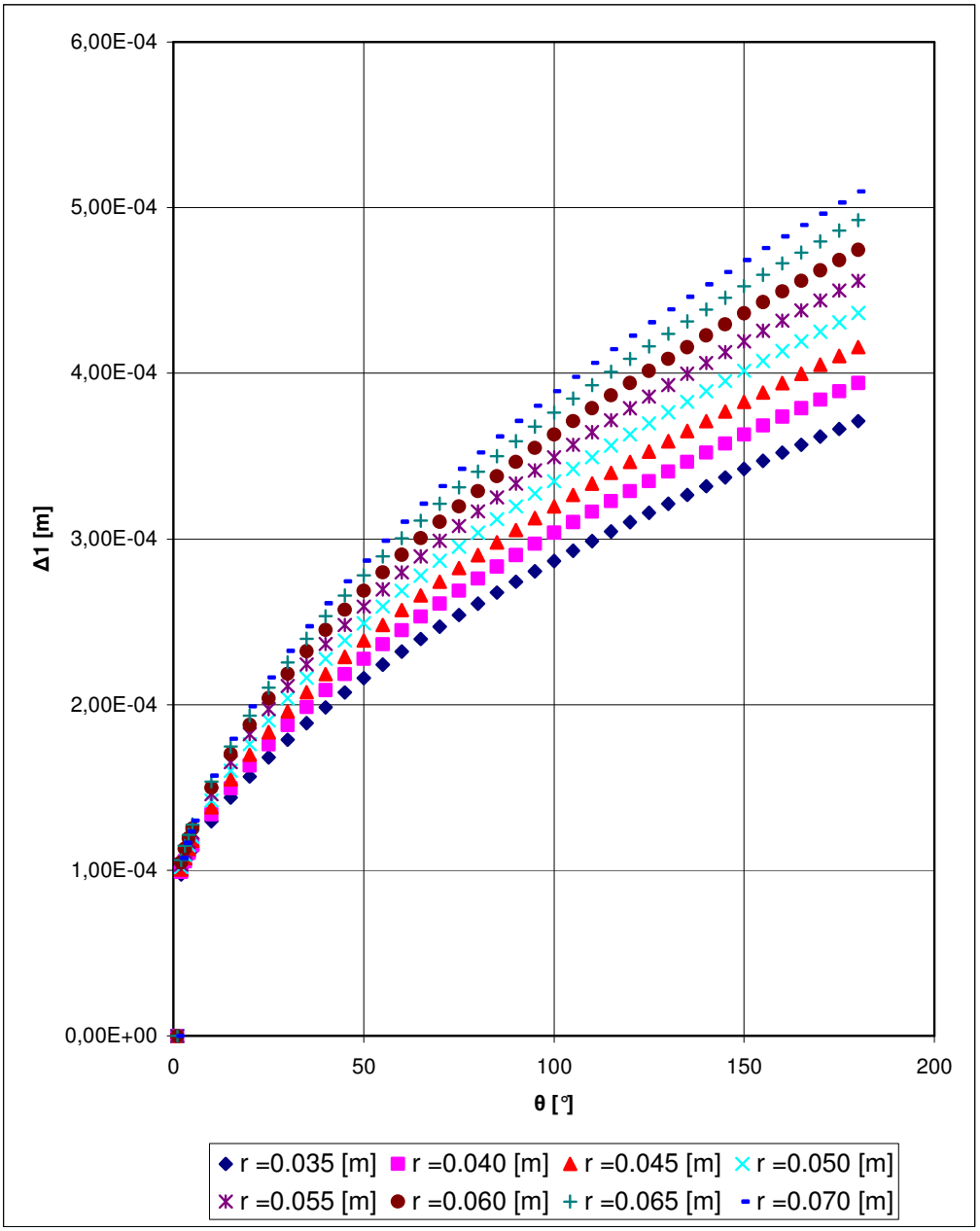

Figure 5.10 Variation of the Vapor Boundary Layer Thickness of the Inner Cylinder with the Angular Position at Different Radiuses of the Inner Cylinder for U= 5 m/s

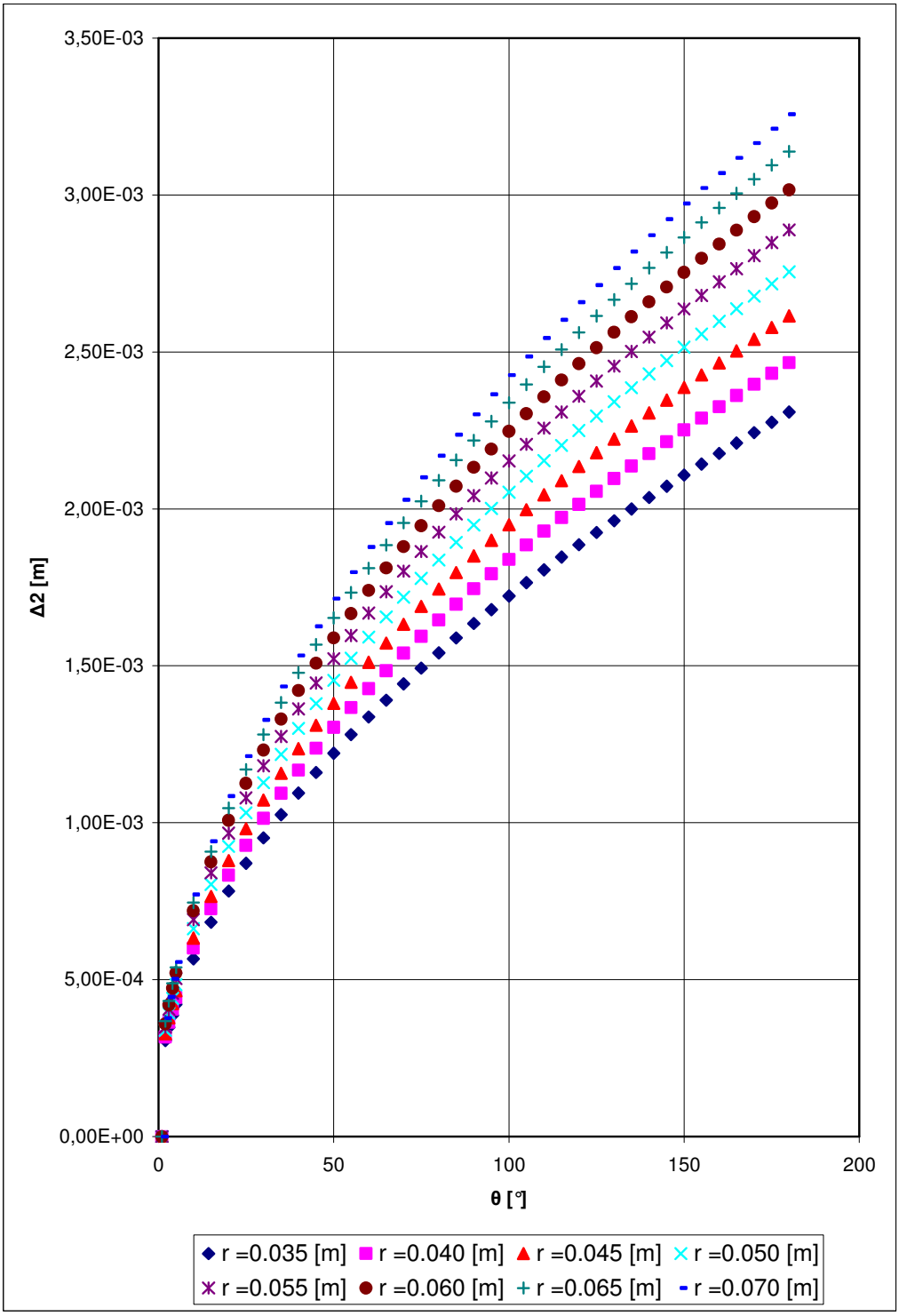

Figure 5.11 Variation of the Vapor Boundary Layer Thickness of the Outer Cylinder with the Angular Position at Different Radiuses of the Inner Cylinder for U= 5 m/s

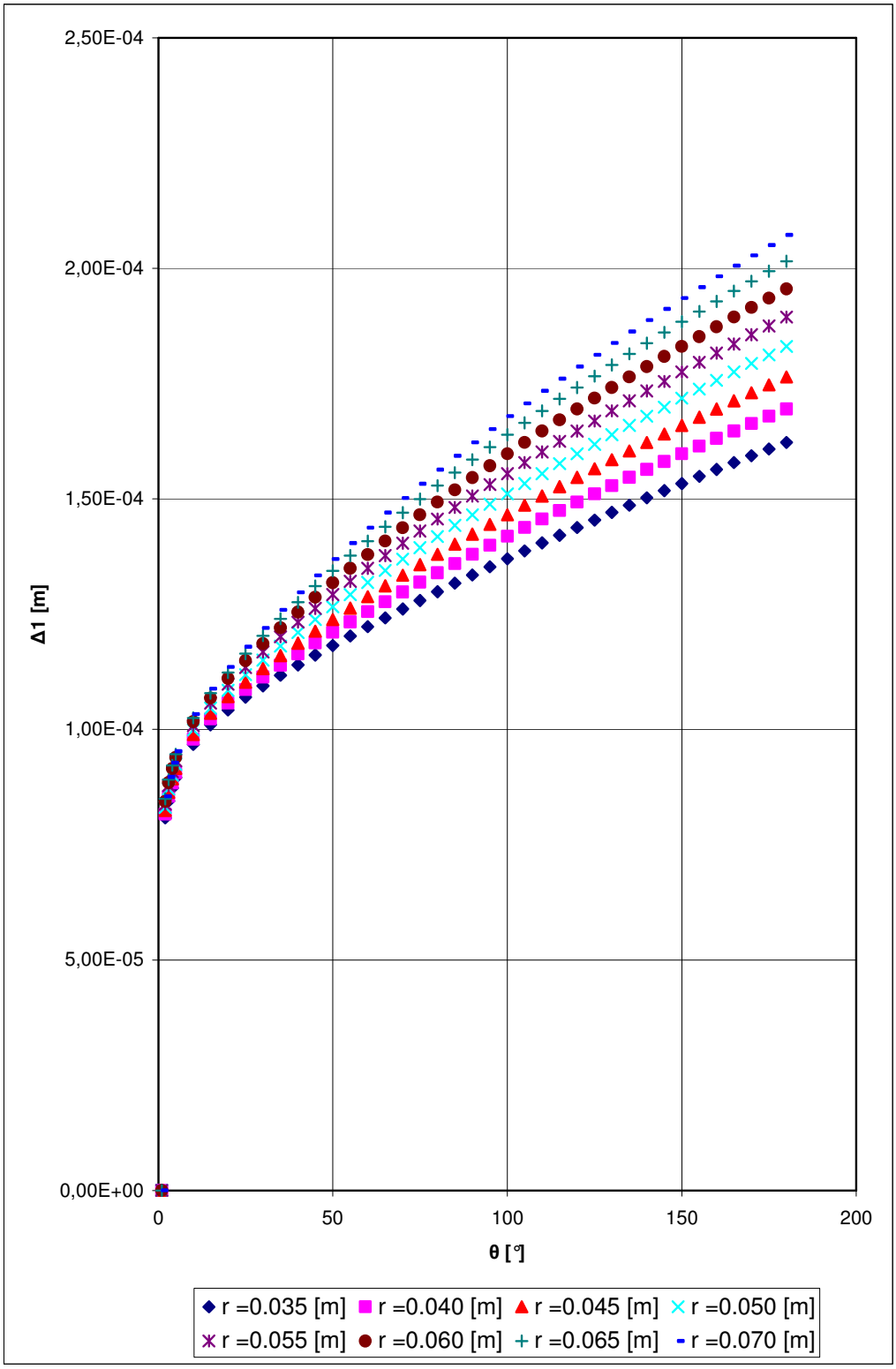

Figure 5.12 Variation of the Vapor Boundary Layer Thickness of the Inner Cylinder with the Angular Position at Different Radiuses of the Inner Cylinder for U= 40 m/s

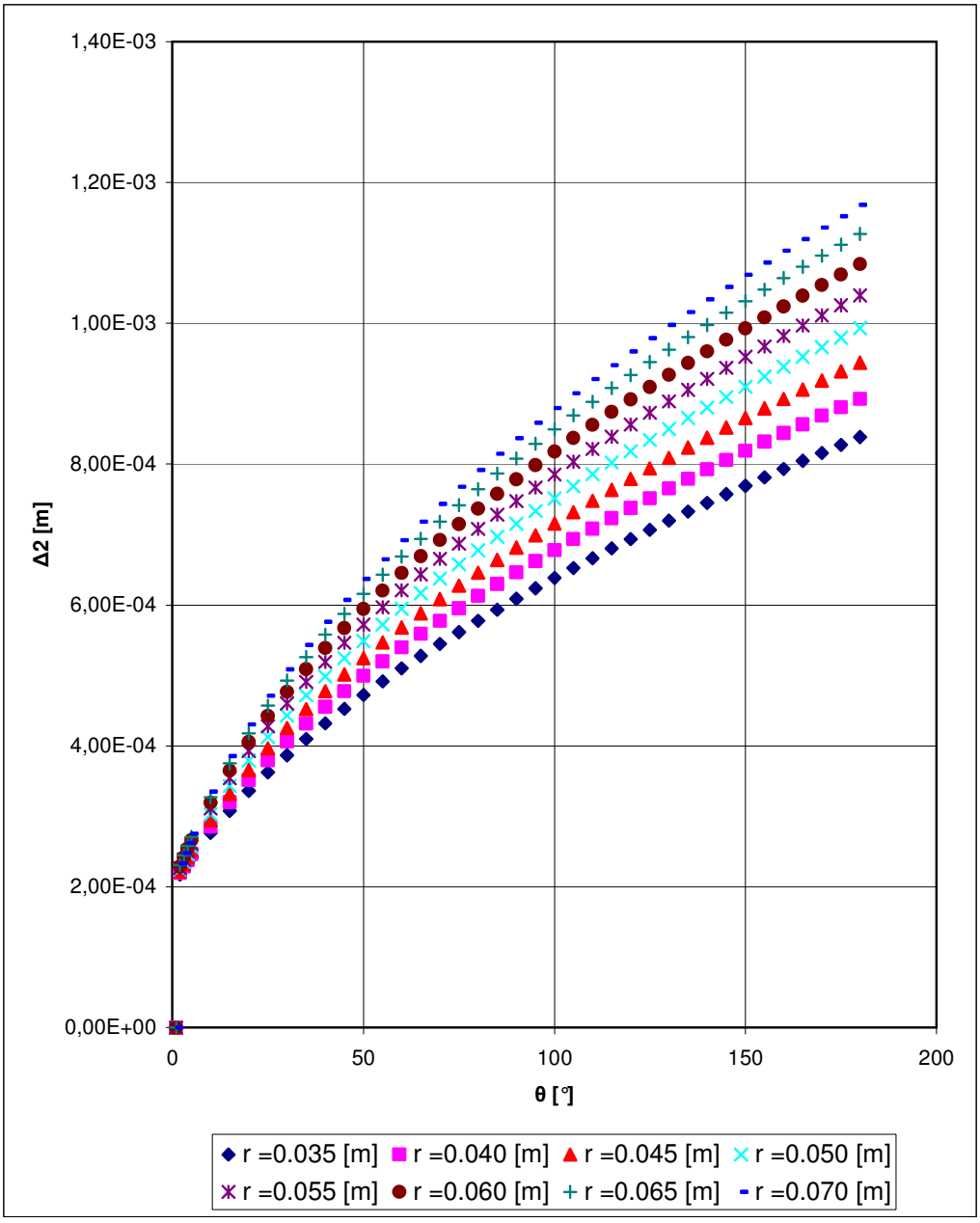

Figure 5.13 Variation of the Vapor Boundary Layer Thickness of the Outer Cylinder with the Angular Position at Different Radiuses of the Inner Cylinder for U= 40 m/s

Effect of changing the radius of the inner cylinder on heat flux was shown in Figures 5.14 and 5.15 for free stream velocities of 5 and 40 m/s of the vapor in the

core respectively. In Figure 5.5, the heat was increased by increasing the free stream velocity of the vapor in the core.

In Figure 5.14, for free stream of the velocity of the vapor at 5 m/s, the heat flux decreases by increasing the radius of the inner cylinder. This is expected because, as seen in Figures 5.8 and 5.9, by increasing the free stream velocity, the film thickness also increases. Moreover, in Figure 5.15, the effect of changing the radius of the inner cylinder on the heat flux is similar to the one which is observed in Figure 5.14. in which the heat flux decreases by increasing the radius of inner cylinder.

In Figures 5.16 and 5.17, for the free stream velocity of the vapor at the effect of changing the radius of the inner cylinder on local heat transfer coefficient was shown. As it was occurred for the heat flux, local heat transfer coefficient decreases by increasing the radius of the inner because of the inversely proportionality between the local heat transfer coefficient and the film thickness as seen in Equation 3.35 again.

As it was seen in Figure 5.14, 5.15, 5.16 and 5.17, the difference between the values of the heat flux for each radius of the inner cylinder at 40 m/s free stream velocity of the vapor in the core is greater than the situation at 5 m/s. Moreover, it can be also said for the local heat transfer coefficient. Therefore, it can be stated that by increasing the velocity of the vapor in the core, the effect of the changing radius of the inner cylinder on the heat flux and local heat transfer coefficient of the vapor increases. Although it was understood from Figures 5.14, 5.15, 5.16 and 5.17 that there is an effect of changing radius of the inner cylinder on the heat flux and the local heat transfer coefficient both, this effect can be neglected.

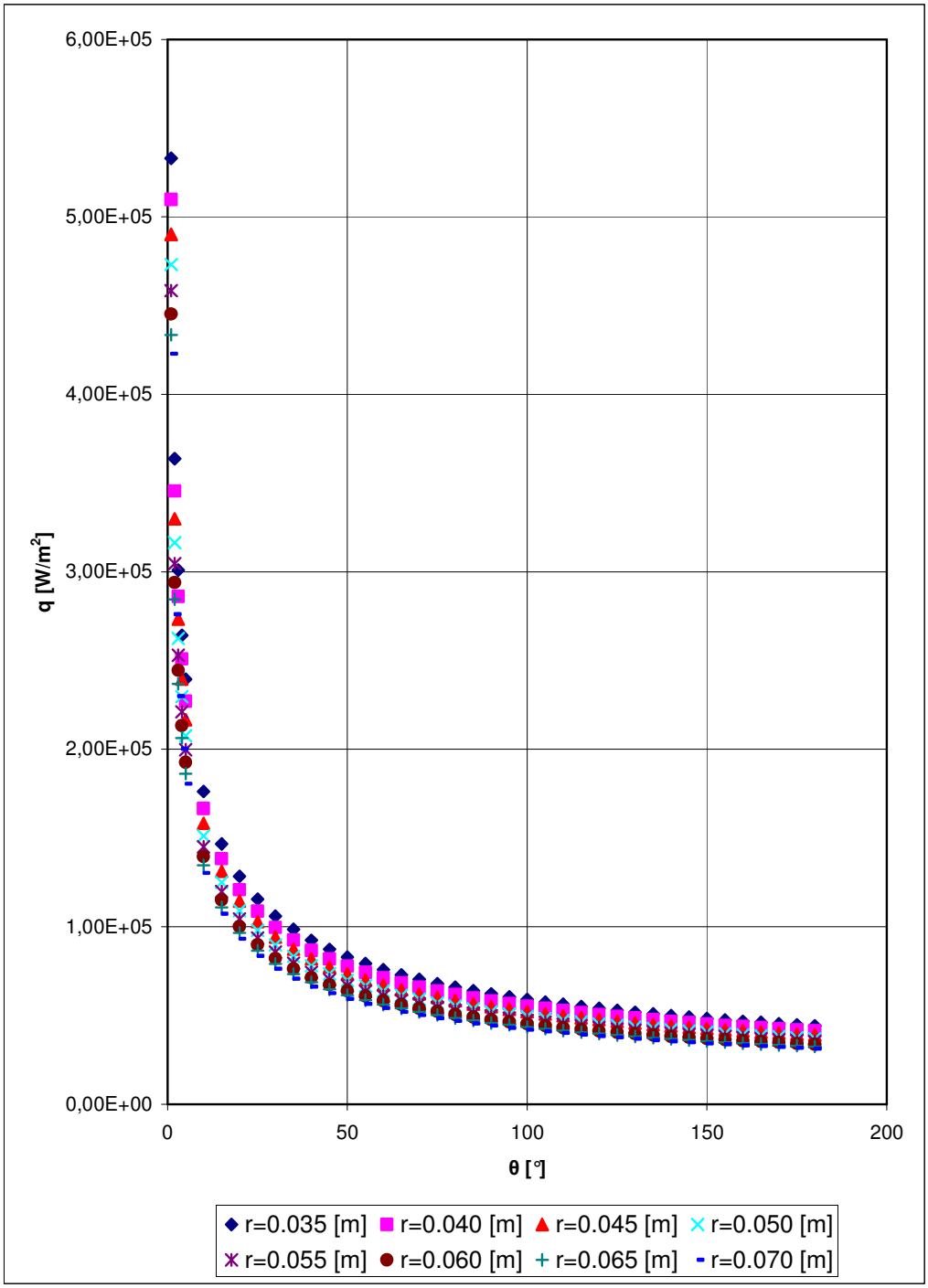

Figure 5.14 Variation of the Heat Flux with the Angular Position at Different Radiuses of the Inner Cylinder for U= 5 m/s

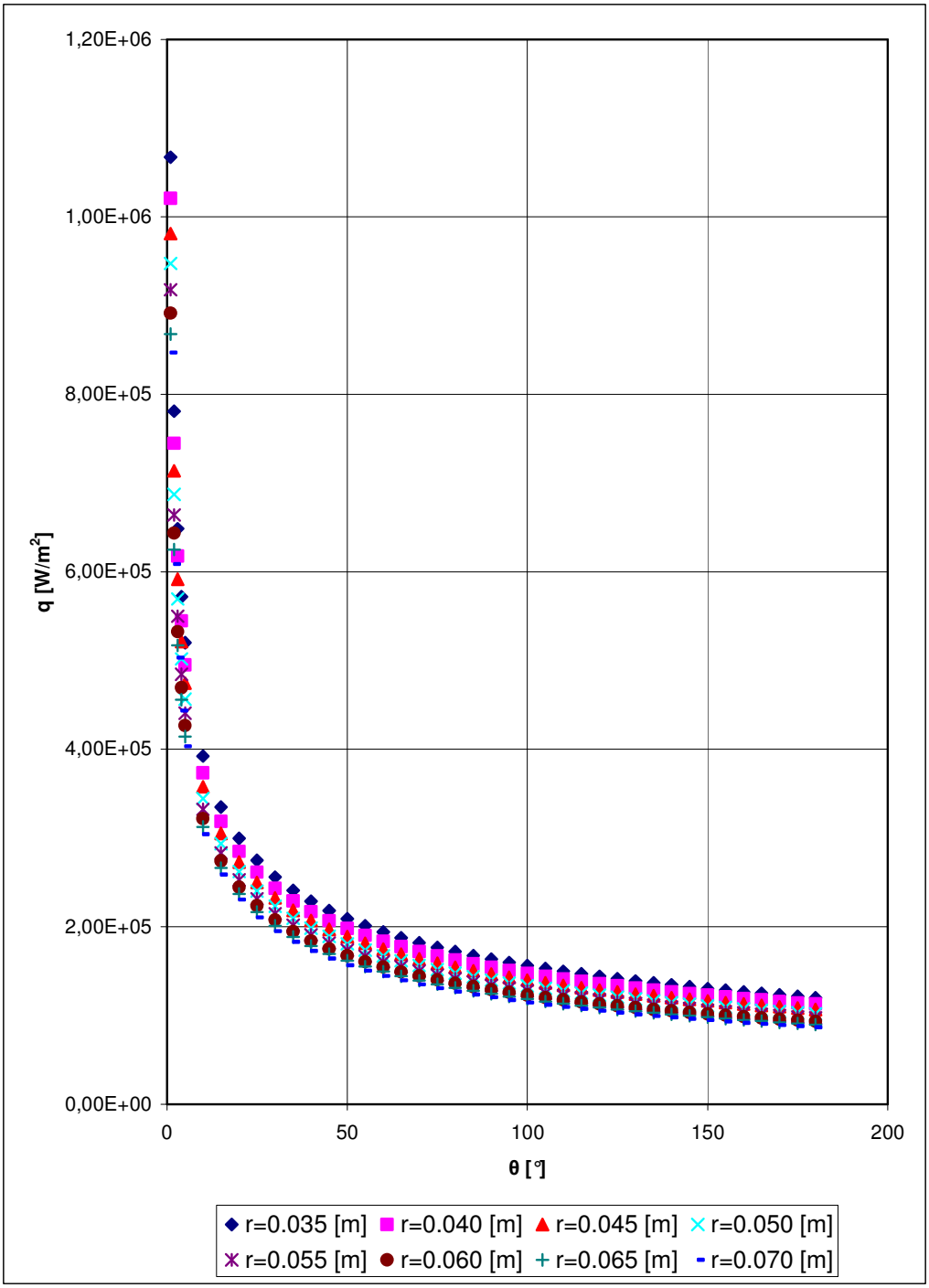

Figure 5.15 Variation of the Heat Flux with the Angular Position at Different Radiuses of the Inner Cylinder for U= 40 m/s

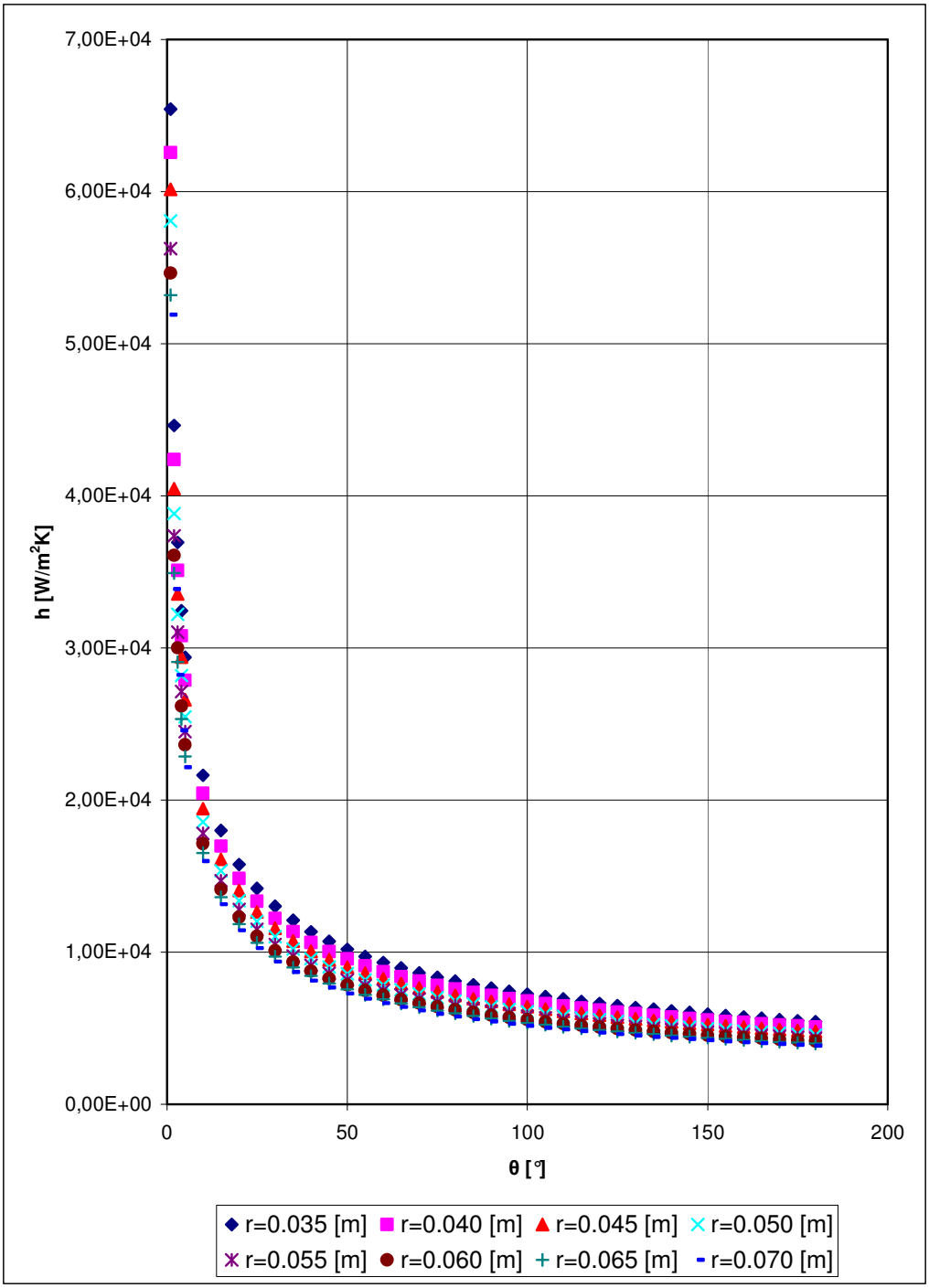

Figure 5.16 Variation of the Local Heat Transfer Coefficient with the Angular Position at Different Radiuses of the Inner Cylinder for U= 5 m/s

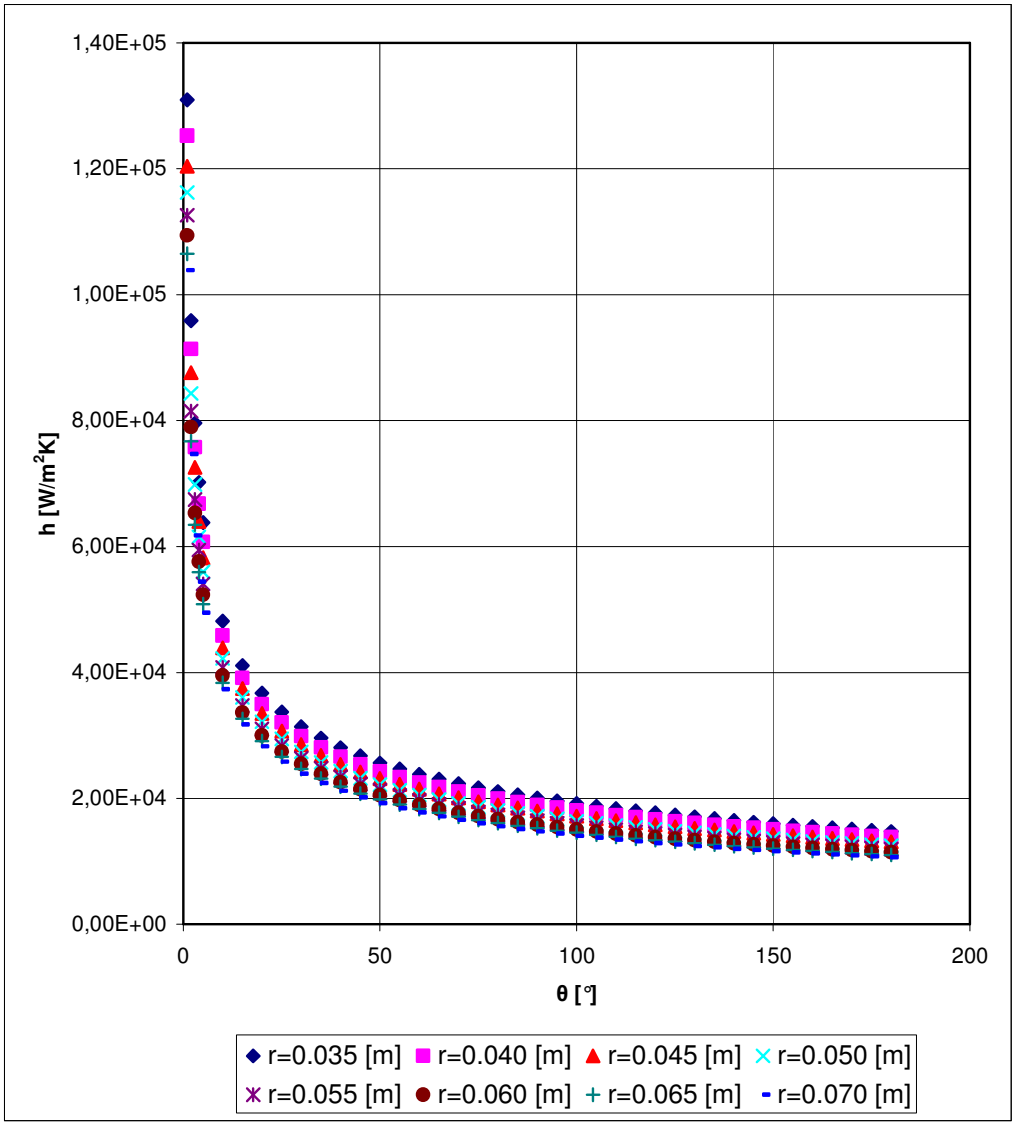

Figure 5.17 Variation of the Local Heat Transfer Coefficient with the Angular Position at Different Radiuses of the Inner Cylinder for U= 40 m/s

After obtained the graphs for the heat flux and the local heat transfer coefficient, the effect of changing the radius of the inner cylinder on the velocity at the interface was investigated in Figures 5.18 and 5.19. According to the Figures 5.18 and 5.19, it can be stated that the velocity at the interface increases by increasing the radius of the inner cylinder. In addition to this the effect of increasing the radius of the inner cylinder on the velocity at the interface for the free stream velocity for the vapor in

the core at 40 m/s is greater than the situation at 5 m/s. According to Figures 5.18 and 5.19, although there is the effect of changing radius of the inner cylinder on the velocity at the interface between the condensate and vapor layer, this effect can be neglected.

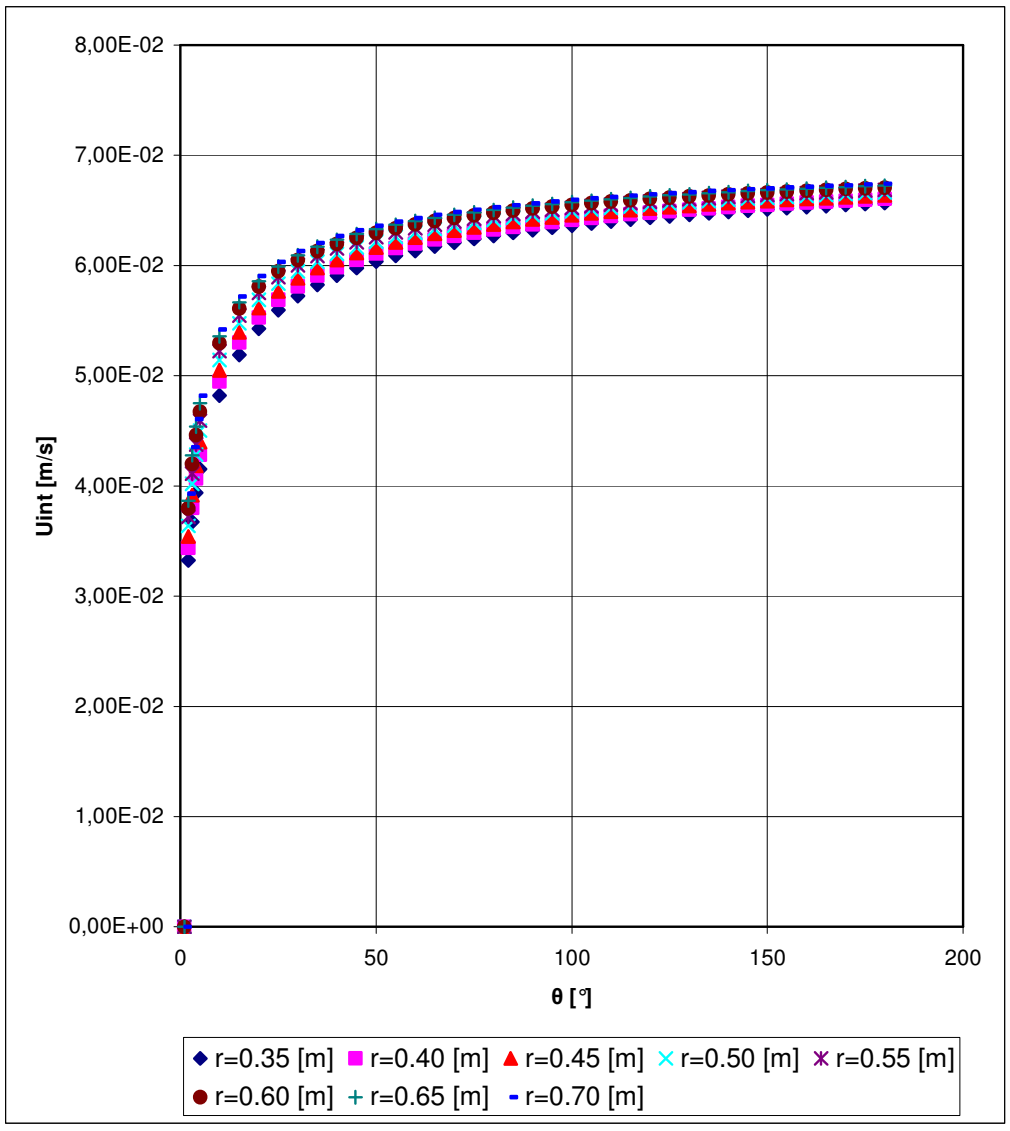

Figure 5.18 Variation of the Velocity at the Interface with the Angular Position at Different Radiuses of the Inner Cylinder for U= 5 m/s

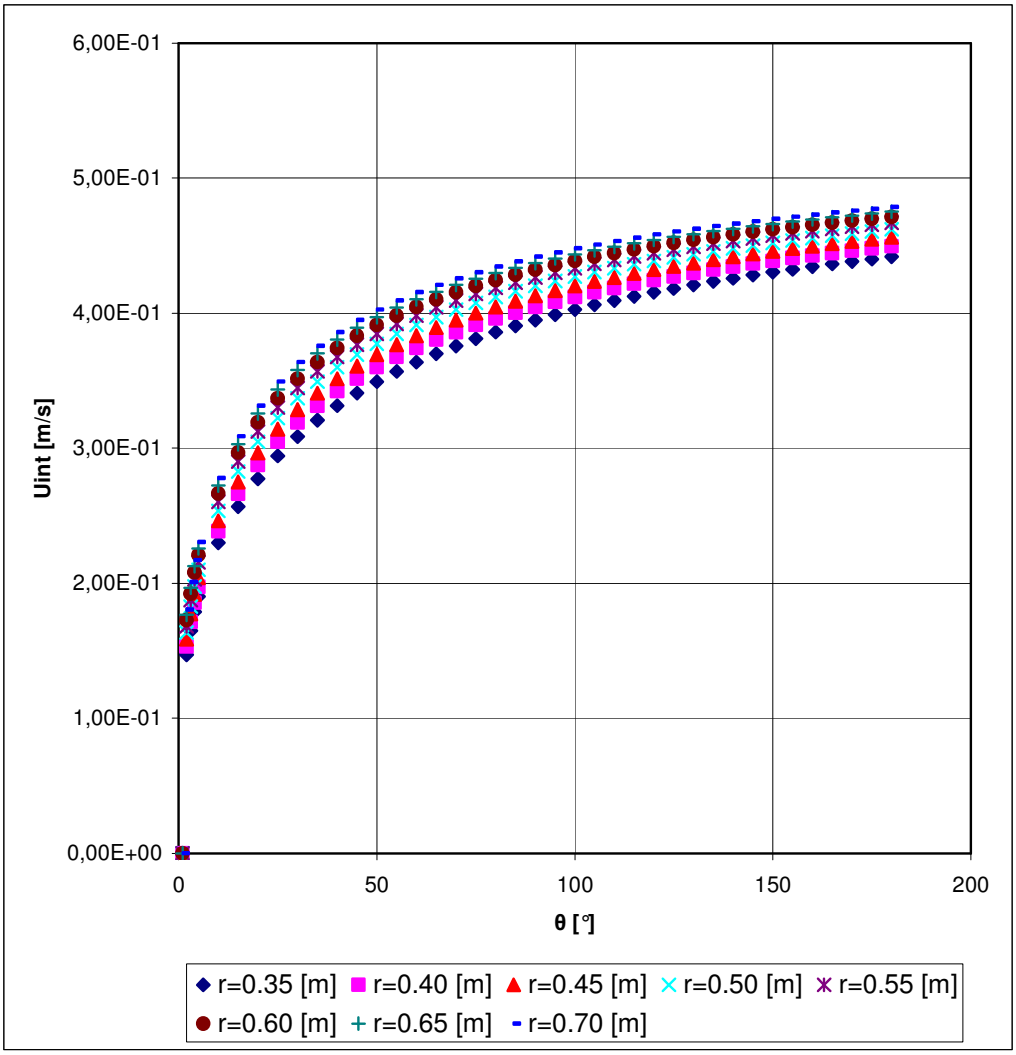

Figure 5.19 Variation of the Velocity at the Interface with the Angular Position at Different Radiuses of the Inner Cylinder for U = 40 m/s

5.2. The Effect of Changing the Temperature Difference Between the Saturated Vapor and the Wall on Condensation Heat Transfer

In the problem, the temperature of the wall was chosen 365 K so the temperature difference between the saturated vapor and the wall was being 8.15 K. In this section the effect of changing temperature difference between the saturated vapor and the

wall on the film thickness of the condensate, the boundary layer thicknesses of the vapor, the heat flux, the local heat transfer coefficient and the velocity at the interface was investigated. By changing the temperature difference, the radius of the inner cylinder was chosen as 0.05 m and the analysis was made for the velocity of the vapor in the core at 5 m/s and 40 m/s. The changed temperature differences are 18.15, 13.15, 8.15 and 3.15 K, respectively.

Firstly the effect of changing the temperature difference between the saturated vapor and the wall on the film thickness of the condensate was investigated in Figures 5.20 and 5.21. According to the graphs, it can be stated that the by increasing the difference between the saturated vapor and the wall caused to increase the film thickness of the condensate also. In other words the effect of changing the temperature difference is directly proportional to the film thickness of the condensate. Because with increasing the temperature difference, the condensate flow increases so the film thickness increases well. And also from the figures, it was understood that the effect of changing the temperature difference on the film the thickness of the condensate for the velocity of the vapor in the core at 5 m/s is greater than the situation at 40 m/s.

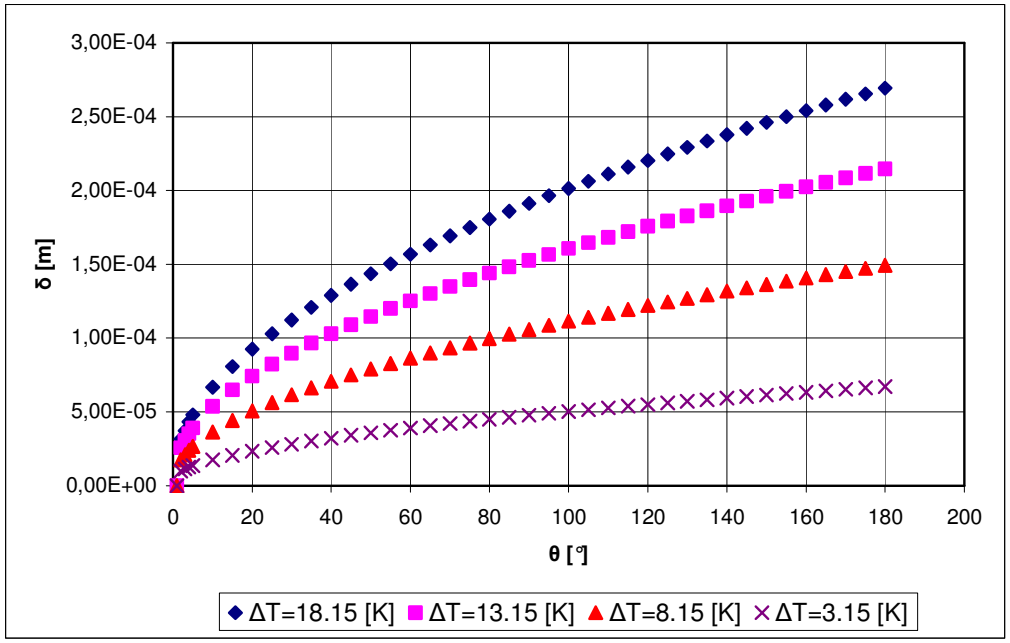

Figure 5.20 Variation of the Condensate Film Thickness with the Angular Position for U = 5 m/s at Different Temperature Differences

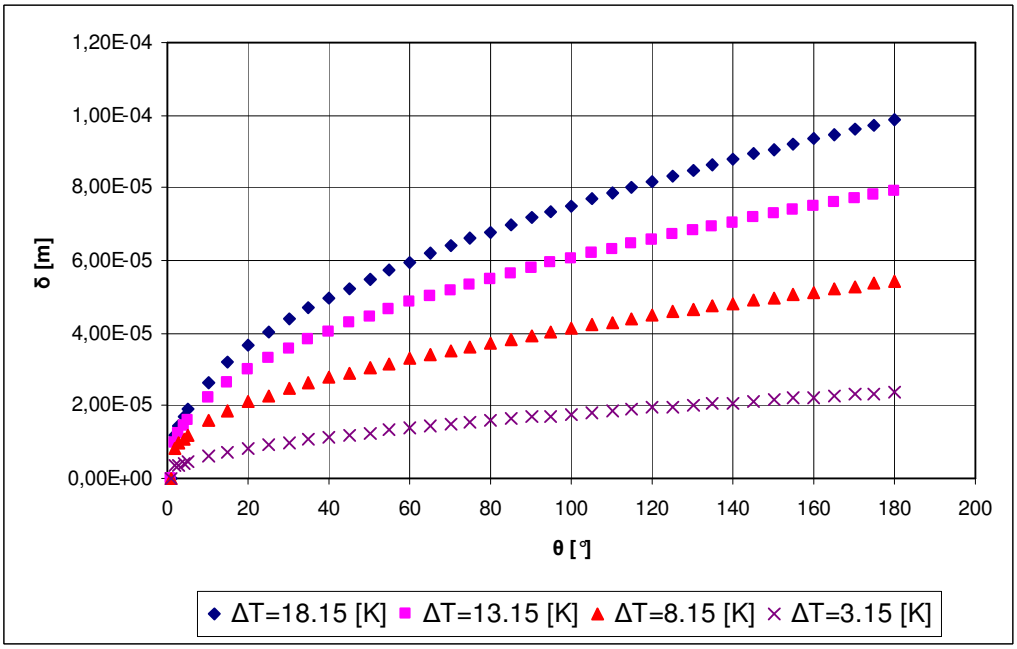

Figure 5.21 Variation of the Condensate Film Thickness with the Angular Position for U = 40 m/s at Different Temperature Differences

The effect of changing the temperature difference between the saturated vapor and the wall on the boundary layer thicknesses of the vapor was investigated in Figures 5.22, 5.23, 5.24 and 5.25 for the velocity of the vapor in the core at 5 m/s and 40 m/s respectively. According to the Figures 5.22 and 5.23, the effect of increasing the temperature difference between the saturated vapor and the wall causes to increase the boundary layer thickness of the vapor of the inner cylinder. When decreasing the temperature difference, the effectiveness of this difference increases on the boundary layer thickness. In other words small temperature difference affects the boundary layer thickness more than the bigger one. By increasing the free stream velocity of the vapor in the core, this effectiveness increases. For the boundary layer thickness of the vapor of the outer cylinder, same things can be said. From the Figures 5.24 and 5.25, the effect of increasing the temperature difference makes an increment on the boundary layer thickness. On the contrary, the effectiveness of the temperature difference between the saturated vapor and the wall on the boundary layer thickness of the vapor of the inner cylinder is much more than the one of the outer cylinder.

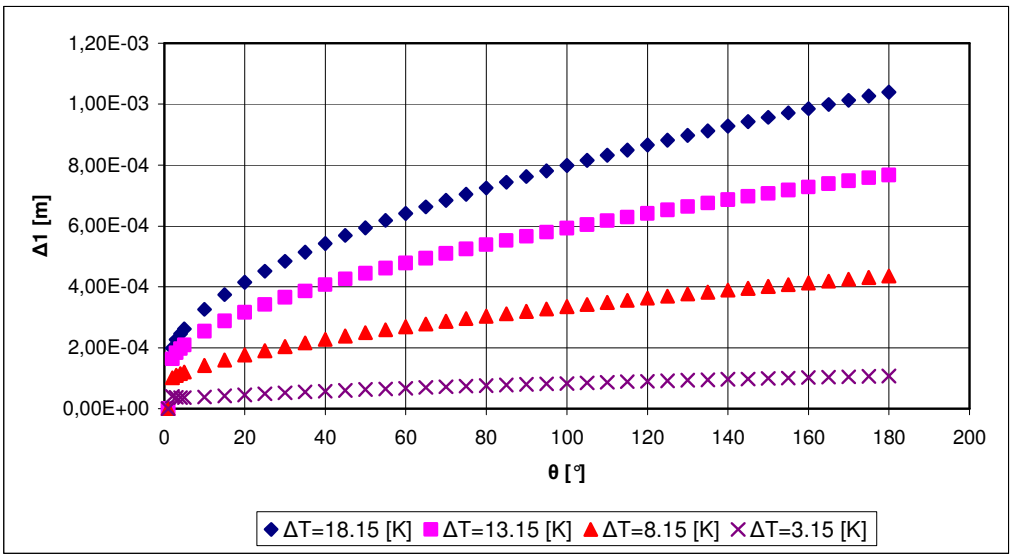

Figure 5.22 Variation of the Vapor Boundary Layer of the Inner Cylinder with the Angular Position for U = 5 m/s at Different Temperature Differences

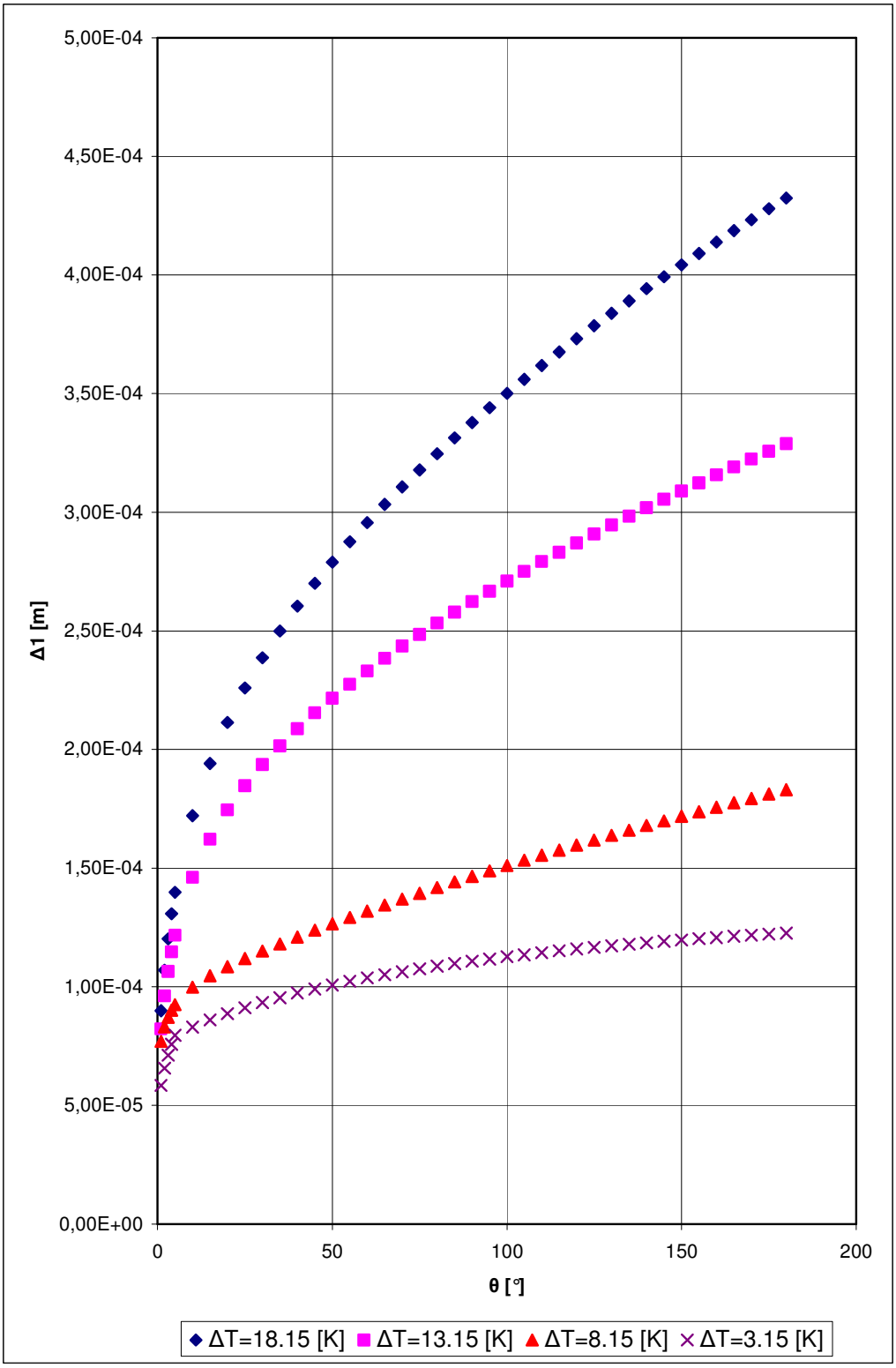

Figure 5.23 Variation of the Vapor Boundary Layer of the Inner Cylinder with the Angular Position for U = 40 m/s at Different Temperature Differences

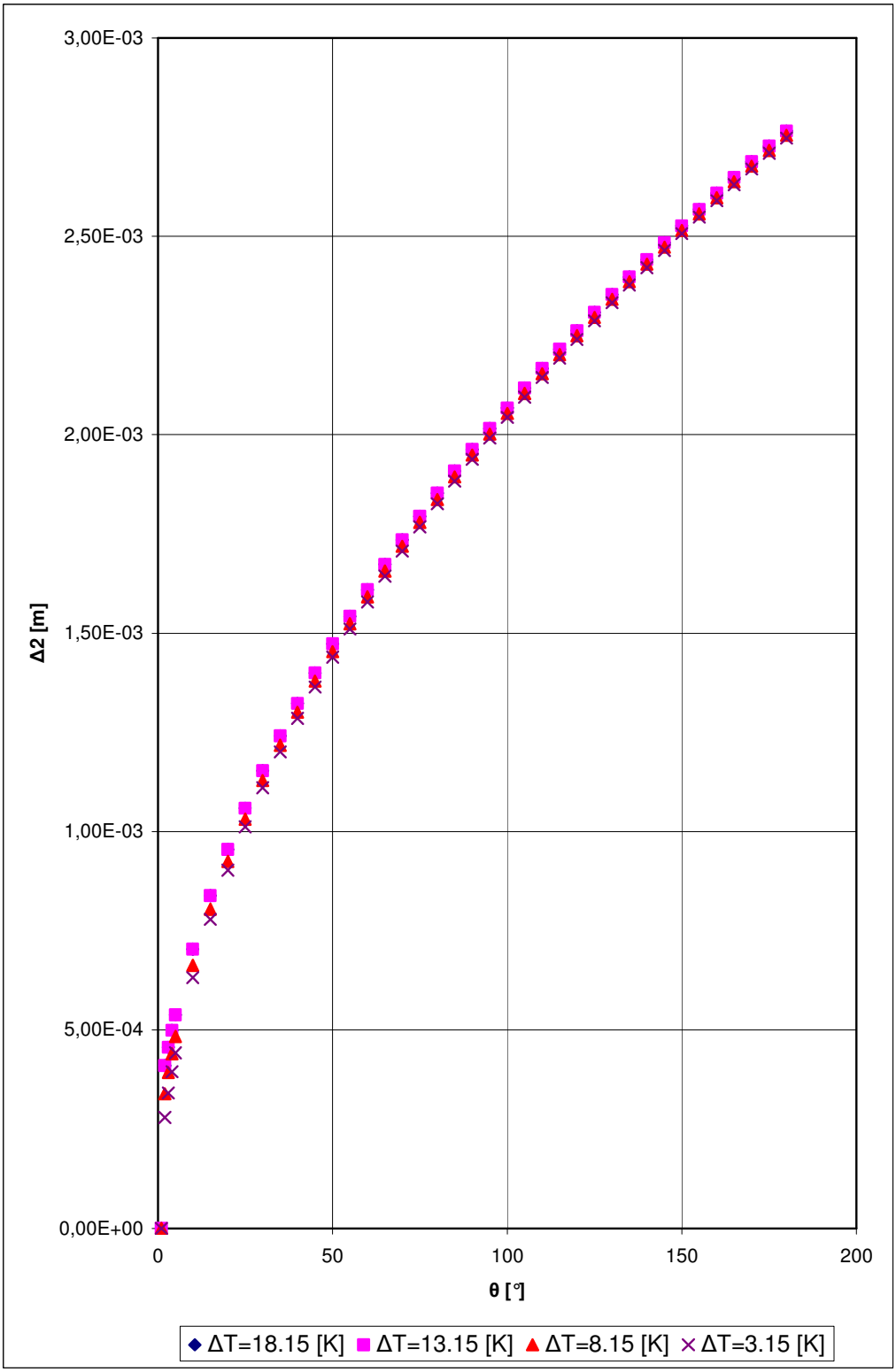

Figure 5.24 Variation of the Vapor Boundary Layer of the Outer Cylinder with the Angular Position for U = 5 m/s at Different Temperature Differences

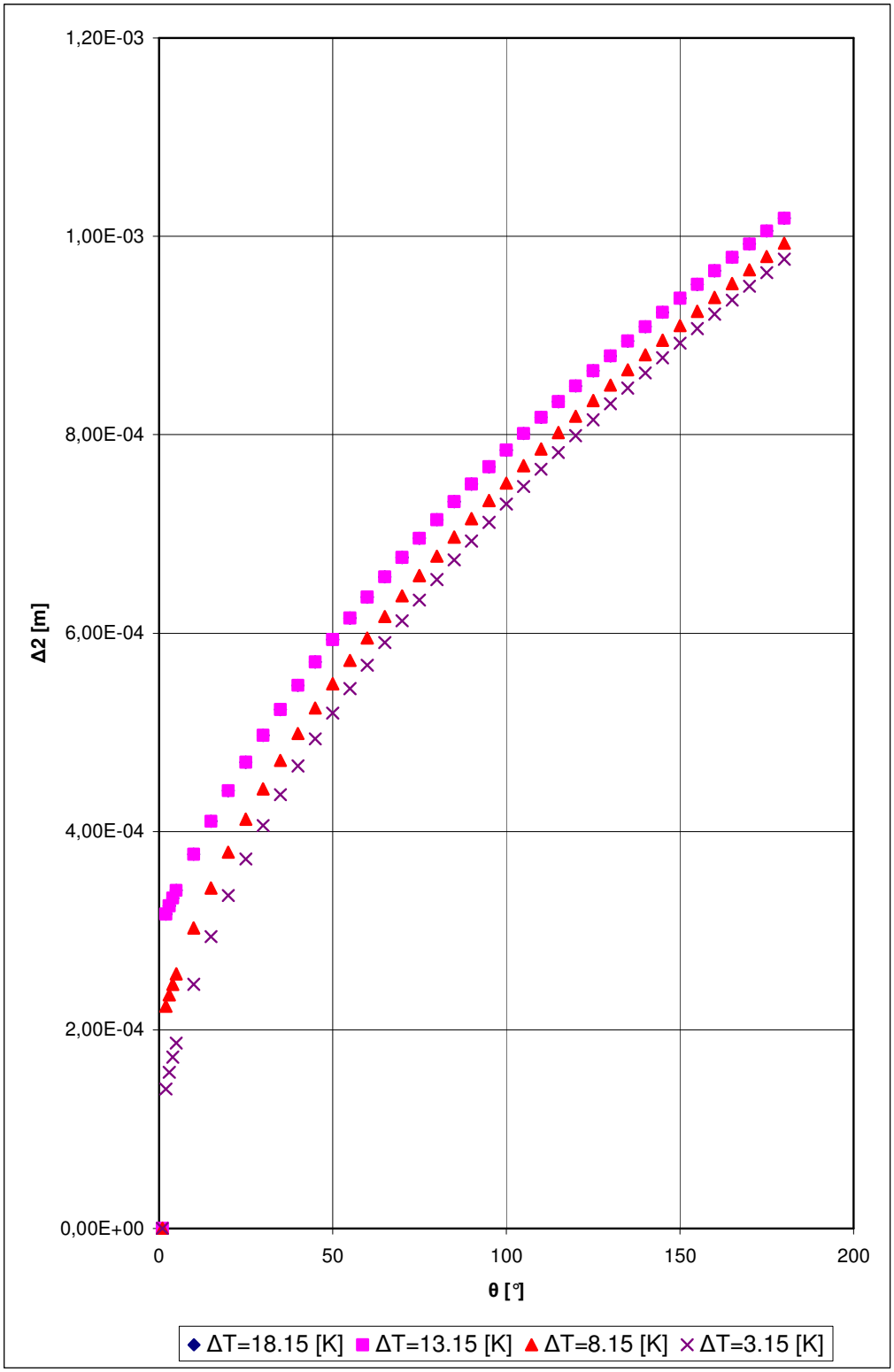

Figure 5.25 Variation of the Vapor Boundary Layer of the Outer Cylinder with the Angular Position for U = 40 m/s at Different Temperature Differences

In Figures 5.26 and 5.27 the effect of changing the temperature difference on the heat flux was shown. By increasing the temperature difference, the heat flux increases. Because the temperature difference is directly proportional to the heat flux as understood from Equation 3.33. The effectiveness of the changing the temperature difference between the saturated vapor and the wall increases by increasing the free stream velocity of the core in the core.

The effect of changing the temperature difference on the local heat transfer coefficient was shown in Figures 5.28 and 5.29. Taking account the effect of the temperature on the heat flux, by increasing the temperature difference, the heat flux had been increased. On the contrary, according to Figures 5.28 and 5.29, the local heat transfer coefficient decreases by increasing the temperature difference because the heat transfer coefficient is inversely proportional to the film thickness. Thicker the film thickness, lower the local heat transfer coefficient. In addition to this the effect of changing the temperature difference between the saturated vapor and the wall on the local heat transfer coefficient is more than the one on the heat flux. The effect of changing the temperature difference can be neglected for the heat flux. And also for the local heat transfer coefficient except the temperature difference is equal to 3.15 K.

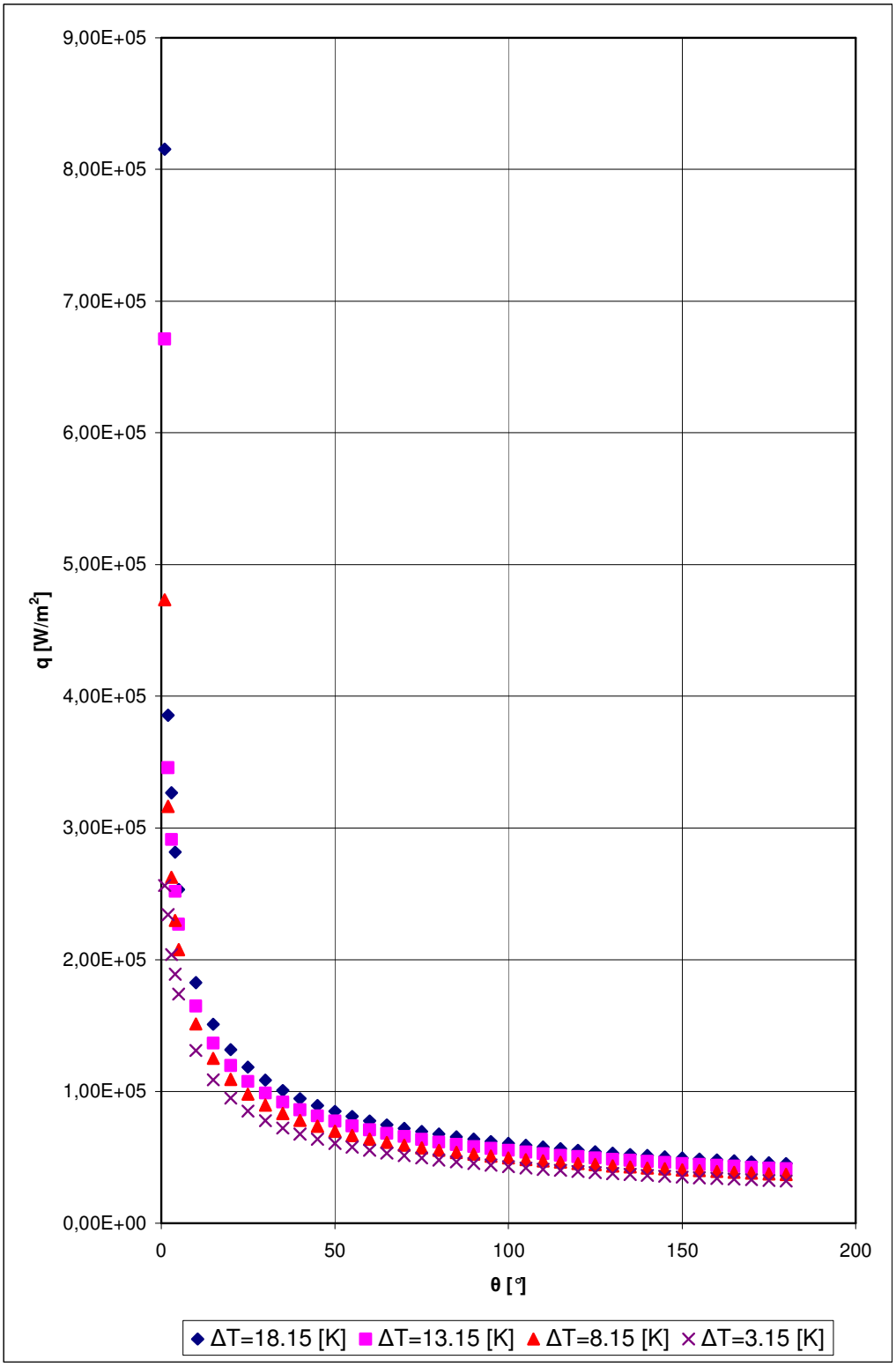

Figure 5.26 Variation of the Heat Flux with the Angular Position for U = 5 m/s at Different Temperature Differences

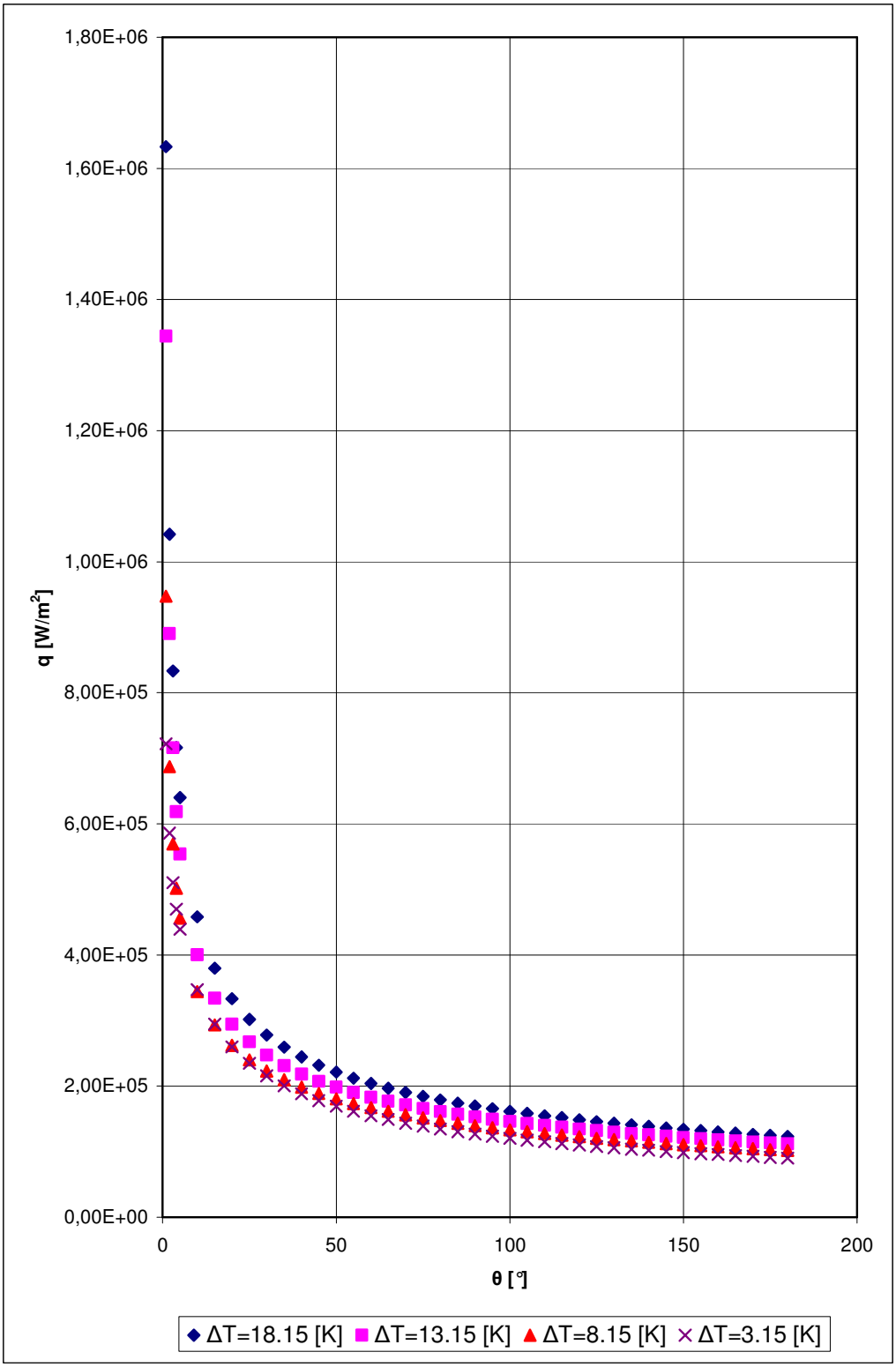

Figure 5.27 Variation of the Heat Flux with the Angular Position for U = 40 m/s at Different Temperature Differences

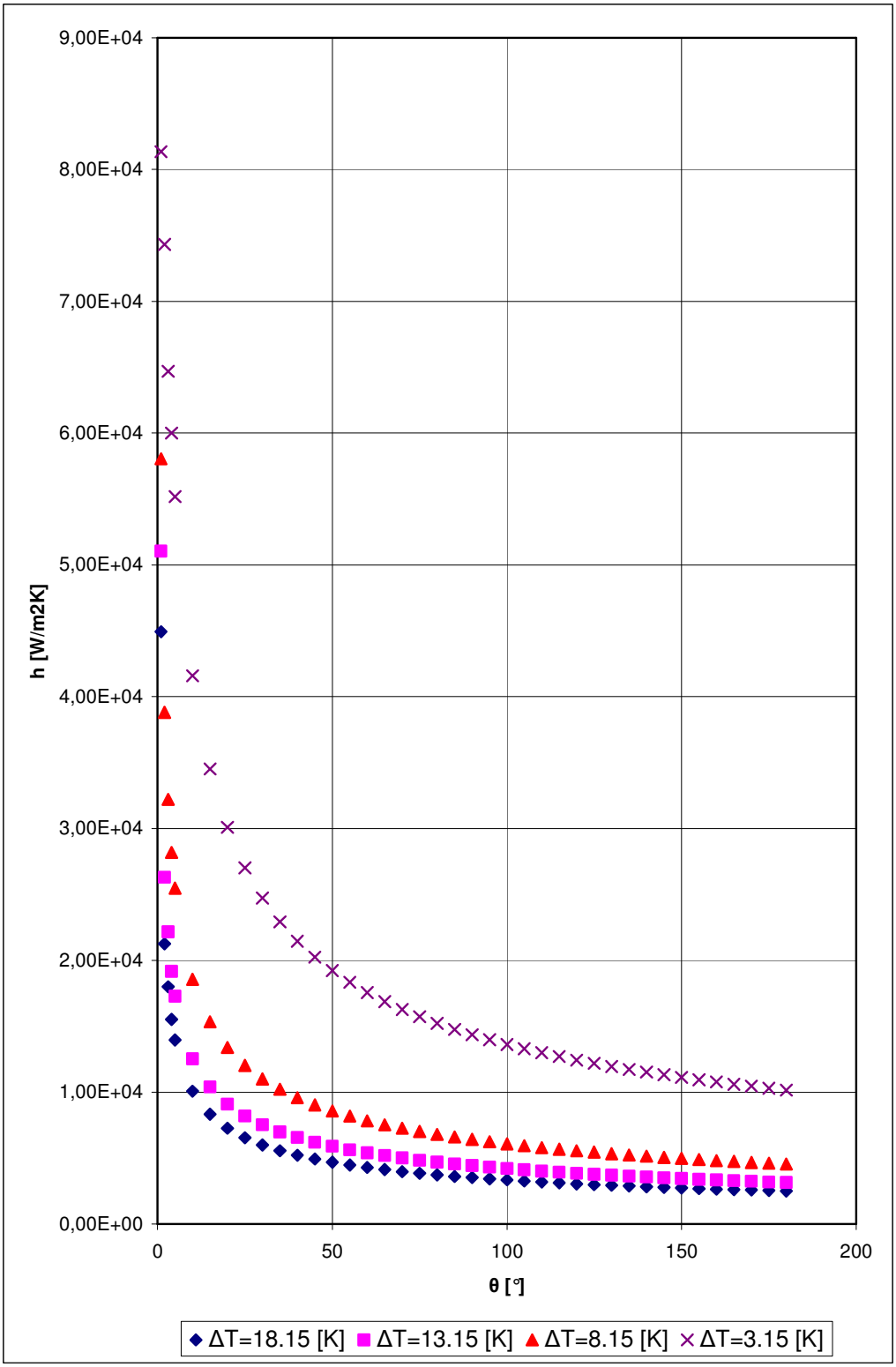

Figure 5.28 Variation of the Local Heat Transfer Coefficient with the Angular Position for U = 5 m/s at Different Temperature Differences

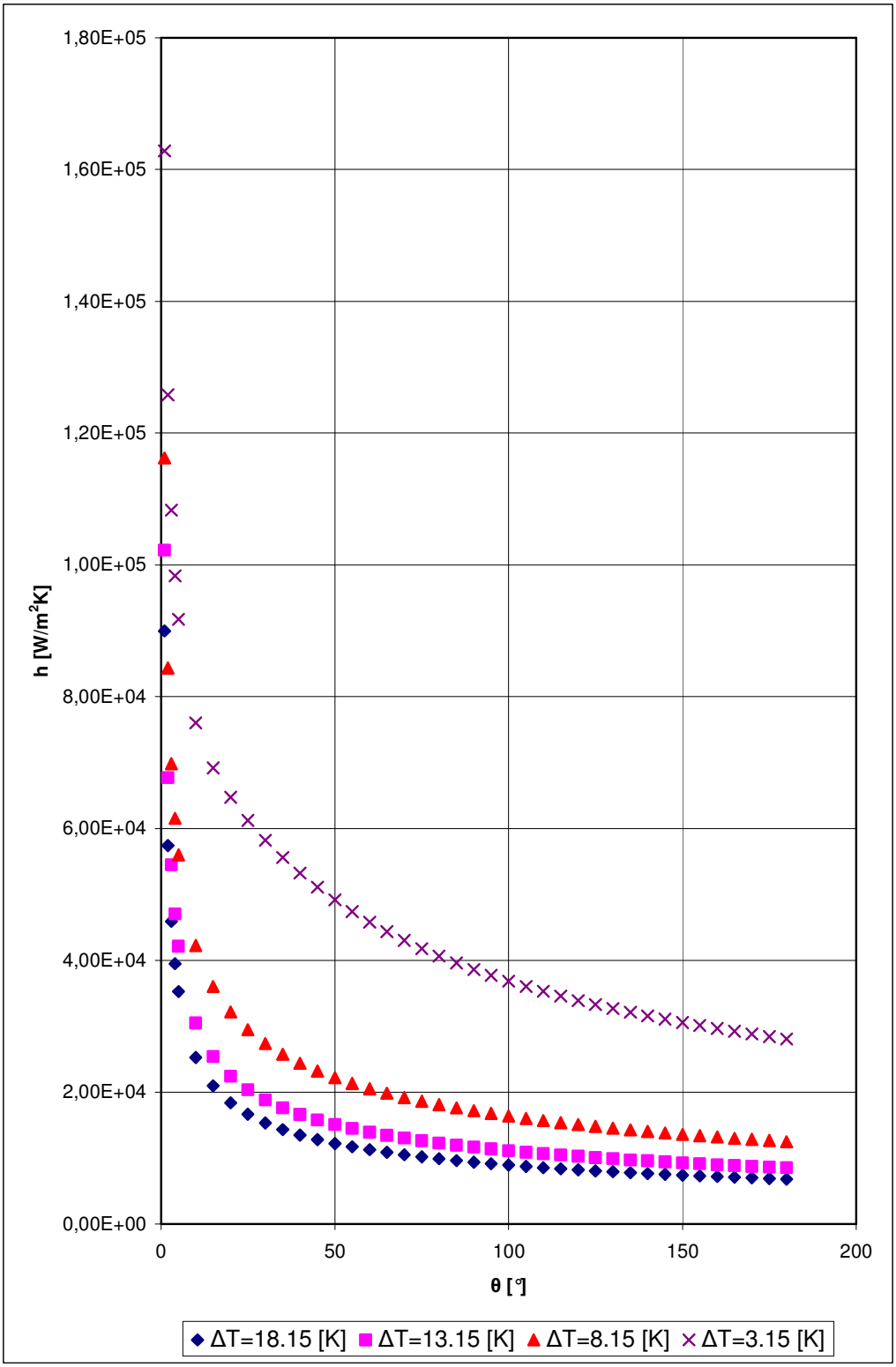

Figure 5.29 Variation of the Local Heat Transfer Coefficient with the Angular Position for U = 40 m/s at Different Temperature Differences

In Figures 5.30 and 5.31, the effect of changing the temperature difference on the velocity at the interface was shown. According to the graphs, by increasing the temperature difference between the saturated vapor and the wall causes to decrease the velocity at the interface for the free stream velocity of the vapor in the core at 5 and 40 m/s both. The effectiveness of changing the temperature difference on the velocity at the interface for the free stream velocity at 40 m/s is more effective than the one at 5 m/s. Moreover, for the free stream velocity of the vapor in the core at 5 and 40 m/s both, the effect of changing the temperature difference between the saturated vapor and the wall on the heat flux and the local heat transfer coefficient can be neglected except the temperature difference is equal to 3.15 K.

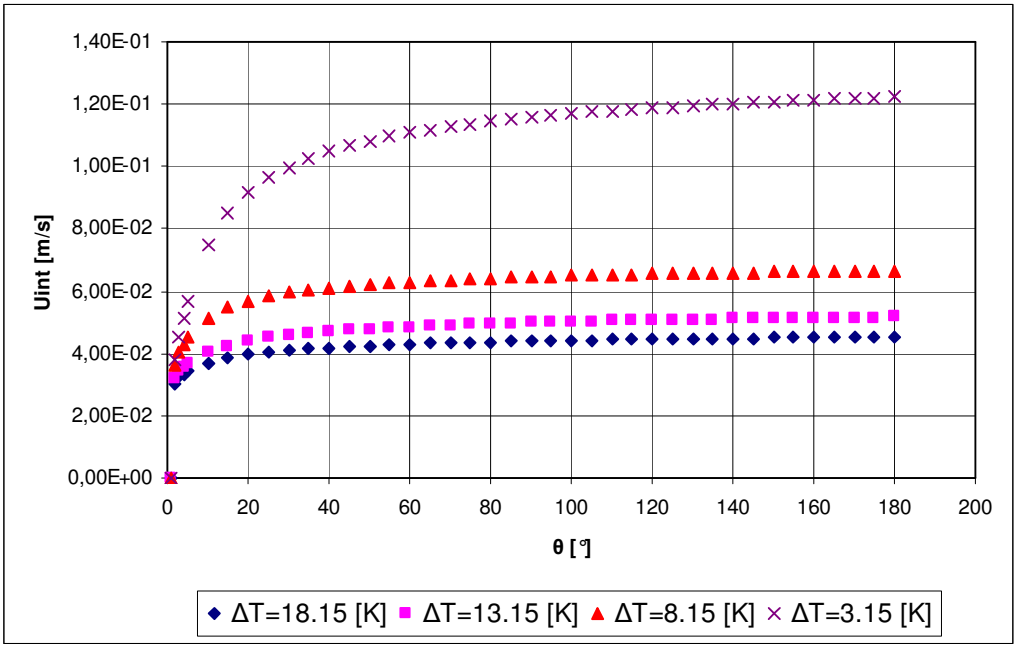

Figure 5.30 Variation of the Velocity at the Interface with the Angular Position for U = 5 m/s at Different Temperature Differences

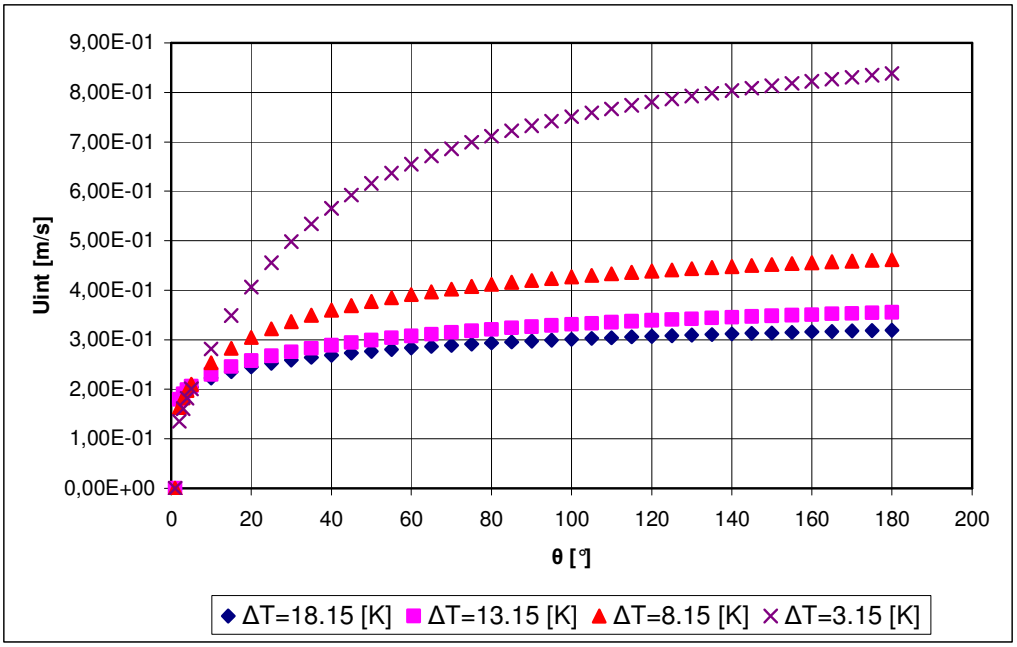

Figure 5.31 Variation of the Velocity at the Interface with the Angular Position for U = 40 m/s at Different Temperature Differences

5.3. The Effect of Changing the Annular Space Between the Concentric Cylinders on Condensation Heat Transfer

In this section by changing the annular space between the concentric cylinders were investigated and the results were shown in following figures. In the analysis, 0.005, 0.010, 0.015 and 0.020 m were chosen as annular space at constant mass flow rate which is 0.1 kg/s.

First, the effect of changing the annular space between the two cylinders was investigated on the condensate film thickness and result was shown in Figure 5.32 below. According to the Figure 5.32, by increasing the annular space between the concentric cylinders, the condensate film thickness increases. In other words, the effect of increasing the annular space is directly proportional to the condensate film thickness. Because entering saturated vapor at constant mass flow rate, by decreasing

the annular space, the area decreases and the velocity of the saturated vapor increases. Therefore, the condensate film thickness decreases.

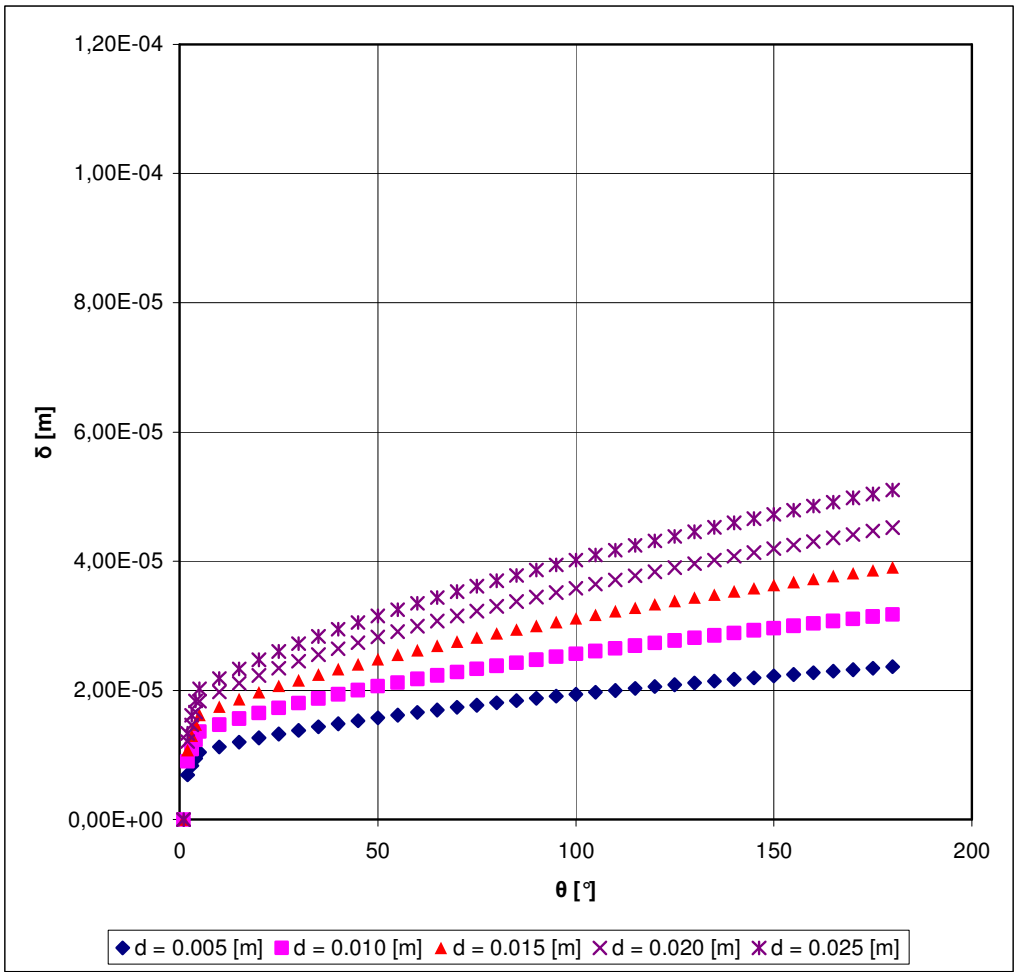

Figure 5.32 Variation of the Condensate Film Thickness with the Angular Position for m = 0.1 kg/s at Different Annular Spaces

In Figures 5.33 and 5.34, the effect of changing the annular space on vapor boundary layer thicknesses was shown. As in the Figure 5.32, by increasing the annular space between the concentric cylinders, vapor boundary layer thicknesses increases

because of the same reason as for the effect of changing the annular space between the concentric cylinders on the condensate film thickness.

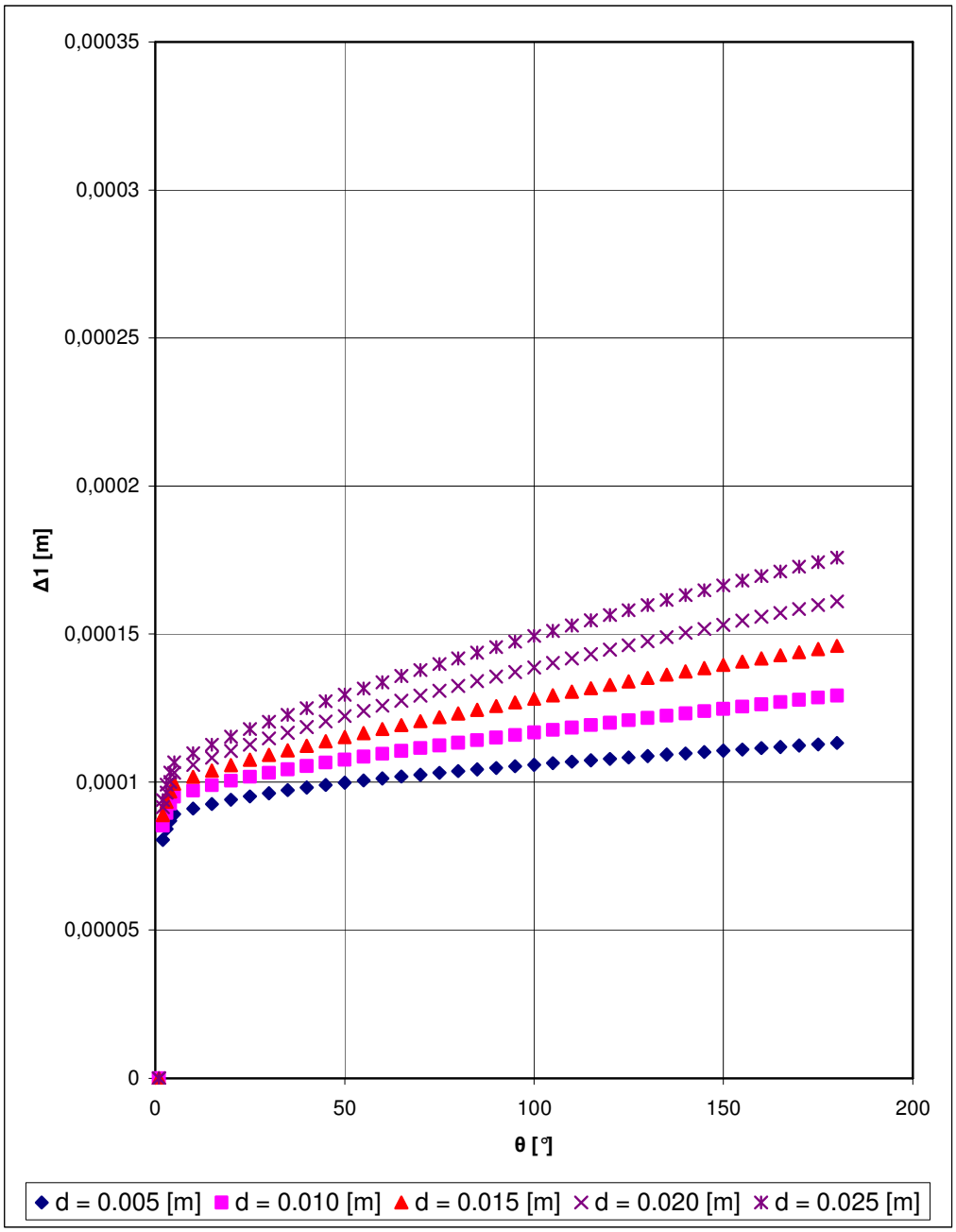

Figure 5.33 Variation of the Vapor Boundary Layer of the Inner Cylinder with the Angular Position for m = 0.1 kg/s at Different Annular Spaces

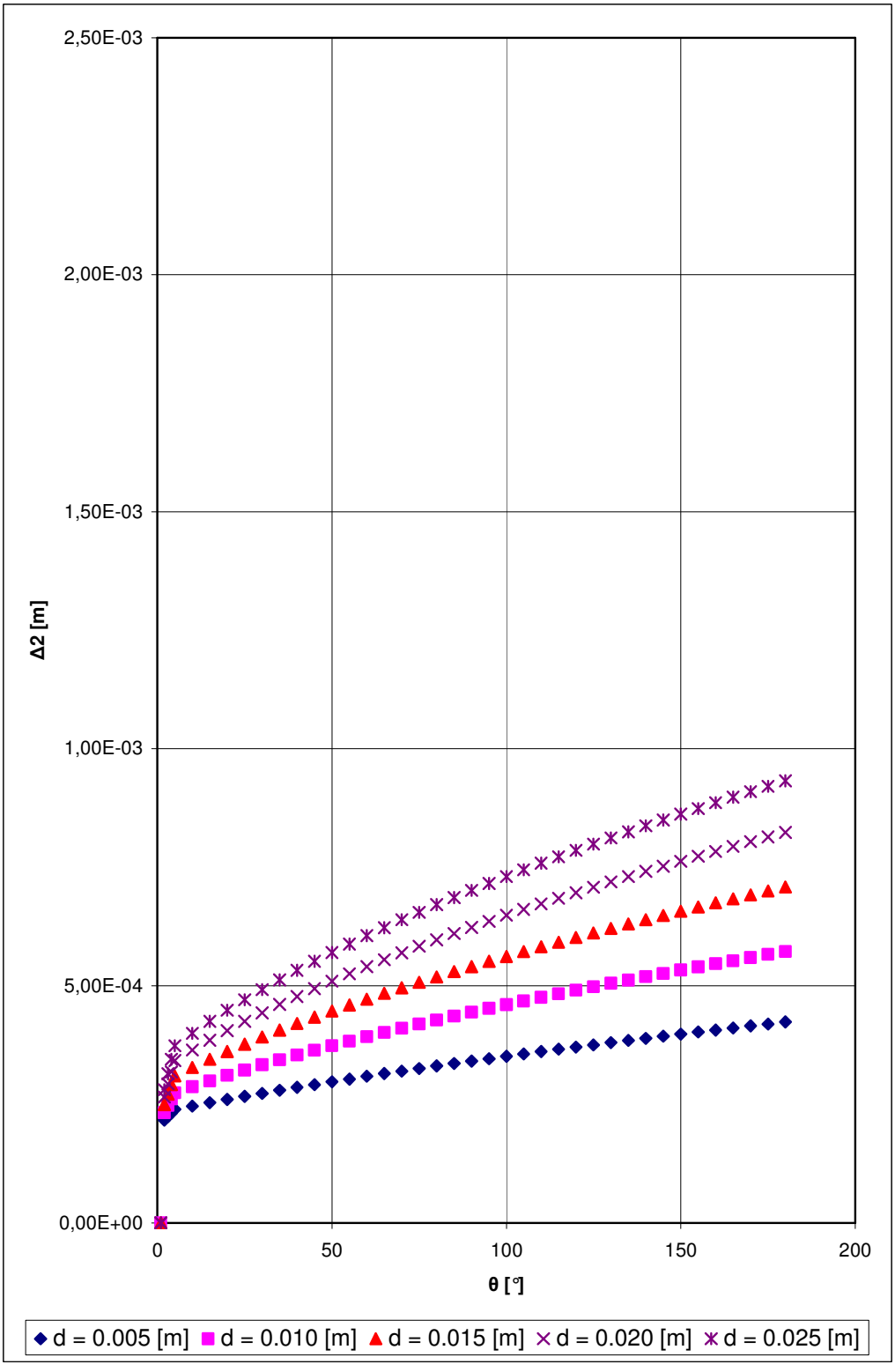

Figure 5.34 Variation of the Vapor Boundary Layer of the Outer Cylinder with the Angular Position for m = 0.1 kg/s at Different Annular Spaces

In Figure 5.35, the effect of changing the annular space between the concentric cylinders on the heat flux was investigated. By increasing the annular space, the heat flux decreases. Because the heat flux is inversely proportional to the condensate film thickness. Therefore, by increasing the annular space, the condensate film thickness increases and the heat flux decreases.

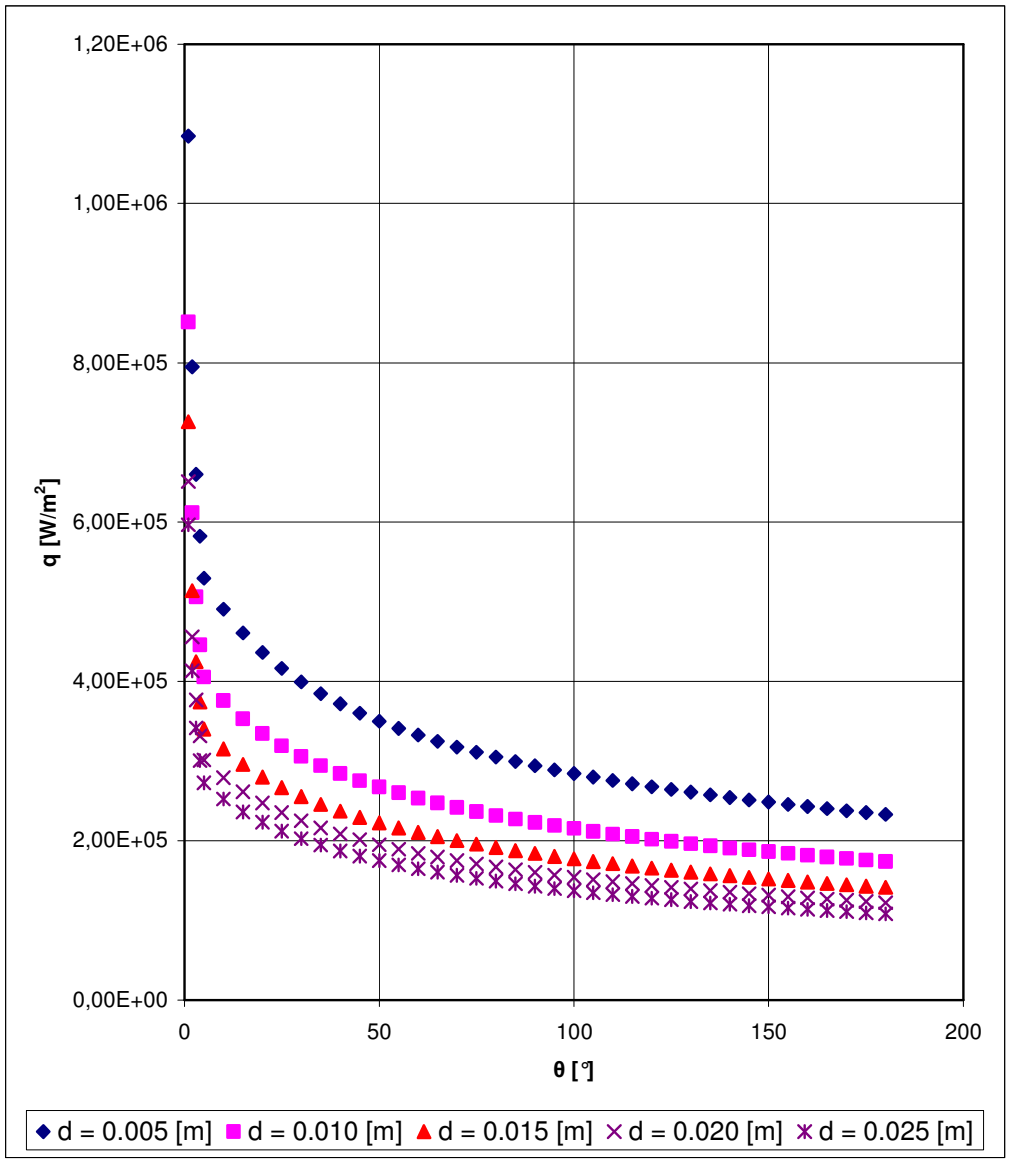

Figure 5.35 Variation of the Heat Flux with the Angular Position for m = 0.1 kg/s at Different Annular Spaces

The effect of changing the annular space between the concentric cylinders on the local heat transfer coefficient was investigated and shown in Figure 5.36. By increasing the annular space, the local heat transfer coefficient decreases as it was in the analysis of the heat flux. Because the local heat transfer coefficient is inversely proportional to the condensate film thickness therefore by increasing the annular space, the condensate film thickness increases and the local heat transfer coefficient decreases.

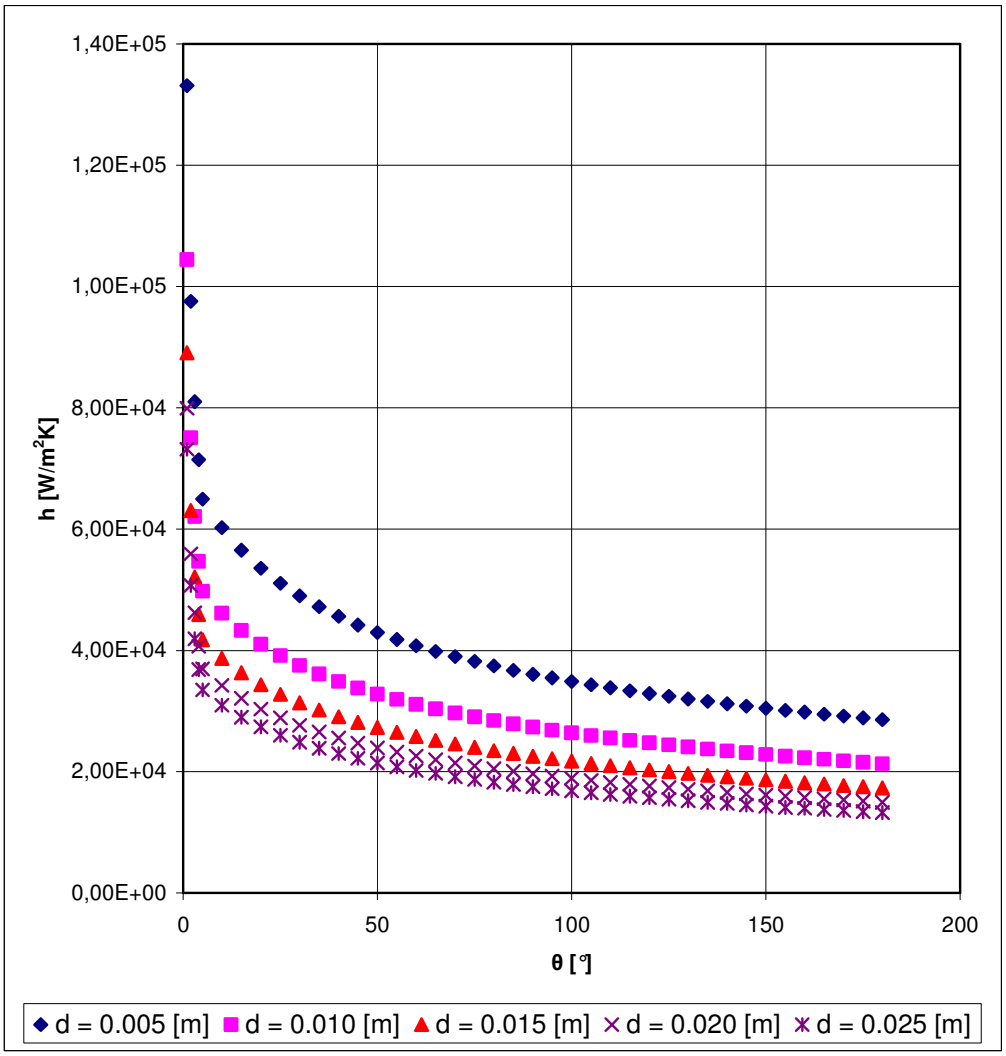

Figure 5.36 Variation of the Local Heat Transfer Coefficient with the Angular Position for m = 0.1 kg/s at Different Annular Spaces

Finally, the effect of changing the annular space between the concentric cylinders on the velocity at the interface was investigated and shown in figure 5.37. According to the Figure 5.37, by increasing the annular space, the velocity at the interface decreases. Because by increasing the annular space at constant mass flow rate, the velocity of the free stream decreases and the velocity at the interface also.

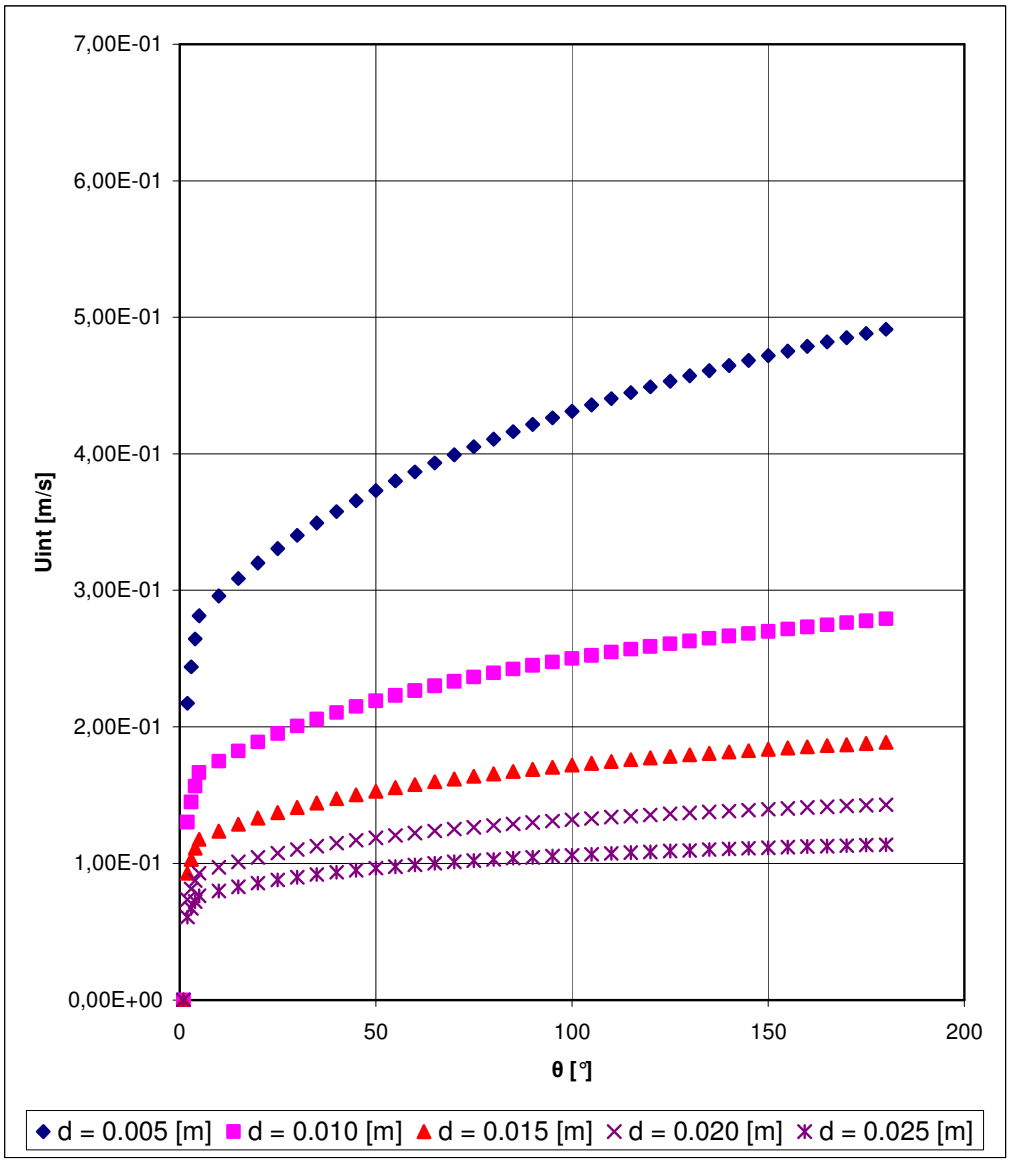

Figure 5.37 Variation of the Velocity at the Interface with the Angular Position for m = 0.1 kg/s at Different Annular Spaces

CHAPTER 6

CONCLUSIONS

Theoretical analysis of laminar forced film condensation of annular outer surface of inner cylinder of two concentric cylinders was started by defining the physical model of the problem in Chapter 3. And then by using conservation of mass and momentum laws, the governing equations were derived by using assumptions and boundary conditions. In Chapter 4, in order to investigate the analysis for the condensation problem, the solution method was mentioned how to solve the equations obtained in Chapter 3. In this section information about the program code which is capable to solve the nonlinear equations related the problem in this study was given also. From the results obtained by the program were investigated and results were graphed as figures in Chapter 5. According to figures in Chapter 5, some conclusions were obtained below:

- By increasing the free stream velocity of the vapor in the core, the film thickness of the condensate and the boundary layer thicknesses the vapor of the inner and outer cylinders decrease. On the contrary, the heat flux, the local heat transfer coefficient and the velocity at the interface increase by increasing the free stream velocity of the vapor in the core.

- The boundary layer thickness of the vapor of the outer cylinder is thicker than the one of the inner cylinder. The reason of this is the mass transfer from the boundary layer of the vapor over the condensate to the condensate layer.

- By increasing the radius of the inner cylinder, the film thickness of the condensate, the boundary layer thickness of the vapor of the inner and outer cylinders and the velocity at thee interface increase. On the other hand, the heat

flux and the local heat transfer coefficient decrease by increasing the radius of the inner cylinder.

- By decreasing the temperature difference between the saturated vapor and the wall, the film thickness of the condensate, the boundary layer thicknesses of the vapor of the inner and outer cylinders and the heat flux decrease but on the other hand, the local heat transfer coefficient and the velocity at the interface increase by decreasing the temperature difference between the saturated vapor and the wall.

- By increasing the annular space between the concentric cylinders, the condensate film thickness and the vapor boundary layers of the inner and outer cylinders increase but on the other hand, the local heat transfer coefficient and the heat flux decrease by increasing the annular space between the concentric cylinders.

In further studies, the geometry of the problem can be changed. In this study, the geometry is concentric two cylinders. In next studies, concentric spheres or by changing the incline of concentric cylinders can be investigated and the effect of this geometry on the film thickness of the condensate, the boundary layer thicknesses of the vapor, the heat flux, the local heat transfer coefficient and the velocity at the interface can be analyzed. In addition to this, beside this geometry the effect of the in the presence of noncondensable gas on the condensation can be investigated on the film thickness of the condensate, the boundary layer thicknesses of the vapor, the heat flux, the local heat transfer coefficient and the velocity at the interface. Instead of saturated vapor, another fluid can be used and its effect can be investigated.

REFERENCES

1. Çengel, Y. A., Heat Transfer – A Practical Approach, International Edition, McGraw-Hill, 1998.

2. Kakaç, S. and Yener, Y., Convective Heat Transfer, 2nd Edition, CRC Press, 1995.

3. Çetinkaya, C., Analytical and Experimental Investigation of Condensation on Circular Disk Under High Gravity, M. S. Thesis, 2001.

4. White, F. M., Viscous Fluid Flow, 2nd Edition, McGraw-Hill, 1991.

5. Fox, R. W. and McDonald, A. T., Introduction to Fluid Mechanics, 4th Edition, John Wiley & Sons, 1994.

6. Nusselt, W., Die Oberflachen-Kondensation des Wasserdamphes, Zeitschrift des Vereines Deutscher Ingenieure, 60, 541-546, 569-575, 1916.

7. Sparrow, E. M. and Gregg, J. L., A Boundary-Layer Treatment of Laminar Film Condensation, Journal of Heat Transfer-Transactions of the ASME, Vol. 81C, 13-18, 1959.

8. Sparrow, E. M. and Gregg, J. L., Laminar Condensation Heat Transfer on A Horizontal Cylinder, Journal of Heat Transfer-Transactions of the ASME, Vol. 81C, 291-296, 1959.

9. Koh, C. Y., Sparrow, E. M. and Harnett, J. P., The Two Phase Boundary Layer in Laminar Film Condensation, International Journal of Heat and Mass Transfer, Vol 2. 69-82, 1961.

10. Chen, M. M., An Analytical Study of Laminar Film Condensation: Part 1 – Flat Plates, Journal of Heat Transfer – Transactions of the ASME, Vol. 83C, 48-54, 1961.

11. Chen, M. M., An Analytical Study of Laminar Film Condensation: Part 2 – Single and Multiple Horizontal Tubes, Journal of Heat Trasnfer-Transactions of the ASME, Vol. 83, 55-60, 1961.

12. Koh, J. C. Y., An Integral Treatment of Two-Phase Boundary Layer in Film Condensation, Journal of Heat Transfer-Transactions of the ASME, Vol. 83, 359-362, 1961.

13. Churchill, S. W., Laminar Film Condensation, International Journal of Heat and Mass Transfer, Vol. 29, No. 8, 1219-1226, 1986.

14. Taghavi, K., Effect of Surface Curvature on Laminar Film Condensation, Journal of Heat Transfer-Transactions of the ASME, Vol. 110, 268-270, 1988.

15. Henderson, C. L. and Marchello, J. M., Role of Surface Tension and Tube Diameter in Film Condensation on Horizontal Tubes, ALCHE Journal, Vol. 13, No. 3, 613-614, 1967.

16. Koh, J. C. Y., Film Condensation in A Forced-Convection Boundary-Layer Flow, International Journal of Heat and Mass Transfer, Vol. 5, 941-954, 1962.

17. Shekriladze I. G. and Gomelauri, V. I., Theoritical Study of Laminar Film Condensation of Flowing Vapor, International Journal of Heat and Mass Transfer, Vol. 9, 581-591, 1966.

18. Denny, E. E. and Mills, A. F., Laminar Film Condensation on a Horizontal Cylinder at Normal Gravity, Journal of Heat Transfer-Transactions of ASME, Vol. 91C, 495-501, 1969.

19. Fujii, T., Uehara, H. and Kurata, C., Laminar Film Condensation of Flowing Vapor on a Horizontal Cylinder, International Journal of Heat and Mass Transfer, Vol. 15, 235-246, 1972.

20. Rose, J. W., Effect of Pressure Gradient in Forced Convection Film Condensation on a Horizontal Tube, International Journal of Heat and Mass Transfer, Vol. 27, No. 1, 39-47, 1984.

21. Gaddis, E. S., Solution of Two Phase Boundary Layer Equations for Laminar Film Condensation of Vapor Flowing Perpendicular to A Horizontal Cylinder, International Journal of Heat and Mass Transfer, Vol. 22, 371-382, 1979.

22. Karabulut, H. and Ataer, Ö. E., Numerical Analysis of Laminar Filmwise Condensation, International Journal of Refrigeration, Vol. 19, No. 2, 117-123, 1996.

23. Memory, S. B., Adams, V. H. and Marto, P. J., Free and Forced Convection Laminar Film Condensation on Horizontal Elliptical Tubes, International Journal of Heat and Mass Transfer, Vol. 40, No. 14, 3395-3406, 1997.

24. Rao, V. D. and Sarma, P. K., Condensation Heat Transfer on Laminar Falling Film, Journal of Heat Transfer, Vol. 106, 518-523, 1984.

25. Hsu, C. H. and Yang, S. A., Pressure Gradient and Variable Wall Temperature Effects During Filmwise Condensation from Downward Flowing Vapor onto A Horizontal Tube, International Journal of Heat and Mass Transfer, Vol. 42, 2419-2426, 1999.

26. Mosaad, M., Combined Free and Forced Convection Laminar Film Condensation on An Inclined Circular Tube with Isothermal Surface, International Journal of Heat and Mass Transfer, Vol. 42, 4017-4025, 1999.

27. Browne, M. W. and Bansal, P. K., An Overview of Condensation Heat Transfer on Horizontal Tube Bundles, Applied Thermal Engineering, Vol. 19, 565-594, 1999.

28. Kutaleladze, S. S. and Gogonin, I. I., Investigation of Heat Transfer in Film Condensation of Flowing Vapor on Horizontal Tube Banks, International Journal of Heat and Mass Transfer, Vol. 28, 1831-1836, 1985.

29. Kutaleladze, S. S., Gogonin, I. I., Sosunov, V. L., The Influence of Condensate Flow Rate on Heat Transfer in Film Condensation of Stationary Vapor on Horizontal Tube Banks, International Journal of Heat and Mass Transfer, Vol. 28, 1011-1018, 1985.

30. Kutaleladze, S. S. and Gogonin, I. I., Heat Transfer in Condensation of Flowing Vapor on A Single Horizontal Cylinder, International Journal of Heat and Mass Transfer, Vol. 28, 1019-1030, 1985.

31. Arpacı, V., Lecture Notes, University of Michigan, 8.9-8.14.

APPENDIX A

PROGRAM CODE FOR THE PROGRAM IN MATLAB

```
1. Clear
2. Clc
3. format long g
4. Tliq=370;
5. Tsat=373.15;
6. muliq=0.000289;
7. roliq=961;
8. kliq=679*10^(-3);
9. rovap=0.596;
10. muvap=0.00001202;
11. deltaT=Tsat-Tliq;
12. hfg=2257*10^(3);
13. g=9.81;
14. r=0.050;
15. l=0;
16. deltax=1*2*pi/360*r;
17. d=0.005;
18. uint0=0.00001;
19. uinf0=5;
```

```
20. delta0=0;
21. deltain0=0.00007;
22. deltain20=0.0002
23. x0 = [0.000000000001; uint0; deltain0; uinf0; deltain20];
24. for i=1:180
25. l=l+deltax
26. teta=l/r;
27. options=optimset('Display','iter','TolX',1e-8, 'Diagnostics', 'on')
28. [x,fval] = fsolve(@(x)
29. myfun_denemeson8(x, uint0, delta0, deltax, kliq, deltaT, roliq, hfg, muliq, muvap, uinf0,
    deltain0, deltain20, g, teta, rovap, d), x0, options);
30. delta0=x(1);
31. uint0=x(2);
32. deltain0=x(3);
33. uinf0=x(4);
34. deltain20=x(5);
35. h=kliq/x(1);
36. hflux=kliq*deltaT/x(1);
37. difference=x(5)-x(3);
38. z(1,i)=delta0;
39. z(2,i)=uint0;
40. z(3,i)=deltain0;
41. z(4,i)=uinf0;
42. z(5,i)=deltain20;
43. z(6,i)=h;
44. z(7,i)=hflux;
45. z(8,i)=difference;
```

46. end

APPENDIX B

SUBPROGRAM CODE FOR THE MAIN PROGRAM IN MATLAB

```
1. function F = myfun_denemeson8(x, uint0, delta0, deltax, kliq, deltaT, roliq, hfg, muliq,
   muvap, uinf0, deltain0, deltain20, g, teta, rovap, d)

2. F = [

3. (x(2)*x(1)/2-uint0*delta0/2)/deltax-kliq*deltaT/(roliq*hfg*x(1));

4. (x(2)^2*x(1)/3-uint0^2*delta0/3)/deltax-
   x(2)*kliq*deltaT/(roliq*hfg*x(1))+muliq*x(2)/(x(1)*roliq)-muvap*(x(4)-x(2))/(roliq*deltain0)-
   x(1)*rovap/roliq*x(4)*(x(4)-uinf0)/deltax;

5. (x(4)^2*x(5)/3-uinf0^2*deltain20/3)/deltax-x(4)*(x(4)*x(5)/2-
   uinf0*deltain20/2)/deltax+muvap/rovap*x(4)/x(5);

6. (x(3)*(x(4)+x(2))/2-deltain0*(uinf0+uint0)/2)/deltax+kliq*deltaT/(rovap*hfg*x(1))+(x(4)*
   (d-x(1)-x(3)-x(5))-uinf0*(d-delta0-deltain0-deltain20))/deltax+(x(4)*x(5)/2-
   uinf0*deltain20/2)/deltax;

7. (x(4)^2*(d-x(1)-x(3)-x(5))-uinf0^2*(d-delta0-deltain0-deltain20))/deltax-x(4)*((x(4)*
   (d-x(1)-x(3)-x(5))-uinf0*(d-delta0-deltain0-deltain20)))/deltax-(d-(x1)-x(3)-x(5))*x(4)*
   (x(4)-uinf0)/deltax;

8. ];
```